UNIVERSITY OF ALBERTA

AN ADAPTIVE DIGITAL TECHNIQUE FOR RF POWER AMPLIFIER LINEARIZATION FOR CELLULAR RADIO

BY

ANIT LOHTIA

A thesis submitted to the Faculty of Graduate Studies and Research in partial fulfillment of the requirements for the degree of **MASTER OF SCIENCE.**

DEPARTMENT OF ELECTRICAL ENGINEERING

EDMONTON, ALBERTA

FALL 1993

National Library
of Canada

Acquisitions and
Bibliographic Services Branch

395 Wellington Street
Ottawa, Ontario
K1A 0N4

Bibliothèque nationale
du Canada

Direction des acquisitions et
des services bibliographiques

395, rue Wellington
Ottawa (Ontario)
K1A 0N4

Your file Votre référence

Our file Notre référence

The author has granted an irrevocable non-exclusive licence allowing the National Library of Canada to reproduce, loan, distribute or sell copies of his/her thesis by any means and in any form or format, making this thesis available to interested persons.

L'auteur a accordé une licence irrévocable et non exclusive permettant à la Bibliothèque nationale du Canada de reproduire, prêter, distribuer ou vendre des copies de sa thèse de quelque manière et sous quelque forme que ce soit pour mettre des exemplaires de cette thèse à la disposition des personnes intéressées.

The author retains ownership of the copyright in his/her thesis. Neither the thesis nor substantial extracts from it may be printed or otherwise reproduced without his/her permission.

L'auteur conserve la propriété du droit d'auteur qui protège sa thèse. Ni la thèse ni des extraits substantiels de celle-ci ne doivent être imprimés ou autrement reproduits sans son autorisation.

ISBN 0-315-88304-9

Canada

UNIVERSITY OF ALBERTA

RELEASE FORM

NAME OF AUTHOR: **ANIT LOHTIA**

TITLE OF THESIS: **AN ADAPTIVE DIGITAL TECHNIQUE FOR RF POWER AMPLIFIER LINEARIZATION FOR CELLULAR RADIO**

DEGREE: **MASTER OF SCIENCE**

YEAR THIS DEGREE GRANTED: **FALL 1993**

Permission is hereby granted to the University of Alberta Library to reproduce single copies of this thesis and to lend or sell such copies for private, scholarly or scientific research purposes only.

The author reserves all other publication and other rights in association with the copyright in the thesis, and except as hereinbefore provided neither the thesis nor any substantial portion thereof may be printed or otherwise reproduced in any material form whatever without the author's prior written permission.

Anit Lohtia

Anit Lohtia
5419 - 105 Street
Edmonton, Alberta
Canada T6H 2M7

DATE: July 21, 1993

UNIVERSITY OF ALBERTA

FACULTY OF GRADUATE STUDIES AND RESEARCH

The undersigned certify that they have read, and recommended to the Faculty of Graduate Studies and Research for acceptance, a thesis entitled **AN ADAPTIVE DIGITAL TECHNIQUE FOR RF POWER AMPLIFIER LINEARIZATION FOR CELLULAR RADIO** submitted by **ANIT LOHTIA** in partial fulfillment of the requirements for the degree of **MASTER OF SCIENCE**.

Paul A. Goud

Dr. P.A. Goud, Co-Supervisor

C. G. Englefield.

Dr. C.G. Englefield, Co-Supervisor

J. F. Vaneldik

Dr. J.F. Vaneldik, Internal Examiner

W. S. Young

Dr. W.S. Young, External Examiner

DATE: 21st July 1993.

DEDICATED TO

my father Rajinder Paul Lohtia, my mother Chand Lohtia and my brother Sunit Lohtia who have been encouraging and caring for me.

Abstract

The next generation of cellular radio systems will need to have a substantially larger user capacity than the current analog system (AMPS), which uses frequency modulation. One such system is that described by the North American Interim Standard 54 (IS-54), which specifies π/4-DQPSK modulation. π/4-DQPSK modulation has a fluctuating envelope RF signal. It therefore requires a highly linear RF power amplifier, because nonlinear amplification of a fluctuating envelope RF signal results in spectral spreading of the signal as well as intermodulation distortion. An improved adaptive digital technique for the linearization of RF power amplifiers is proposed in this project. In this method, the demodulated amplifier output is compared with the baseband input signal to estimate the amplifier's AM-AM and AM-PM characteristics. The input signal is predistorted using the estimated characteristics, in order to compensate for the amplifier's nonlinearity. The proposed technique has about 23 dB better suppression of third order intermodulation products than that provided by the complex gain predistortion technique. Also, the proposed linearizer has about 8 dB less out-of-band power emission than the cartesian coordinate negative feedback technique of linearization in the first and second adjacent RF channels.

Analog quadrature modulator and demodulator impairments, namely: gain imbalance, phase imbalance, and dc-offset, adversely affect the performance of RF power amplifier linearization techniques. A technique to compensate for these impairments is also investigated in this work. In this technique, part of the RF signal is fed to an envelope detector. The detector output, along with the baseband quadrature components, is used to estimate the impairment values. The estimated impairment values are then used to

compensate for the impairments. Simulation results show that spurious signals can be suppressed by more than 30 dB using this technique.

Acknowledgments

I would like to express my sincere thanks and respect to Dr. Paul A. Goud and Dr. Colin G. Englefield for their inspiring guidance, help and encouragement. I am grateful to Mr. Timothy Neufeld for his help with computer simulations. My special thanks are also due to Ms. Yvonne J. den Otter for allowing me to use her simulation models. This project benefited greatly from the preliminary work carried out by Ms. den Otter under the supervision of Dr. Goud and Dr. Englefield. I would also like to thank to Dr. Andrew S. Wright for several stimulating discussions. I am indebted to Telecommunications Research Laboratories (TR Labs) for providing me with a Graduate Scholarship and their fine facilities during the course of this work. I am also grateful to the Faculty of Graduate Studies and Research for their financial assistance in the form of a Province of Alberta Graduate Scholarship and a Mary Louise IMRIE Graduate Student Award. Further I wish to extend my gratitude to the members of the examining committee for reviewing this work. I would also like to thank my friends, teachers, and everyone who has helped me in one way or another in completing the work reported in this thesis.

Table of Content

Chapter **Page**

1. Introduction.....1

1.1 Cellular Radio Systems.....1

1.2 Digital Cellular Systems.....3

1.3 RF Power Amplifier.....4

1.4 Thesis Outline.....5

2. RF Amplifier Linearization Techniques.....7

2.1 Amplifier Distortion Mechanisms.....7

2.1.1 AM-AM Distortion.....7

2.1.2 AM-PM Distortion.....11

2.2 Criteria for Evaluation of Amplifier Nonlinearity.....11

2.2.1 Intermodulation Products.....11

2.2.2 Out-of-Band Power Emission.....15

2.3 RF Amplifier Linearization Techniques.....16

2.3.1 LINC.....17

2.3.2 Feedforward Technique.....19

2.3.3 CALLUM.....20

2.3.4 Cartesian Coordinate Negative Feedback.....22

2.4 Predistortion Techniques.....24

2.4.1 Complex Gain Predistortion.....26

2.5 Proposed Linearization Technique.....29

2.6 Analog Quadrature Modulator and Demodulator Impairments.....34

2.7 Effects of the Modulator Impairments on a Transmitted Signal.....38

2.7.1 Spurious Signals.....38

2.7.2 Intermodulation Products.....38

2.8 Proposed Method for Compensation of the Quadrature Modulator and Demodulator Impairment.....39

2.8.1 Quadrature Modulator Impairment Compensator.....40

Chapter Page

2.8.2 Demodulator Impairment Compensator....42

3. Computer Simulation Models....45

3.1 Simulation of Communication Systems....45

3.2 BOSS....45

3.3 Basic Transmitter Model....46

3.3.1 Random Data Generator....46

3.3.2 π/4-DQPSK....47

3.3.3 Pulse Shaping Filter....49

3.3.4 Nonlinear Power Amplifier....51

3.4 Spline Interpolation Linearizer....53

3.5 Complex Gain Predistortion....56

3.6 Cartesian Coordinate Negative Feedback....56

3.7 Modulator....58

3.8 Demodulator....59

4. Results....62

4.1 Simulation Plan....62

4.2 Evaluation of Amplifier Linearity....63

4.2.1 Estimation of Power Spectrum....63

4.2.2 Intermodulation Products....65

4.3 RF Power Amplifier Distortion....66

4.4 Cubic Spline Interpolation....70

4.4.1 Number of Spline Points....70

4.4.2 Look-Up Table Size....72

4.4.3 Back Off....73

4.4.4 Class B Amplifier Cubic Spline Linearization....74

4.5 Direct Points Technique....74

4.6 Complex Gain Predistortion....77

4.7 Cartesian Coordinate Negative Feedback....79

4.8 Comparison of Performance of Spline Interpolation, Complex Gain and Cartesian Systems....80

4.9 Modulator Distortion....81

Chapter Page

4.9.1 Effects of Gain Imbalance....82
4.9.2 Effects of Phase Imbalance....83
4.9.3 Effects of DC-Offset....84
4.10 Demodulator Distortion....85
4.10.1 Effects of Gain Imbalance....86
4.10.2 Effects of Phase Imbalance....87
4.10.3 Effects of DC-Offset....88
4.11 Performance of Modulator Impairment Compensator....88
4.12 Performance of Demodulator Impairment Compensator....91
4.13 Performance of Spline Interpolation Linearizer with Modulator and Demodulator Impairment Compensators....92

5. Summary and Conclusions....94

References....98

Appendix A **Cubic Spline Interpolation**....102

Appendix B **Newton-Raphson method**....106

Appendix C **AM-AM and AM-PM Characteristics of Class AB and Class B Amplifiers**....109

Appendix D **Listing of Fortran Codes for BOSS Primitives**....116

List of Tables

Table		Page
3.1	Phase encoding of π/4-DQPSK modulator	49
C.1	Normalized AM-AM and AM-PM conversion factors for the class AB amplifier	110
C.2	Normalized AM-AM and AM-PM conversion factors for the class B amplifier	113

List of Figures

Figure		Page
1.1	Architecture of cellular radio system	2
1.2	Cell configuration of a mobile radio system	2
2.1	Voltage transfer characteristic of a power amplifier	8
2.2	(a) Power transfer characteristic of class AB amplifier (b) Power transfer characteristic of class B amplifier	9
2.3	(a) Phase characteristic of class AB amplifier (b) Phase characteristic of class B Amplifier	12
2.4	Intermodulation products and harmonic distortion spectrum for two-tone input signal	16
2.5	LINC transmitter	18
2.6	Feedforward linearization technique	19
2.7	CALLUM	20
2.8	Region of stable operation for CALLUM	21
2.9	Cartesian coordinate negative feedback system	22
2.10	Feedback amplifier	23
2.11	Adaptive predistortion	25
2.12	Complex gain predistorter	27
2.13	Transmitter with proposed linearizer	30
2.14	Power transfer characteristic of an amplifier	32
2.15	Phase distortion characteristic of an amplifier	33
2.16	Ideal quadrature modulator	35
2.17	Effect of gain imbalance on a sinusoidal input	35
2.18	Effect of phase imbalance on a sinusoidal input	36
2.19	Effect of dc-offset on a sinusoidal input	37

Figure **Page**

2.20 Ideal quadrature demodulator....37

2.21 Spectrum of modulator output for single tone input....39

2.22 Modulator impairment compensator....40

2.23 Demodulator impairment compensator....42

3.1 Simulation model of a π/4-DQPSK transmitter....46

3.2 (a),(b) QPSK signal constellation and transitions, (c) π/4-DQPSK signal constellation and transitions....48

3.3 Impulse response of square-root raised cosine filter....52

3.4 BOSS module of nonlinear power amplifier....53

3.5 Simulation model of π/4-DQPSK transmitter with cubic spline interpolation linearizer....54

3.6 Simulation model of transmitter with spline interpolation linearizer and two-tone input signal....55

3.7 Simulation model of complex gain predistortion system....57

3.8 Simulation model of cartesian coordinate negative feedback system....58

3.9 Simulation model of quadrature modulator....59

3.10 Simulation model of quadrature demodulator....60

3.11 Simulation model of transmitter with spline interpolation linearizer, and modulator and demodulator impairment compensators....61

4.1 Spectrum of two-tone input signal....66

4.2 Power spectral density of π/4-DQPSK modulated signal with square-root raised cosine filtering....67

4.3 Output spectral density of class AB amplifier....67

Figure **Page**

4.4 Output spectrum of class AB amplifier for two-tone input signal (20 kHz and 25 kHz)....68

4.5 Output power spectral density of class B amplifier....68

4.6 Output spectrum of class B amplifier for two-tone input signal (20 kHz and 25 kHz)....69

4.7 Comparison of output power spectral density of class AB and class B amplifiers....69

4.8 Output power spectral density for different number of spline points....71

4.9 Intermodulation products for different number of spline points....71

4.10 Output spectral density for different look-up table sizes....72

4.11 Intermodulation products for different look-up table sizes....73

4.12 Output spectral density for different input power levels....74

4.13 Comparison of output spectral density of class AB and class B amplifiers with spline interpolation linearizer....75

4.14 Output spectral density for direct look-up table points....76

4.15 Comparison of output spectral densities for spline interpolation and direct look-up table points....76

4.16 Output power spectral density of class AB amplifier with complex gain predistorter....78

4.17 Output spectrum of class AB amplifier with complex gain predistorter for two-tone input signal....78

4.18 Output power spectral density of class AB amplifier with cartesian coordinate feedback....79

4.19 Comparison of output power spectral densities of class AB amplifier....80

Figure **Page**

4.20 Comparison of intermodulation products of class AB amplifier with spline interpolation, complex gain and cartesian coordinate negative feedback linearizers....81

4.21 Gain imbalance versus undesired sideband level....82

4.22 Signal constellation of π/4-DQPSK modulated signal with raised cosine filtering....83

4.23 Effect of gain Imbalance on a π/4-DQPSK modulated signal....84

4.24 Phase imbalance versus undesired sideband level....85

4.25 Effect of phase imbalance on a π/4-DQPSK modulated signal....85

4.26 DC-Offset versus undesired carrier signal....86

4.27 Effect of dc-offset on a π/4-DQPSK modulated signal....86

4.28 Gain imbalance versus image signal level....87

4.29 Phase imbalance versus image signal level....88

4.30 DC-offset versus undesired dc signal level....89

4.31 Gain imbalance versus undesired sideband level....90

4.32 Undesired sideband level versus convergence bound of compensated modulator....90

4.33 Gain imbalance versus image signal level....91

4.34 Image signal level versus convergence bound of demodulator impairment compensator....92

4.35 Output power spectral density of class AB amplifier with spline interpolation linearizer and modulator and demodulator impairment compensators....93

List of Abbreviations

A/D	Analog to Digital
AMPS	Advanced Mobile Phone Service
AM-AM	Amplitude to Amplitude
AM-PM	Amplitude to Phase
BOSS	Block Oriented System Simulator (COMDISCO Inc.)
CALLUM	Combined Analog Locked Loop Universal Modulator
C/N	Carrier to Noise Ratio
D/A	Digital to Analog
DFT	Discrete Fourier Transform
DSP	Digital Signal Processor
EIA	Electronic Industries Association
FFT	Fast Fourier Transform
FM	Frequency Modulation
IN	Intelligent Network
IS-54	Interim Standard 54
ISDN	Integrated Service Digital Network
LINC	Linear Amplification using Nonlinear Components
MTSO	Mobile Telephone Switching Office
π/4-DQPSK	π/4 shifted Differentially Encoded Quadrature Phase Shift Keying
PSD	Power Spectral Density

PSTN	Public Switching Telephone Network
QPSK	Quadrature Phase Shift Keying
S/N	Signal to Noise Ratio
SS-7	Signaling System 7
TDMA	Time Division Multiple Access
TIA	Telecommunication Industry Association
VCO	Voltage Controlled Oscillator

List of Symbols

α	roll-off factor for the transmit filter (square-root raised cosine)
β	transfer function of feedback network
d_A	open loop distortion of forward path
ϕ	phase
f	frequency
f_1	frequency of tone 1 (two-tone input)
f_2	frequency of tone 2 (two-tone input)
G	amplifier gain
i	in-phase component of complex signal
IM_3	third-order intermodulation product
IM_5	fifth-order intermodulation product
q	quadrature-phase component of complex signal
T	symbol period
v	voltage
ω_c	carrier frequency

1. Introduction

Mobile communication systems have experienced tremendous growth in the past decade. In mobile communication systems, the mobile terminals are not physically linked to the network, but use radio links instead.

1.1 Cellular Radio Systems

Cellular radio systems are high-capacity mobile communication systems. These systems employ radio frequency reuse in order to enhance their communications traffic capacity. The service area is divided into a large number of cells. Each cell has a base station or cell site and is allocated a set of radio frequency channels for wireless communications with the mobile users in that particular cell. Base stations link the mobile users to the public switching telephone network (PSTN) via a mobile telephone switching office (MTSO). Fig. 1.1 shows the system architecture of a cellular network.

Adjacent cells are assigned different radio frequencies; these same frequencies are reused in nonadjacent cells, as shown in Fig. 1.2. The problem of co-channel radio interference is controlled by ensuring a minimum distance between base-stations using the same frequency channels, and by controlling the radio frequency (RF) power level of the transmitters.

Another feature of cellular systems is the "hand-off" concept. The system hands-off an ongoing call in one channel in one cell to another channel in an adjacent cell as the user moves from one cell to the next cell. This is done automatically by the system. The cell site monitors the signal strength of all users in the cell and uses these data to adjust the transmitter powers of the mobile users, and to determine when a handoff is needed. During a handoff, the

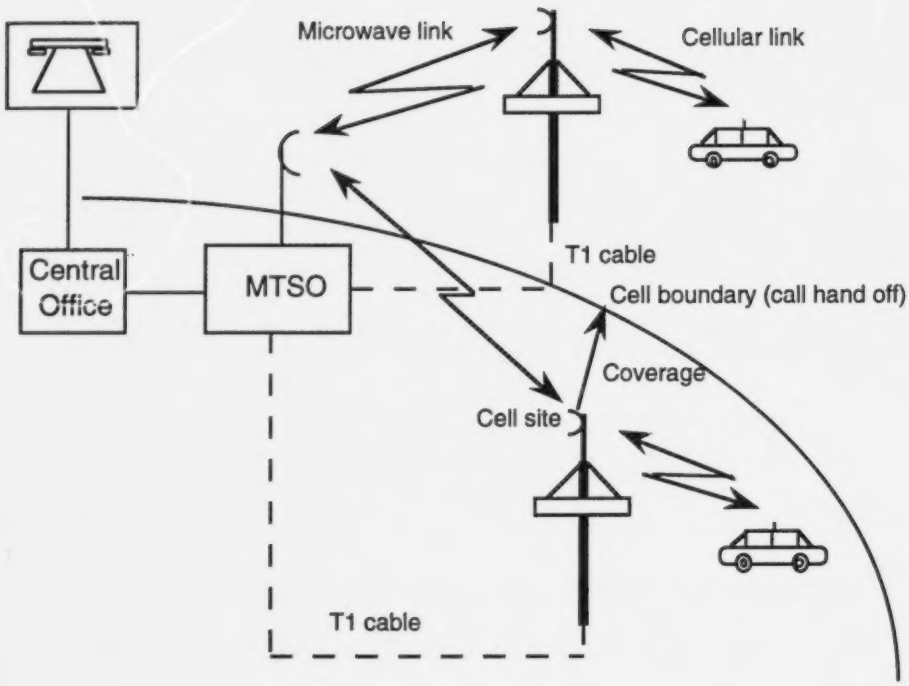

Fig. 1.1 Architecture of cellular radio system

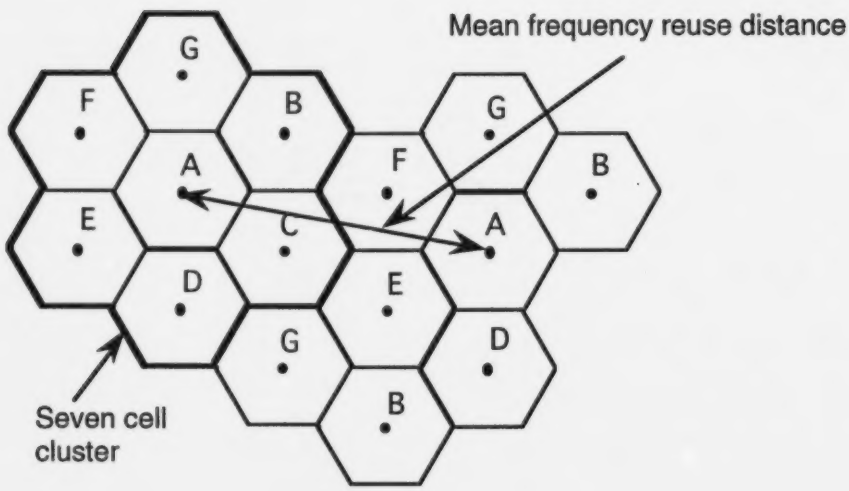

Fig. 1.2 Cell configuration of a cellular radio system

cell uses data-control links to inform the neighboring cell through the MTSO that a user is approaching.

In North America, there is a 50-MHz frequency band allocated for cellular communications in the 800-MHz band. The initial increase in demand for cellular service was met by increased spectral and trunk efficiency and by reducing the cell sizes (cell splitting). However, these techniques have nearly been stretched to their full extent in some cities [1]. Therefore, a significantly higher capacity cellular system is needed to meet the growing demand for mobile service.

1.2 Digital Cellular Systems

Digital cellular systems can provide increased capacity without requiring additional frequency spectrum. An interim standard (IS-54) for digital cellular systems in North America has been prepared by the EIA / TIA (Electronic Industries Association / Telecommunication Industries Association), subcommittee TR 45.3 on Digital Cellular Systems (1990). This standard specifies a dual mode system, supporting both the existing analog and the future digital mode systems [2].

IS-54 digital cellular systems use time division multiple access (TDMA). Each 30-kHz RF channel will initially carry three user signals, multiplexed in the time domain. This system is compatible with the currently used Advanced Mobile Phone Service (AMPS) system. The advantages of TDMA for the cellular system are [1,3]: less expensive base-stations, since no new frequency combiners are needed, and future capacity increase when lower bit rate speech encoding becomes possible.

Apart from enhanced capacity, digital systems have the advantage of being able to operate with lower S/N (signal to noise) and C/N (carrier to noise) ratios as compared to analog systems. The digital cellular system is compatible with the digital telephone network. It can incorporate ISDN (integrated service digital network), SS-7 (signaling system 7) and IN (intelligent network) services in the future. Digital systems also provide better security of communications.

AMPS systems use frequency modulation (FM) for transmission, a modulation format that has a constant envelope. In an RF power amplifier, the amount of distortion produced is dependent upon the amplitude variation of the input signal. Since a frequency modulated signal has a constant envelope, the amplifier will not cause distortion of such a signal. Therefore, a power efficient nonlinear amplifier can be used. However, frequency modulation is not a spectrally efficient technique. Departing from constant envelope modulation, the IS-54 standard specifies $\pi/4$ shifted differentially encoded quadrature phase shift keying ($\pi/4$-DQPSK) with square-root raised cosine filtering at the transmitter and receiver. A $\pi/4$-DQPSK modulated signal has a fluctuating envelope. Nonlinear amplification of a fluctuating envelope RF signal will result in intermodulation distortion products and spectral spreading of the signal, which can cause interference in adjacent channels. Therefore, a $\pi/4$-DQPSK modulated signal requires a highly linear RF power amplifier for amplification.

1.3 RF Power Amplifier

The transmitter RF power amplifier amplifies a low level input signal to the desired power level. An ideal amplifier has constant gain independent of input power level. However, in a practical amplifier, the gain decreases as the amplifier approaches saturation. Also, the phase delay in the amplifier is a

function of the input signal level. As mentioned above, the nonlinear behavior of an amplifier causes intermodulation distortion and spectral spreading of the signal, resulting in interference in the adjacent frequency channels of a cellular system.

A major challenge in RF power amplifier design is to build a linear amplifier without compromising its power efficiency. A number of techniques for linearization of RF power amplifier have been reported in last several years. These techniques fall under one of the following categories; namely, 1) Feedforward, 2) Linear amplification using nonlinear components, 3) Negative Feedback, 4) Predistortion. The predistortion technique for linearizing an RF power amplifier has been improved and extended in this research project. This technique is based on predistorting the input signal of the amplifier to compensate for its nonlinearities. The predistortion coefficients are computed using the estimated amplitude-to-amplitude (AM-AM) and amplitude-to-phase (AM-PM) characteristics of the amplifier. The amplifier distortion is taken to be dependent on the amplitude of the input signal and not on its phase.

The linearization technique uses an analog quadrature modulator and demodulator, which can introduce phase dependent distortion. This can adversely affect the performance of the proposed linearizer. An adaptive technique for compensation of the modulator and demodulator impairments is therefore also investigated in this project.

1.4 Thesis Outline

Chapter 2 describes the effects of RF amplifier nonlinearities in the IS-54 digital cellular system and quantifies these nonlinearities. An overview of RF power amplifier linearization techniques is presented. The proposed amplifier

linearization technique is described. The effects of the quadrature modulator and demodulator impairments are discussed. The structures of the modulator and demodulator impairment compensators are described.

Chapter 3 explains the computer simulation models used for this work. The models for the proposed linearization technique, the complex gain predistortion method, and the cartesian coordinate negative feedback method are described.

Chapter 4 presents the results obtained in this project. The performance of the above-mentioned linearization techniques is compared. The results for the performance of the modulator and demodulator impairment compensators are also presented.

Chapter 5 concludes the thesis with a summary of the research results, and indicates areas of possible future work in this field.

2 RF Amplifier Linearization Techniques

This chapter describes amplifier distortion mechanisms and linearization techniques. An adaptive digital linearizer for RF amplifiers is proposed, using the well-known method of predistorting the input signal to compensate for the amplifier nonlinearity. It takes advantage of the very good physical approximation that the amplifier distortion is dependent only on the magnitude of the input signal. A phase-dependent distortion can occur due to imperfections of the quadrature modulator and demodulator, which are a part of the feedback loop. These imperfections can be compensated for by using digital signal processing techniques. Methods for compensating for the quadrature modulator and demodulator impairments are proposed, and are described in this chapter.

2.1 Amplifier Distortion Mechanisms

The output of an ideal amplifier is a simple scaled replica of the original input signal. However, practical amplifiers introduce nonlinear distortion. The amplifier gain decreases as saturation is approached. These distortions occur due to power supply and other gain mechanism limitations. Amplifier distortion can be characterized using amplitude-to-amplitude (AM-AM) and amplitude-to-phase (AM-PM) distortion. If a nonlinear amplifier is used for the amplification of a multiple carrier signal, cross modulation may occur due to AM-AM and AM-PM conversion.

2.1.1 AM-AM Distortion

AM-AM distortion is an amplitude distortion arising from the nonlinear power transfer characteristics of an amplifier. Fig. 2.1 shows a representative input-output voltage characteristic of a power amplifier. When the input voltage (v_i) is less than some threshold voltage (v_t), the amplifier transistors are

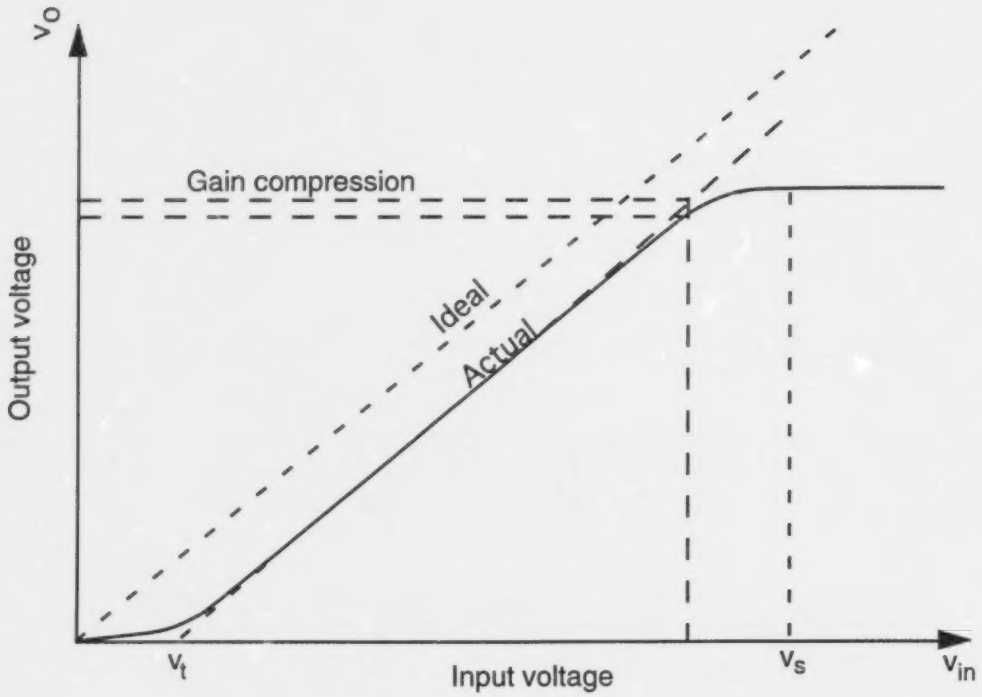

Fig. 2.1 Voltage transfer characteristic of a power amplifier

conducting weakly and the output voltage (v_o) is very small. This deadband is present in class B amplifiers and results in so-called cross-over distortion. As the input voltage is increased above v_t, the transistors operate in their active region and a quite linear operating region is obtained. Raising the input voltage beyond the saturation voltage (v_s), drives the transistors into saturation. Representative power transfer characteristics of practical class AB and class B amplifiers are shown in Fig. 2.2. The 0 dB input power level corresponds to the 1 dB gain compression point. The power gain of an amplifier is the slope of its power transfer characteristic. Ideally the gain should be constant; that is, it should be independent of the input signal level. An ideal linear response can be characterized by a straight line passing through the origin.

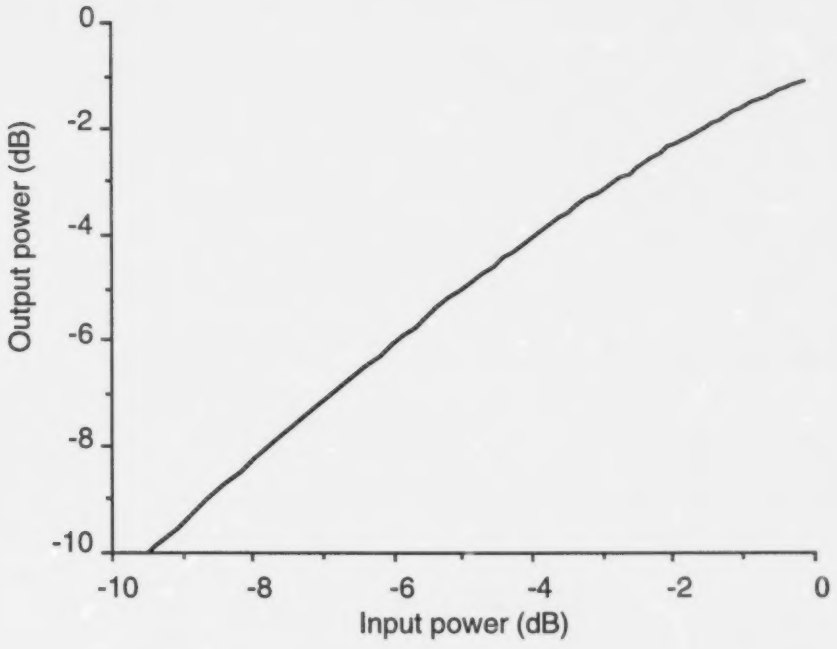

(a)

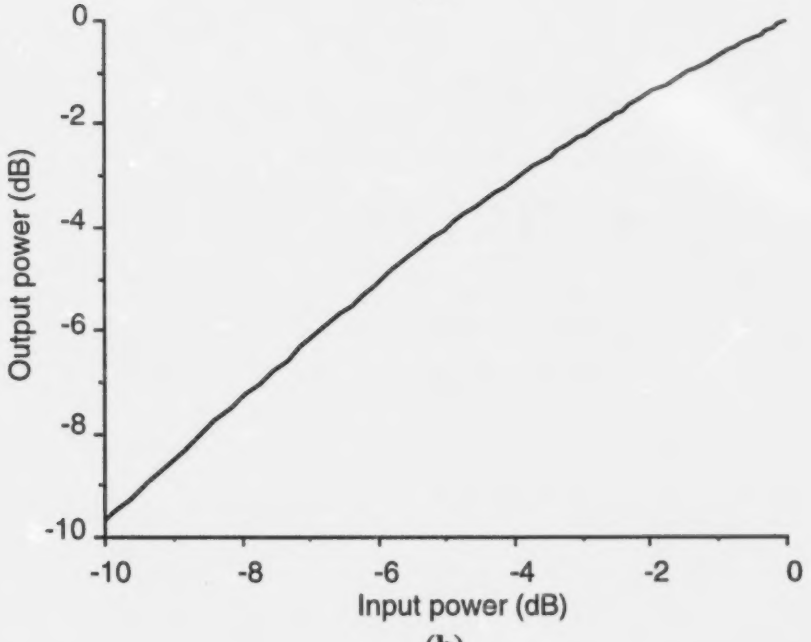

(b)

Fig 2.2 (a) Power transfer characteristic of class AB amplifier
(b) Power transfer characteristic of class B amplifier

It can be seen from Fig. 2.1 that there is a fairly constant gain region. However, operating in this linear region has the distinct disadvantage of a low DC-to-RF conversion efficiency. This efficiency can be increased by operating an amplifier close to saturation. Saturation implies that the gradient of the transfer function is zero. In other words, the output power does not increase with a further increase of the input power. The output signal suffers increasing gain compression with increasing input amplitude as saturation is approached. This results in the generation of harmonics and intermodulation distortion products. Harmonic distortion is the generation of second or higher harmonics of the input signal. Intermodulation distortion products are generated when two or more frequencies are present in the input signal. Intermodulation distortion products result in spurious signals within as well as outside the frequency band of the input signal.

If the input signal has a bandwidth over which the characteristics of the amplifier do not depend upon frequency, the amplifier can be considered as memoryless in that bandwidth. The output voltage ($v_o(t)$) of a memoryless amplifier is a function of the instantaneous input voltage ($v_i(t)$). The output voltage can be represented by a power series of the input voltage:

$$v_o(t) = c_1 v_i(t) + c_2 {v_i}^2(t) + c_3 {v_i}^3(t) + \ldots\ldots$$

....(2.1)

If $v_i(t) = A\cos\omega t$, then the first three terms of $v_o(t)$ can be written as:

$$v_o(t) = c_1 A\cos\omega t + c_2 A^2\cos^2\omega t + c_3 A^3\cos^3\omega t$$

....(2.2)

which can be rewritten as:

$$v_o(t) = 0.5c_2A^2 + \left(c_1A + 0.75c_3A^3\right)\cos\omega t + 0.5c_2A^2\cos 2\omega t + 0.25c_3A^3\cos 3\omega t$$

....(2.3)

The third and fourth terms represent the second and third harmonics of the input signal, respectively. Harmonics are normally filtered out. However they do represent a waste of power and reduce the magnitude of the desired amplified signal. Intermodulation distortion products cannot be filtered and cause a further waste of power and adjacent channel interference.

2.1.2 AM-PM Distortion

AM-PM distortion is caused by nonconstant phase delay, that is, the phase shift introduced by an amplifier is a function of the instantaneous input signal level. Fig. 2.3 shows typical phase characteristics of class AB and class B amplifiers. The phase shift is not constant with the input power. This causes amplitude-to-phase (AM-PM) conversion. This in turn results in the generation of the harmonics and intermodulation distortion products. AM-PM distortion can severely degrade the performance of a modulation scheme that encodes the information in the phase of a RF signal, such as quadrature phase shift keying (QPSK).

2.2 Criteria for Evaluation of Amplifier Nonlinearity

2.2.1 Intermodulation Products

Intermodulation distortion is evaluated by using two or more tones as the input signal. Let the voltage transfer function of a quasi-linear amplifier be represented by

$$v_o(x) = c_1x + c_2x^2 + c_3x^3$$

....(2.4)

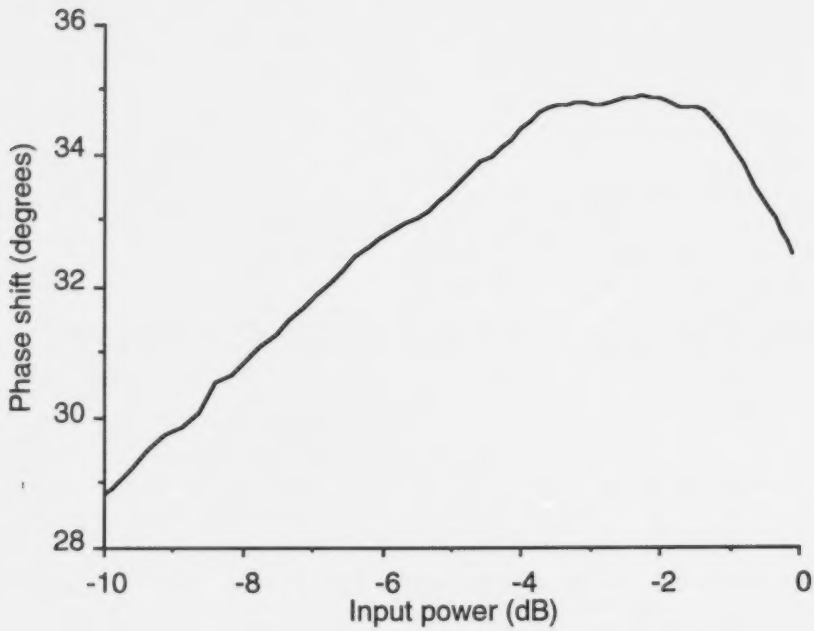

(a)

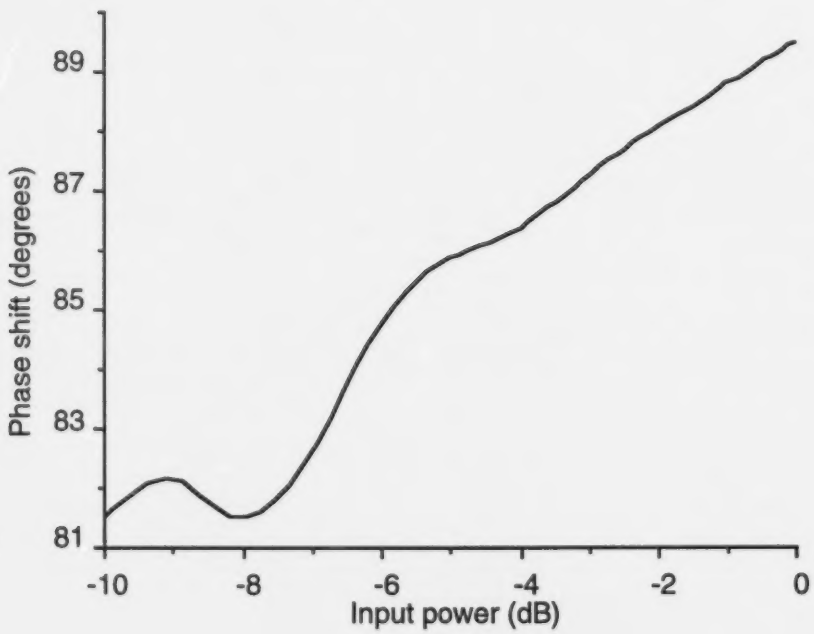

(b)

Fig. 2.3 (a) Phase characteristic of class AB amplifier
(b) Phase characteristic of class B amplifier

where x is the input voltage, and the coefficients, c_1, c_2 and c_3 are determined by the amplifier characteristics and its operating conditions.

If a three-tone input is assumed, then

$$x = A_1 \cos \omega_1 t + A_2 \cos \omega_2 t + A_3 \cos \omega_3 t$$

....(2.5)

and the output is

$$\begin{aligned} v_o(x) = {} & c_1\left(A_1 \cos \omega_1 t + A_2 \cos \omega_2 t + A_3 \cos \omega_3 t\right) \\ & + c_2\left(A_1 \cos \omega_1 t + A_2 \cos \omega_2 t + A_3 \cos \omega_3 t\right)^2 \\ & + c_3\left({A_1}^3 \cos^3 \omega_1 t + {A_2}^3 \cos^3 \omega_2 t + {A_3}^3 \cos^3 \omega_3 t\right) \\ & + c_3 \begin{pmatrix} 3{A_1}^2 A_2 \cos^2 \omega_1 t \cos \omega_2 t + 3A_1 {A_2}^2 \cos \omega_1 t \cos^2 \omega_2 t + \\ 3{A_1}^2 A_3 \cos^2 \omega_1 t \cos \omega_3 t + 3A_1 {A_3}^2 \cos \omega_1 t \cos^2 \omega_3 t + \\ 3{A_2}^2 A_3 \cos^2 \omega_2 t \cos \omega_3 t + 3A_2 {A_3}^2 \cos \omega_2 t \cos^2 \omega_3 t \end{pmatrix} \\ & + c_3\left(6A_1 A_2 A_3 \cos \omega_1 t \cos \omega_2 t \cos \omega_3 t\right) \end{aligned}$$

....(2.6)

Generally for a narrow band signal, the carrier frequency is much larger than the amplifier bandwidth, so that harmonics of the signal can be filtered out. The odd power terms, however, generate in-band spurious signals. Eq. 2.6 can be simplified using the following trigonometric identities:

$$\cos^2 A \cos B = \frac{1}{4}\left[2\cos B + \cos(2A - B) + \cos(2A + B)\right]$$

....(2.7)

$$\cos A \cos B \cos C = \frac{1}{4}\begin{bmatrix} \cos(A+B-C)+\cos(A-B-C)+ \\ \cos(A-B+C)+\cos(A+B+C) \end{bmatrix}$$

....(2.8)

The terms of the type (2A-B) and (A+B-C) fall into the frequency band of the required signal. Taking only these terms, the output of a nonlinear amplifier is given by Eq. 2.9. The fourth and fifth terms on the right hand side of Eq. 2.9, give the third-order intermodulation products.

$$y = \left[c_1 A_1 + \frac{3}{2} c_3 \left(A_1 {A_2}^2 + A_1 {A_3}^2 \right) + \frac{3}{4} c_3 {A_1}^3 \right] \cos \omega_1 t$$

$$+ \left[c_1 A_2 + \frac{3}{2} c_3 \left({A_1}^2 A_2 + A_2 {A_3}^2 \right) + \frac{3}{4} c_3 {A_2}^3 \right] \cos \omega_2 t$$

$$+ \left[c_1 A_3 + \frac{3}{2} c_3 \left({A_1}^2 A_3 + {A_2}^2 A_3 \right) + \frac{3}{4} c_3 {A_3}^3 \right] \cos \omega_3 t$$

Intermodulation Products

$$+ \frac{3}{4} c_3 \begin{bmatrix} {A_1}^2 A_2 \cos(2\omega_1 t - \omega_2 t) + A_1 {A_2}^2 \cos(2\omega_2 t - \omega_1 t) \\ {A_1}^2 A_3 \cos(2\omega_1 t - \omega_3 t) + A_1 {A_3}^2 \cos(2\omega_3 t - \omega_1 t) \\ {A_2}^2 A_3 \cos(2\omega_2 t - \omega_3 t) + A_2 {A_3}^2 \cos(2\omega_3 t - \omega_2 t) \end{bmatrix}$$

$$+ \frac{3}{2} c_3 A_1 A_2 A_3 \begin{bmatrix} \cos(\omega_1 t + \omega_2 t - \omega_3 t) + \cos(-\omega_1 t + \omega_2 t + \omega_3 t) + \\ \cos(\omega_1 t - \omega_2 t + \omega_3 t) \end{bmatrix}$$

....(2.9)

The intermodulation distortion products can be used as a parameter for specifying the distortion of an amplifier. An intermodulation distortion product may be expressed as the power in decibels below the amplifier's peak power or

below that of one of the tones employed to produce the test signal. The test signal may consist of two equal level tones, say at frequencies f_1 and f_2. The frequency difference (f_2 - f_1) is generally small as compared to the individual frequencies f_1 and f_2.

The third-order intermodulation product, IM_3, is defined as the ratio of the output power at a third-order product frequency, $2f_2 - f_1$ or $2f_1 - f_2$, to the output power at one of the input tones:

$$IM_3(dB) = 10\log\left[\frac{P_3}{P_{1,2}}\right]$$

....(2.10)

where P_3 = Power at a third-order product frequency, $2f_2 - f_1$ or $2f_1 - f_2$, and

$P_{1,2}$= Power at f_1 or f_2

Similarly, the fifth-order intermodulation product is defined as

$$IM_5(dB) = 10\log\left[\frac{P_5}{P_{1,2}}\right]$$

....(2.11)

where P_5 = Power at a fifth-order product frequency $3f_2 - 2f_1$ or $3f_1 - 2f_2$.

Fig. 2.4 shows a frequency spectrum of the output of a nonlinear amplifier for a two-tone input signal.

2.2.2 Out-of-Band Power Emission

Spectral spreading is another measure of amplifier nonlinearity. When a band-limited signal is applied to an amplifier, the amplifier nonlinearity results in an output power spectrum that is wider than the frequency band of the original signal. The proposed bandwidth of the North American digital cellular channel is 30 kHz. The IS-54 standard [2] specifies that the maximum power transmitted in the adjacent channel (centered 30 kHz away) be 26 dB below the mean output

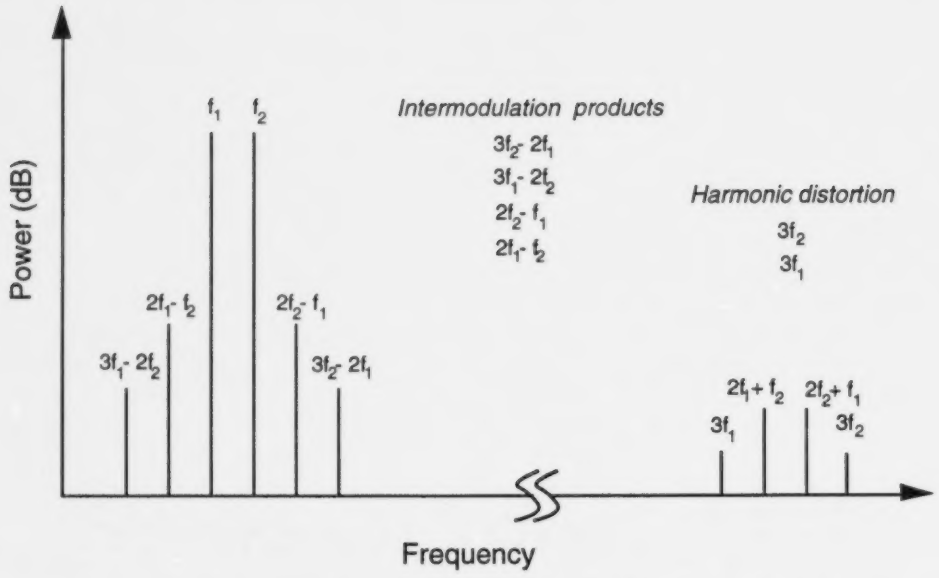

Fig. 2.4 Intermodulation products and harmonic distortion spectrum for two-tone input signal

power in the main channel. The allowed power emission is -45 dB in the next 30 kHz channel. The total power emitted in the channel 90 kHz away from the main channel should be below -60 dB.

2.3 RF Amplifier Linearization Techniques

Nonlinear amplification of linearly modulated signals causes spectral spreading, thereby losing the advantage of using spectrally efficient linear modulation techniques. Therefore, a linear RF power amplifier is essential for amplification of linearly modulated signals. A simple method to achieve linear amplification is to operate in the linear region well below the saturation region. This technique is known as the back-off technique [4], since the amplifier is not used at its full rated power output. The advantages of this technique are :

- It does not require any additional circuitry.

- It can be used for amplification of wideband signals. The signal bandwidth is restricted only by the frequency response of the amplifier.

However, backing-off results in the need for an amplifier with a higher power rating and in a reduction of the amplifier's DC-to-RF conversion efficiency. The power efficiency of an amplifier is a very important factor, especially for mobile communication equipment that may need to be operated from a battery. A major challenge, therefore, in RF power amplifier design is to maintain linearity without compromising the power efficiency. A number of RF power amplifier linearization techniques have been investigated over the past several years. The following sections describe the linearization techniques that are suitable for digital mobile radio systems.

2.3.1 LINC

LINC [5-7], Linear Amplification using Nonlinear Components, is a method for producing linear amplification using nonlinear amplifiers. A block diagram for a LINC transmitter is shown in Fig. 2.5. The LINC technique exploits the fact that a bandpass signal, $s(t)$, can be split into two constant envelope phase modulated components, $s_1(t)$ and $s_2(t)$:

$$s(t) = A(t)\cos[\omega_c t + \phi(t)] \quad \text{....(2.12)}$$

$$s_1(t) = C\cos[\omega_c t + \phi(t) + \beta(t)] \quad \text{....(2.13)}$$

$$s_2(t) = C\cos[\omega_c t + \phi(t) - \beta(t)] \quad \text{....(2.14)}$$

where $2s(t) = s_1(t) + s_2(t)$ and $\beta(t) = \cos^{-1}\left[\frac{A(t)}{C}\right]$

Note that $s_1(t)$ and $s_2(t)$ are constant amplitude vectors rotating in opposite directions with an increasing value of $\beta(t)$. These phase modulated constant amplitude signals can be amplified separately with nonlinear amplifiers. The amplified signals are then passively combined to produce an amplified replica of the original input signal.

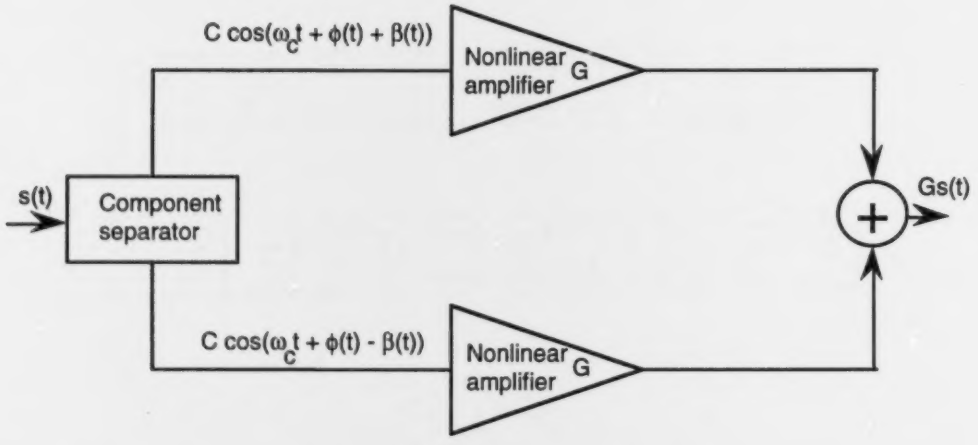

Fig. 2.5 LINC transmitter

The LINC technique can provide, in principle, linear amplification using two power-efficient nonlinear amplifiers. However, the characteristics of the two RF amplifiers must be well-matched for cancellation of the unwanted distortion products at the output. Also, this system is sensitive to the phase and gain imbalances between two RF paths [8]. It is not easy to generate the constant amplitude phase modulated signals accurately using analog techniques. However, digital processing techniques have made component separation significantly easier. Another drawback of this technique is that it cannot adapt to changes in the characteristics of the amplifiers.

2.3.2 Feedforward Technique

Fig. 2.6 shows a block diagram of a feedforward correction circuit. It consists of a main amplifier whose distortion is to be reduced, an auxiliary amplifier, an attenuator, and two delay elements. The power handling capacity of the auxiliary amplifier is normally much less than that of the main amplifier [9]. A part of the main amplifier output is fed to the attenuator, where it is compared with a delayed version of the original input signal. If the main amplifier has no distortion, then these signals will be identical and the signal to the auxiliary amplifier will be zero, due to signal cancellation. Any distortion in the main amplifier, however, generates an error signal. This error signal is amplified using the auxiliary amplifier and subtracted from the delayed main amplifier output to cancel the distortion products. This cancellation requires the signal components to have appropriate phases and amplitudes. Gain changes in the main and auxiliary amplifiers will affect the first and second cancellation, respectively.

The feedforward configuration is an open loop configuration. It cannot

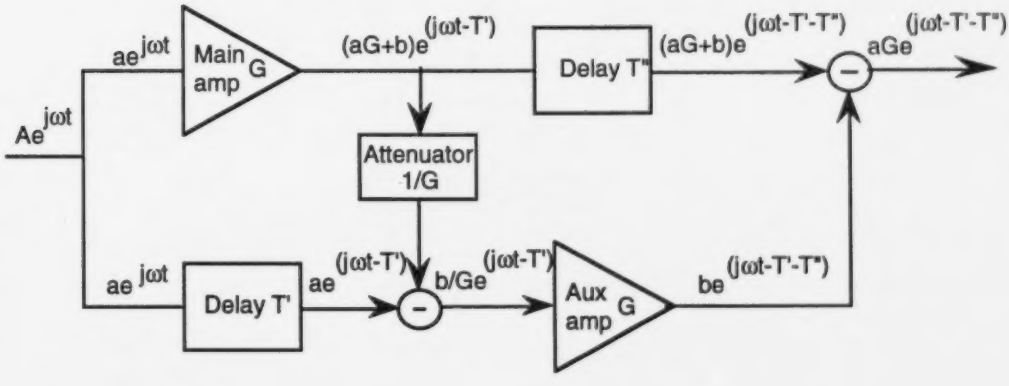

Fig. 2.6 Feedforward linearization technique

compensate for drifts in the auxiliary amplifier characteristics. The auxiliary amplifier must have linear characteristics. This method primarily reduces the third-order intermodulation products.

2.3.3 CALLUM

The CALLUM (Combined Analog Locked Loop Universal Modulator) [10] technique is similar to the LINC technique. There are two nonlinear amplifiers which amplify constant amplitude phase modulated signals. However, CALLUM has a feedback loop to control the amplifier matching. The feedback loop incorporates the component separation, up-conversion, amplification, and the final summation at the output. This method uses two voltage controlled oscillators (VCOs) for frequency translation and component separation, as shown in Fig. 2.7. Unlike a conventional modulator system, the channel frequency is set by the local oscillator in the demodulator. Since the output of a

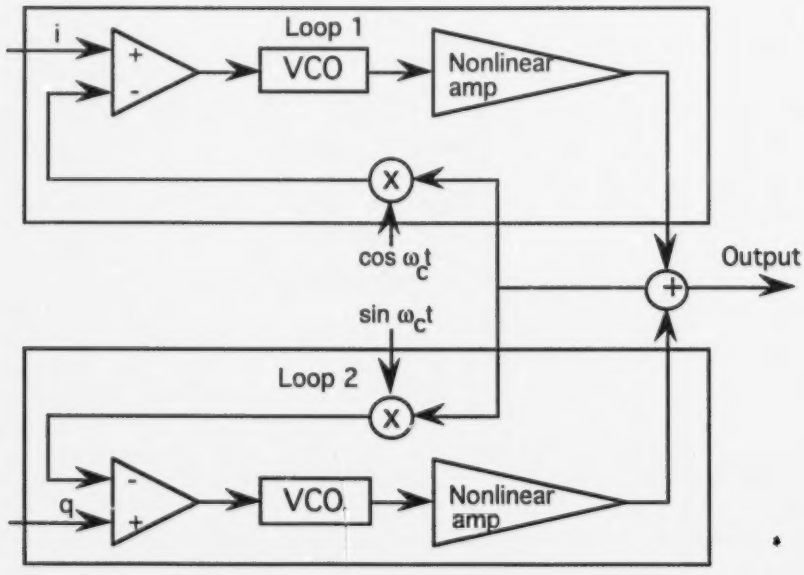

Fig. 2.7 CALLUM

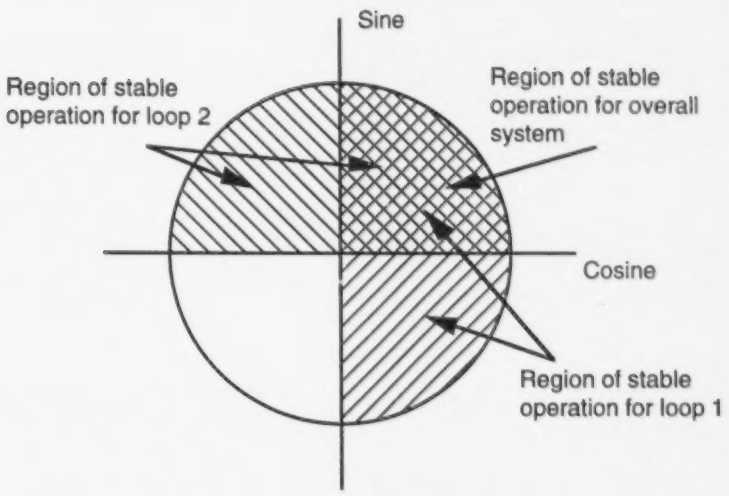

Fig. 2.8 Region of stable operation for CALLUM

VCO is inherently a constant amplitude signal, therefore, a nonlinear amplifier can be used for amplification. An error signal is generated from the difference between the input component and the demodulated output of the summation port. Assuming the demodulation process to be perfect, and the loop gain to be infinite, the error signal would go to zero. In other words, the summation port output would be a scaled replica of the original input signal.

Stability is a major limitation of this technique. The modulator is a combination of two phase locked loops. A phase locked loop has stable operation as long as the phase of the input signal is within $\pm 90^0$ of the local oscillator phase. This limits the operation of CALLUM to the first quadrant (see Fig. 2.8). For stable operation in all the quadrants, a modulation format dependent switching matrix must be put in the feedback path. This makes the control circuitry complicated and modulation format dependent. Another limitation of the CALLUM modulator is the restriction on the loop gain and bandwidth.

2.3.4 Cartesian Coordinate Negative Feedback

The cartesian coordinate negative feedback system [11-16] operates in the same way as a simple feedback loop. Part of the amplifier output is synchronously demodulated into its quadrature components, i' and q'. The demodulated components are subtracted from the i and q input drive signals to produce loop error signals which, after suitable filtering, are used to drive the quadrature modulator and the power amplifier. A block diagram of the system is shown in Fig. 2.9. If the loop gain is sufficiently high, the distortion caused by the amplifier will be reduced. The cartesian feedback system is a closed loop configuration, and may, therefore, be unstable. The loop stability is dependent upon the phase shift introduced by the amplifier and the feedback path, and on the loop gain. The higher the loop gain, the more critical is the phase requirement. Therefore, a phase adjustment circuitry may be required to avoid oscillations in the feedback loop.

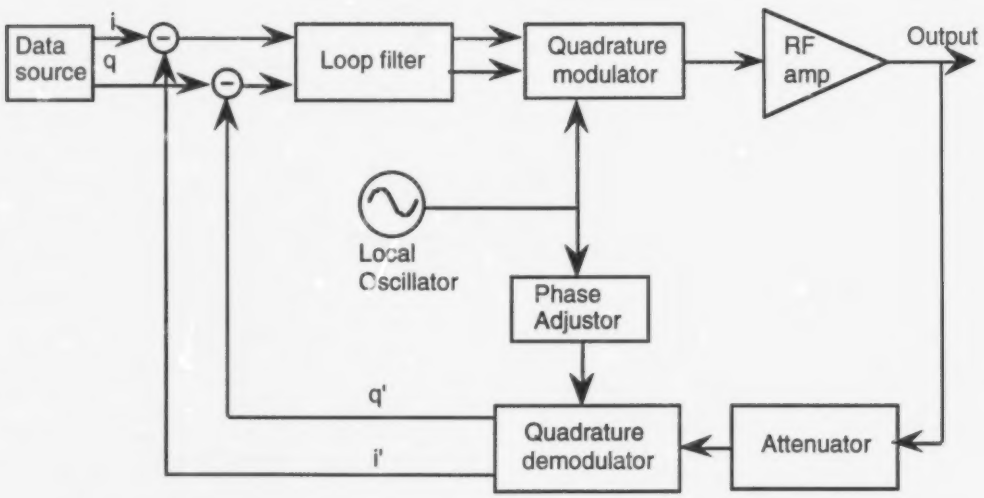

Fig. 2.9 Cartesian coordinate negative feedback system

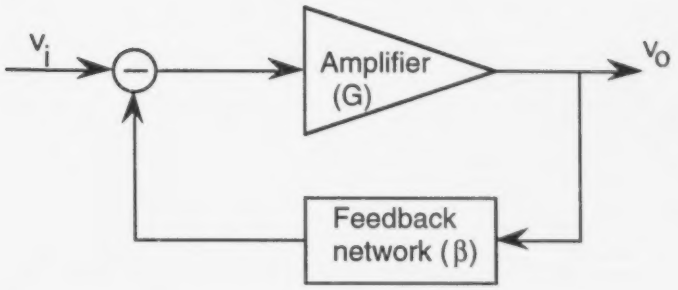

Fig. 2.10 Feedback amplifier

Fig. 2.10 shows a basic negative feedback amplifier. The reduction in the distortion, d_A, introduced by the amplifier can be estimated using feedback theory. If the amplifier voltage gain is G, the open loop output voltage is

$$v_o = Gv_i + d_A \qquad \text{....(2.15)}$$

If the feedback transfer function is β, then the closed loop output voltage (for $G\beta >> 1$) is

$$v_o = \frac{v_i}{\beta} + \frac{d_A}{G\beta} - d_F \qquad \text{....(2.16)}$$

where d_F is the distortion in the feedback loop.

Eq. 2.16 indicates that the use of feedback cannot correct for the distortion introduced in the feedback path, whereas the distortion in the forward path is reduced by a factor equal to the loop gain. Therefore, it is important to use highly linear and low noise components in the feedback path.

The main advantage of the cartesian coordinate negative feedback system is that it is simple to implement. It continuously corrects for any nonlinearity in the forward path, and can also compensate for the drifts in the characteristics of the amplifier. However, the phase delay in the feedback

depends on the carrier frequency, and may require a phase adjustment when the carrier frequency is changed.

2.4 Predistortion Techniques

Predistortion techniques [17-28] operate on the principle of providing an appropriately predistorted signal to an amplifier so that the output of the amplifier is a scaled replica of the original input signal. Predistortion linearization techniques can be characterized into three categories. The first uses analog predistortion. In this method, the low level modulated signal is passed through a network of active and passive components to compensate for the amplifier nonlinearity. Diodes may be used to provide the nonlinear compensation. The characteristics of active components can drift, and it can be difficult to compensate for these drifts. The second type uses fixed baseband predistortion. The signal constellation points are predistorted so that they are present at their correct constellation positions after nonlinear amplification. This type of linearizer cannot compensate for changes in the characteristics of the amplifier. The third type of predistortion linearizers uses look-up tables to predistort the baseband input signals. Fig. 2.11 shows the schematic diagram of a typical predistorter. The amplifier output is sampled by a directional coupler and demodulated using the same local oscillator that is used for the modulator. This eliminates need for carrier recovery. The demodulated output is compared with the baseband input to characterize the gain and phase distortion of the amplifier. There are various different methods for predistorting the input signal, and updating the look-up table. Y. Nagata [17] proposed a linearizer that uses a two dimensional look-up table for storing predistortion coefficients for all the

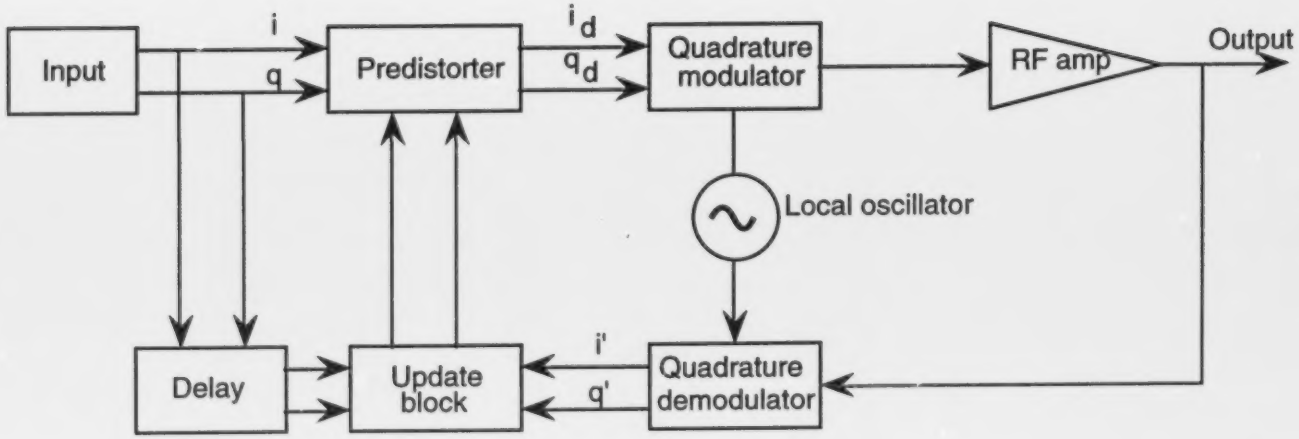

Figure 2.11 Adaptive predistorter

complex signal points of the modulating signal trajectory. This requires a large look-up table.

The complex gain predistortion technique was proposed by J. Cavers [28]. This method takes advantage of the amplitude dependence of the amplifier distortion to reduce the look-up table size, and to decrease the time for updating the look-up table. This technique is discussed in detail in the following section.

2.4.1 Complex Gain Predistortion

RF power amplifier distortion is characterized by the AM-AM and AM-PM characteristics of the amplifier. Both distortion mechanisms are dependent on the magnitude of the input signal and are independent of the phase of the input signal. Therefore, the gain of an RF amplifier can be represented by a complex number, $G(|v_d|^2)$, where $|v_d|^2$ denotes the squared magnitude of the input signal. Since the complex gain depends only on the amplitude of the input signal, a one dimensional look-up table can be used to characterize the required predistortion characteristic. The square of the instantaneous magnitude of the input signal, $|v_m|^2$, is used as an index to the look-up table. The input signal, v_m, is multiplied by the appropriate value from the look-up table, in order to generate the predistorted signal, v_d. A block diagram of the complex gain predistorter is shown in Fig. 2.12. The predistorted signal is upconverted and amplified. A part of the amplifier output is synchronously demodulated. The demodulated output is compared with the input signal and used for updating the look-up table.

The output of the amplifier is given by

$$v_a = v_d G\left(|v_d|^2\right) \qquad \text{....(2.17)}$$

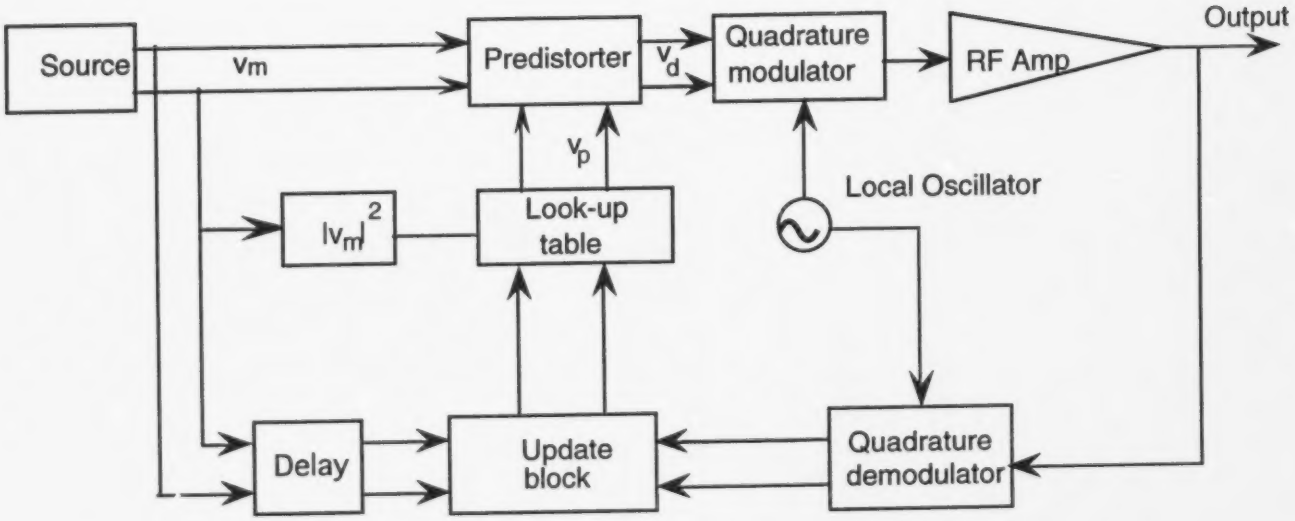

Fig. 2.12 Complex gain predistorter

Also,

$$v_d = v_m F\left(|v_m|^2\right)$$

....(2.18)

where F is the transfer characteristic of the predistorter. Using Eq. 2.18, v_a can be rewritten as:

$$v_a = v_m F\left(|v_m|^2\right) G\left(|v_m|^2 \left| F\left(|v_m|^2\right)\right|^2\right)$$

....(2.19)

If K is the value of the desired gain of the amplifier, the following relation must be satisfied in order to achieve an overall linear response of the system.

$$v_a = K v_m = v_m F\left(|v_m|^2\right) G\left(|v_m|^2 \left| F\left(|v_m|^2\right)\right|^2\right)$$

....(2.20)

If $|v_m|^2 = x_m$, then

$$K = F(x_m) G\left(x_m |F(x_m)|^2\right)$$

....(2.21)

The value of the predistortion function, $F(x_m)$, is a root of the following equation:

$$e_g\left(F(x_m)\right) = v_a\left(F(x_m)\right) - K v_m$$

....(2.22)

The secant algorithm [29] is used to solve this equation. The method has a reasonable convergence speed.

The main advantage of the complex gain predistorter is the low memory requirement. Because of the small look-up table size, the update time for the

look-up table is also small. This system has essentially an open loop configuration (the feedback loop is closed only for the look-up table update), therefore, it is unconditionally stable. A major drawback of the technique is that convergence of the secant method is sensitive to the initial conditions [30,31]. An incorrect choice for the initial conditions can prevent convergence of the algorithm.

2.5 Proposed Linearization Technique

The proposed method is a predistortion linearization technique, in which the input signal is appropriately predistorted in order to compensate for the amplifier nonlinearity. The AM-AM and AM-PM characteristics of the amplifier are estimated, using cubic spline interpolation, from a look-up table of distortion values that are obtained directly from the amplifier itself using synchronous demodulation. These measured characteristics are then used to calculate the predistortion coefficients, which are then stored in a look-up table. Since the amplifier distortion is dependent only on the magnitude of the input signal, a one dimensional look-up table is sufficient. The magnitude of the input signal acts as a pointer to the look-up table.

A block diagram of a transmitter with the proposed linearizer is shown in Fig. 2.13. The signal source bits are encoded into in-phase (i_k) and quadrature-phase (q_k) components. The i_k and q_k components pass through pulse shaping filters. The square of the magnitude of the resulting complex signal, $|v_m|^2$, is an index to the look-up table that contains predistortion coefficients for the magnitude and phase of the signal. The predistorted signals, i_d and q_d, are converted into two analog signals by a pair of D/A converters, which are

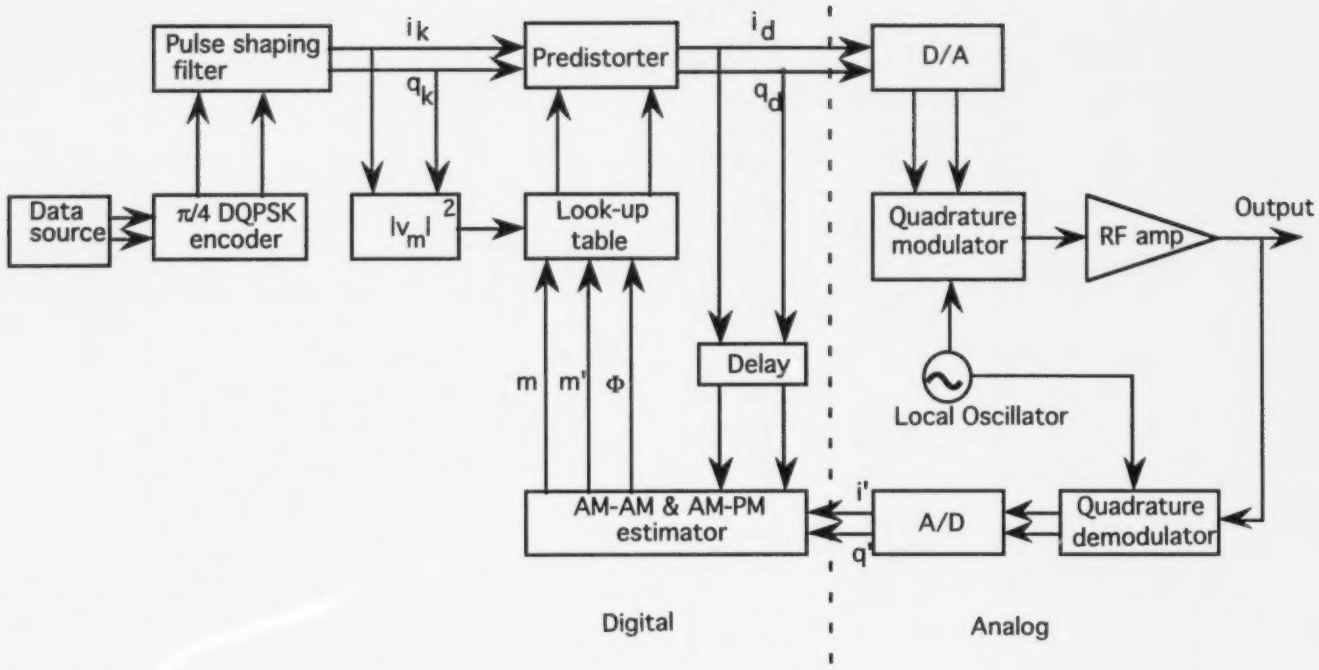

Fig. 2.13 Transmitter with proposed linearizer

then used to drive the quadrature modulator that generates the RF signal. The input to the amplifier can be written as:

$$x(t) = i_d \cos \omega_c t + q_d \sin \omega_c t$$

$$= \left(i_d{}^2 + q_d{}^2\right)^{1/2} \cos\left(\omega_c t - \phi_d\right)$$

....(2.23)

where $\phi_d = tan^{-1}\left(\frac{q_d}{i_d}\right)$

ω_c = carrier frequency

A portion of the amplifier output is synchronously demodulated in order to obtain a sample of the i and q components of the transmitted signal. These outputs (i', q') are compared with the inputs to the quadrature modulator, i_d and q_d, in order to estimate the AM-AM and AM-PM characteristics of the amplifier.

The magnitude of the input signal of the amplifier can be written as:

$$m = \left(i_d{}^2 + q_d{}^2\right)^{1/2}$$

....(2.24)

The magnitude and phase of the demodulated signal are given by:

$$m' = \left(i'^2 + q'^2\right)^{1/2}$$

....(2.25)

$$\phi' = tan^{-1}\left(\frac{q'}{i'}\right)$$

....(2.26)

$\Phi = \phi' - \phi_d$, is the phase distortion introduced by the amplifier.

For a small number of the values of m, taken over the entire input magnitude range, the corresponding values of m' and Φ are stored in

memory. Since there is a delay in the feedback path, the input signals, i_d and q_d, must be delayed by the same amount, so that the i' and q' samples correspond properly to the samples of i_d and q_d.

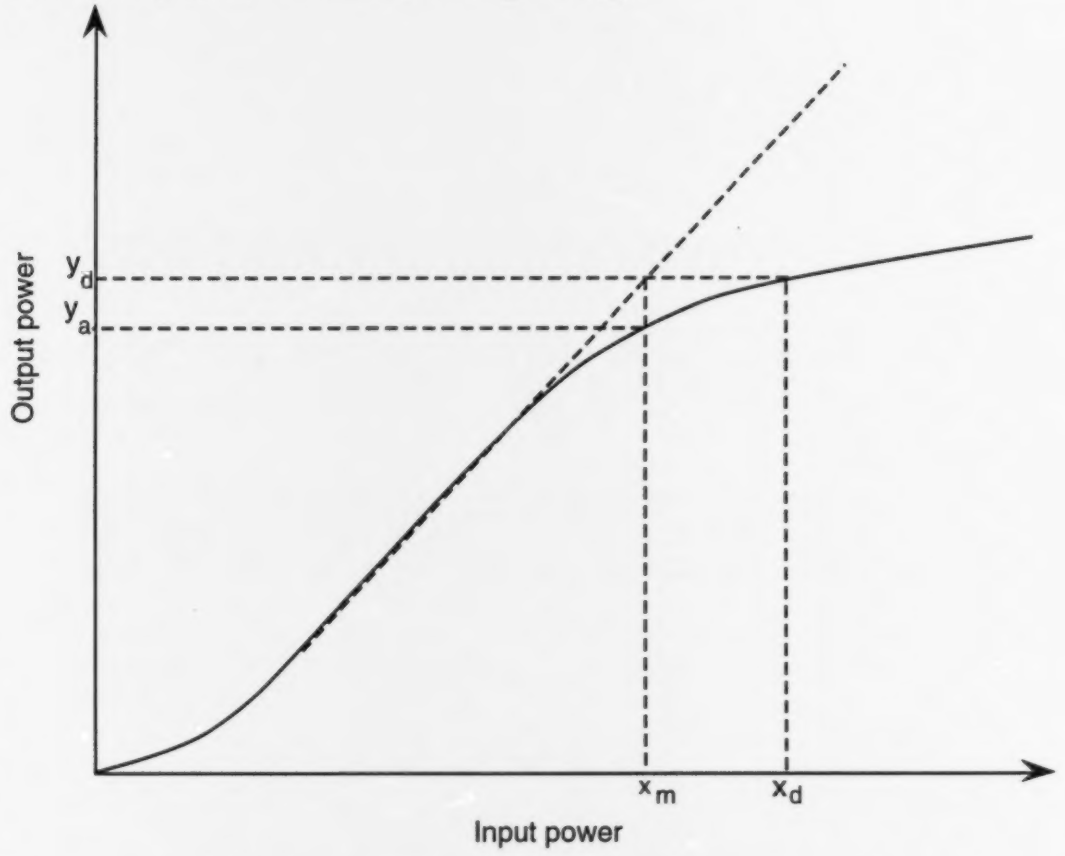

Fig. 2.14 Power transfer characteristic of an amplifier

For computing the predistortion coefficient for a given input power level, x_m, the desired output power level, y_d, is known from the required linear characteristic. If the input signal, x_m, is fed to the amplifier without predistortion, the output would be y_a, which does not lie on the linear characteristic, as shown in Fig. 2.14. To obtain the desired output power, y_d, the input to the amplifier should be x_d. For the corrected value, x_d, of the magnitude of the signal, the

corresponding phase distortion (Φ_d) can be read from the AM-PM characteristics, as shown in Fig. 2.15.

Cubic spline interpolation [29] is used to estimate the AM-AM and AM-PM characteristics for any particular $|v_m|^2$ value using the values stored in the look-up table. Cubic spline interpolation uses a third order polynomial for interpolation between two adjacent sample points (see Appendix A).

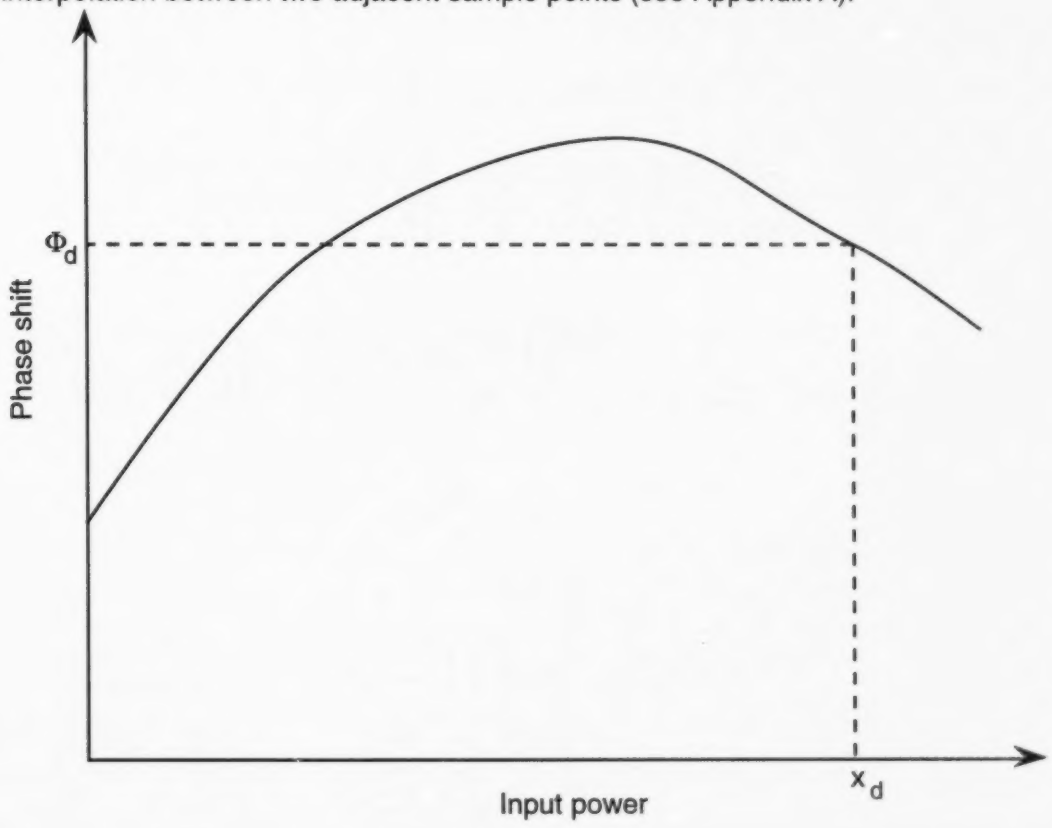

Fig. 2.15 Phase distortion characteristic of an amplifier

The feedback loop is closed only for determining the AM-AM and AM-PM characteristics of the amplifier. Unlike the complex gain predistortion method, this method does not use a recursive algorithm for computation of the predistortion coefficients. Therefore, convergence of the algorithm is not

dependent on the initial conditions. The proposed linearization technique is not restricted by the modulation format because the signal is predistorted after the pulse shaping. The linearizer is suitable for baseband implementation using a digital signal processor.

The linearizer assumes the distortion to be dependent only on the magnitude of the input signal. However, phase-dependent distortion can occur due to imperfections in the quadrature modulator. The quadrature demodulator in the feedback path can also have impairments. These impairments are discussed in the following section.

2.6 Analog Quadrature Modulator and Demodulator Impairments

A quadrature modulator is an essential block for generating the amplitude- and phase- modulated RF signals. Fig. 2.16 shows a block diagram for an ideal quadrature modulator. The i and q components are applied to double balanced mixers fed by cosine and sine references, respectively. If the i and q components are of equal amplitude and have a 90^0 phase difference, the output of an ideal quadrature modulator will be a single sideband signal. However, phase and gain imperfections in the mixers result in unbalanced transmission through two RF paths of the modulator. When the unbalanced components are summed at the output combiner, imperfect cancellation occurs in the undesired sideband. A rigorous analysis of the modulator errors is tedious [32]. The combined effect of the imperfections can be represented by gain imbalance, phase imbalance and carrier feedthrough or dc offset [33-37].

The gain imbalance is the ratio of the gains of the i and q channels, caused by the mixers, filters and D/A converters. The effects of the gain imbalance on a sinusoidal input (cosine wave as i component and sine wave

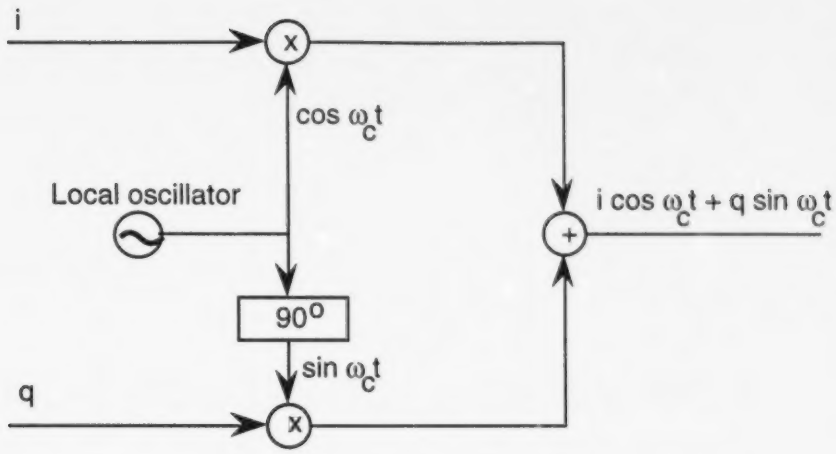

Fig. 2.16 Ideal quadrature modulator

as q component) is illustrated in Fig. 2.17. The phase vector travels on an ellipse instead of a circle.

Phase imbalance can occur due to two possible sources of error. Firstly, the phase difference between the local oscillator signals that multiply the i and q components may not be exactly 90^0. This error is independent of the input signal. Secondly, any difference in the lengths of the RF signal paths will cause

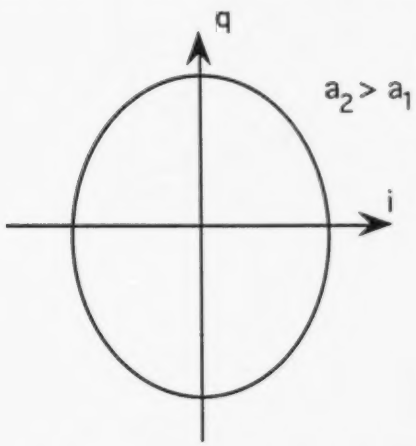

Fig. 2.17 Effect of gain imbalance for a sinusoidal input

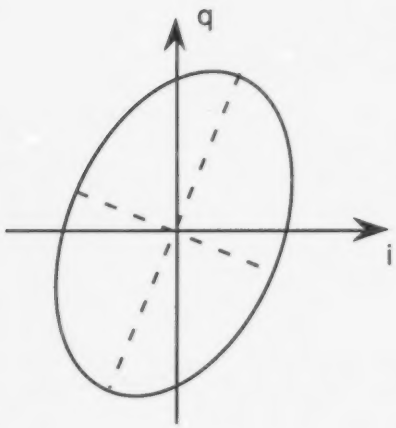

Fig. 2.18 Effect of phase imbalance for a sinusoidal input

a phase error, which will, in general, be frequency dependent. However, this error is not significant in the monolithic modulators. Fig. 2.18 illustrates the effect of the phase imbalance on a sinusoidal signal. The phase vector lies on a rotated ellipse whose axes are not aligned with the i and q channels.

The third type of modulator error, dc-offset, is caused by carrier leakage in the mixer. The local oscillator signal leaks through into the RF port, which causes dc-offset. The D/A converters and filters also cause dc-offset. Fig. 2.19 illustrates the effect of dc-offset on a sinusoidal input signal.

Fig. 2.20 shows a block diagram of an ideal quadrature demodulator. A quadrature demodulator recovers baseband i and q components from the RF signal. Quadrature demodulators contain power splitters, mixers, filters, A/D converters and 90^0 phase splitters. These components also have imperfections. As in the case of the modulator, the effects of the imperfections of these components can be represented by gain imbalance, phase imbalance and dc-offset. The gain imbalance can occur due to mixers, filters and A/D converters.

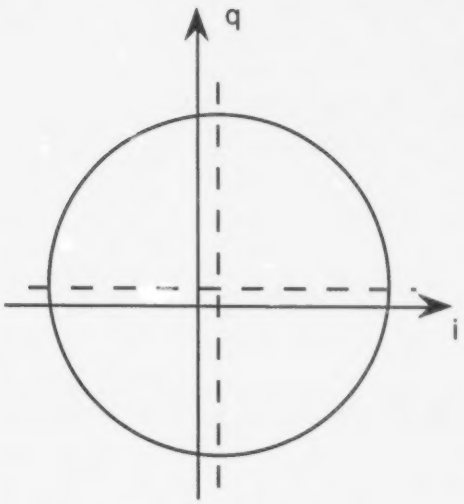

Fig. 2.19 Effect of dc-offset for a sinusoidal input

The phase shifter at the local oscillator may not produce an exact 90^0 phase shift and the length of the RF signal paths may be different, both of these can cause phase imbalance. The leakage in the mixer causes self mixing of the

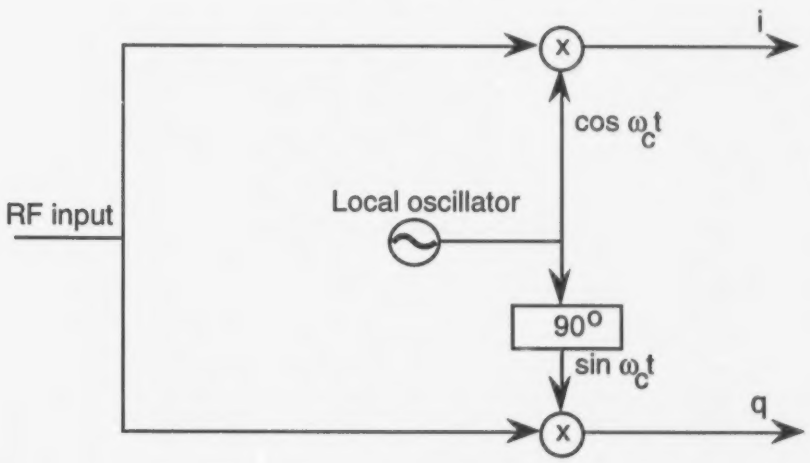

Fig. 2.20 Ideal quadrature demodulator

local oscillator signals, resulting in dc-offsets in both the i and q channels. The effects of these impairments on a demodulated signal, are similar to the effects of the modulator impairments.

2.7 Effects of the Modulator Impairments on a Transmitted Signal

The gain and phase imbalances in the i and q channels cause imperfect cancellation of the signals in the undesired sideband. This generates spurious frequency components in the undesired sideband, which can interact with the amplifier nonlinearity to generate intermodulation distortion products, thereby, degrading the performance of a transmission system.

2.7.1 Spurious Signals

Fig. 2.21 shows the frequency spectrum of the output signal of an analog quadrature modulator when the input to the modulator is a complex tone of frequency, f_m. The output spectrum consists of a tone at the desired frequency $f_c + f_m$, a spurious tone at the channel centre, that is at the RF carrier frequency, f_c, and a second spurious tone at $f_c - f_m$. The spurious tone at $-f_m$ is due to the gain and phase imbalances, and the tone at the carrier frequency is caused by the carrier leakage in the modulator. It is important to keep these spurious signals at the lowest possible level.

2.7.2 Intermodulation Products

The quadrature modulator distortion can interact with the power amplifier nonlinearity to produce intermodulation products. Consider a two-tone input (f_1, f_2) to the modulator followed by a nonlinear power amplifier. If the modulator is perfect, then the output of the modulator would be a two-tone signal. For this

case, the intermodulation products generated due to nonlinear amplification will be combinations of frequencies f_1 and f_2. However, if the modulator is not perfect, there would be additional tones at the frequencies $-f_1$ and $-f_2$ away from the channel centre, as discussed above. With an imperfect modulator, therefore, there will be five tones interacting to produce the intermodulation products. This causes additional amplitude and phase distortion at the amplifier output.

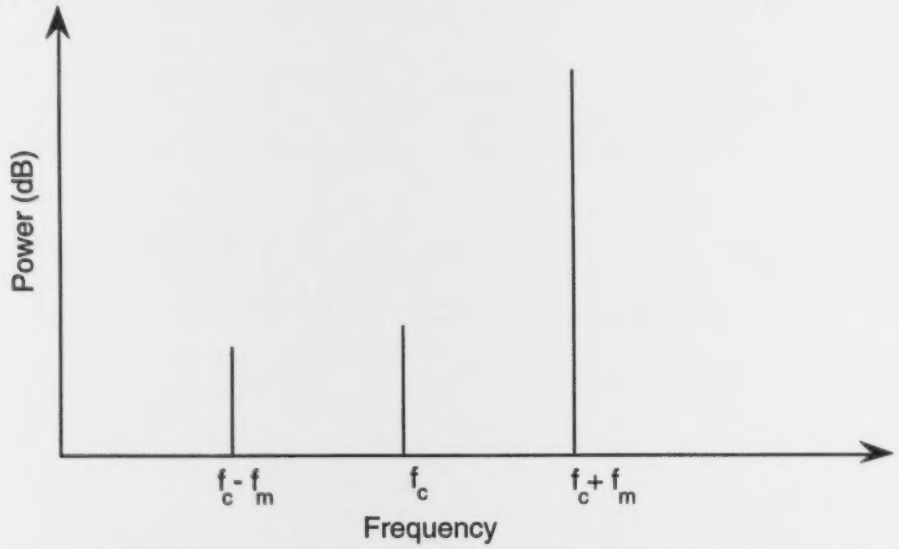

Fig. 2.21 Spectrum of modulator output for single tone input

2.8 Proposed Method for Compensation of the Quadrature Modulator and Demodulator Impairments

The quadrature modulator and demodulator impairments can adversely affect the performance of a predistortion linearizer. The modulator impairments distort the signal constellation of the signal, which can introduce phase-dependent distortion in the transmitter. Any imperfection in the demodulator, since it is the feedback loop, cannot be compensated for by the overall

feedback loop. Therefore to obtain good overall amplifier linearization, it is essential to correct for the quadrature modulator and demodulator impairments.

2.8.1 Quadrature Modulator Impairment Compensator

A block diagram of the proposed compensator for the modulator impairments is shown in Fig. 2.22. A portion of the modulator output, $s(t)$, is fed to an envelope detector. The envelope detector output is digitized using a A/D converter. The digitized value, m, is stored in memory along with the corresponding values of quadrature inputs (i_d, q_d) to the modulator.

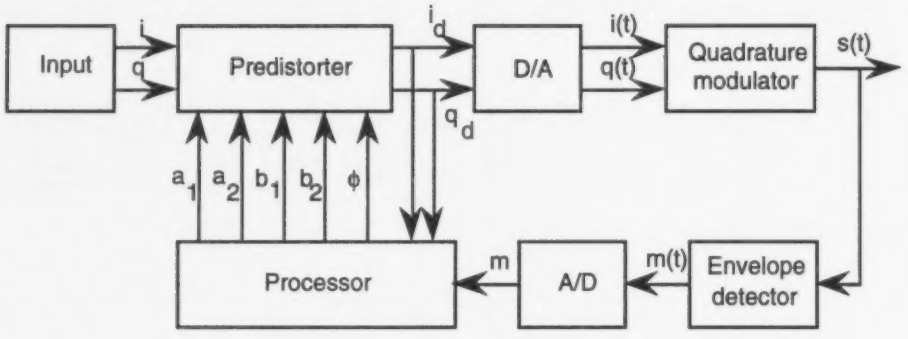

Fig. 2.22 Modulature impairment compensator

The output of an ideal quadrature modulator can be written as:

$$s(t) = i(t)\cos\omega_c t + q(t)\sin\omega_c t \qquad \text{....(2.27)}$$

where $i(t)$ and $q(t)$ are the in-phase and quadrature-phase inputs, respectively. However, a practical quadrature modulator has gain imbalance, phase imbalance and dc-offset. Therefore, the output of a practical quadrature modulator is given by:

$$s(t) = \left(a_1 i(t) + b_1\right)\cos\left(\omega_c t + \phi\right) + \left(a_2 q(t) + b_2\right)\sin\omega_c t$$

....(2.28)

where a_1 and a_2 are the gains in the i and q channels.

b_1 and b_2 are the dc-offsets for the i and q channels.

and ϕ is the phase imbalance.

The modulator output, $s(t)$, can be written as

$$s(t) = \left(a_1 i(t) + b_1\right)\cos\phi\cos\omega_c t + \begin{pmatrix}\left(a_1 i(t) + b_1\right)\sin(-\phi) + \\ \left(a_2 q(t) + b_2\right)\end{pmatrix}\sin\omega_c t$$

$$= m\cos\left(\omega_c t - \theta\right)$$

....(2.29)

where

$$m(t) = \left(\left(\left(a_1 i(t) + b_1\right)\cos\phi\right)^2 + \begin{pmatrix}\left(a_1 i(t) + b_1\right)\sin(-\phi) + \\ \left(a_2 q(t) + b_2\right)\end{pmatrix}^2\right)^{1/2}$$

....(2.30)

$$\theta(t) = \tan^{-1}\left(\frac{\left(a_1 i(t) + b_1\right)\sin(-\phi) + \left(a_2 q(t) + b_2\right)}{\left(a_1 i(t) + b_1\right)\cos\phi}\right)$$

....(2.31)

m is value of the envelope detector output. Five sets of values of m, i_d and q_d are stored in memory. Eq. 2.30 is solved for a_1, a_2, b_1, b_2 and ϕ using the Newton-Raphson method (see Appendix B). With values of a_1, a_2, b_1, b_2 and ϕ known, the i and q signals may be predistorted to counter the modulator imperfections. The predistorted values, i_d and q_d, are given by

$$i_d = \frac{1}{a_1}\left(\frac{i}{\cos\phi} - b_1\right) \quad \text{....(2.32)}$$

$$q_d = \frac{1}{a_2}\left(q - \left(b_2 + \left(a_1 i + b_1\right)\sin(-\phi)\right)\right) \quad \text{....(2.33)}$$

An advantage of this method is that it does not require test vectors. The predistortion coefficients can be calculated while the transmitter is in operation. The compensator does not require component or bias adjustments, and can be implemented using a digital signal processor.

2.8.2 Demodulator Impairment Compensator

The structure of the demodulator impairment compensator, as shown in Fig. 2.23, is similar to the modulator compensator. The input to the envelope detector is a fraction of the RF signal. The digitized envelope detector output, m, is stored in memory along with the corresponding demodulated values i' and q'.

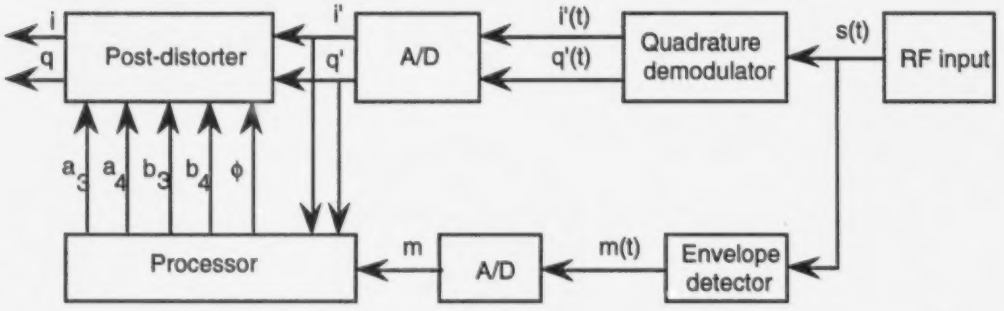

Fig. 2.23 Demodulator impairment compensator

Let the RF signal, $s(t)$ be

$$s(t) = i(t)\cos\omega_c t + q(t)\sin\omega_c t \qquad \text{....(2.34)}$$

Then the magnitude of $s(t)$ is given by:

$$m(t) = |s(t)| = \left(i^2(t) + q^2(t)\right)^{1/2} \qquad \text{....(2.35)}$$

The demodulated signals i' and q' are given by:

$$i'(t) = a_3\left(i(t)\cos\phi + q(t)\sin(-\phi)\right) + b_3 \quad \text{....(2.36)}$$

$$q'(t) = a_4 q(t) + b_4 \quad \text{....(2.37)}$$

where a_3 and a_4 are gains in the i and q channels.

b_3 and b_4 are dc-offsets in the i and q channels.

ϕ is the phase imbalance.

From Eqs. 2.36 and 2.37, i and q can be written as:

$$i = \frac{1}{\cos\phi}\left(\frac{(i'-b_3)}{a_3} + \frac{(q'-b_4)}{a_4}\sin\phi\right) \quad \text{....(2.38)}$$

$$q = \left(\frac{q'-b_4}{a_4}\right) \quad \text{....(2.39)}$$

Using Eqs. 2.38 and 2.39, m can be rewritten as:

$$m = \left(\left(\frac{1}{\cos\phi}\left(\frac{(i'-b_3)}{a_3} + \frac{(q'-b_4)}{a_4}\sin\phi\right)\right)^2 + \left(\frac{q'-b_4}{a_4}\right)^2\right)^{1/2} \quad \text{....(2.40)}$$

Five independent equations are generated using five sets of values of m, i' and q'. These equations are solved for a_3, a_4, b_3, b_4 and ϕ, using the Newton-Raphson method. The calculated values of a_3, a_4, b_3, b_4 and ϕ are then used to correct i' and q', to compensate for the demodulator impairments. The corrected values of i and q are given by:

$$i = \frac{1}{\cos\phi}\left(\frac{(i'-b_3)}{a_3} + \frac{(q'-b_4)}{a_4}\sin\phi\right) \quad \text{....(2.41)}$$

$$q = \left(\frac{q' - b_4}{a_4} \right) \qquad \text{....(2.42)}$$

The demodulator compensator can be implemented using a digital signal processor. It does not require any component adjustment to adapt for changes in the demodulator impairments. Simulation results of the performance of the proposed compensators and RF amplifier linearization methods are presented in chapter 4.

3. Computer Simulation Models

3.1 Simulation of Communication Systems

Computer simulation is a convenient and cost efficient method for modeling, analyzing and designing communication systems. In this project, computer simulations were used to evaluate the performance of amplifier linearization techniques and of modulator and demodulator impairment compensators. This chapter describes simulation models for the various systems used in the project.

Actual measurements of the performance of a hardware prototype are ultimately necessary for its evaluation. However, this approach is normally time consuming, and generally is not very flexible. Trade off studies which are important for the design can be performed easily by simulation.

3.2 BOSS

The Block Oriented System Simulator (BOSS), provided by Comdisco Systems, Inc. (Cupertino, CA), is a software package that allows the user to develop a communication system model using a block diagram representation of the various components. BOSS provides a modular structure approach in which each functional block is represented by a block diagram. Block diagrams of complex systems are constructed in hierarchical fashion from the bottom up. If a module cannot be constructed using the library modules, a new module can be created by entering a FORTRAN subroutine.

BOSS is written in LISP [38], and uses pop-up command menus, on-line help and a powerful post-processor to provide a friendly and visual simulation environment. Version 2.7 of BOSS was used on a SUN-SPARC workstation in this project.

3.3 Basic Transmitter Model

BOSS simulations use an equivalent low-pass complex-envelope representation of band pass signals rather than the true RF signal, in order to reduce the sampling rate and computing time. North American digital cellular systems currently have carrier frequencies in the 800-MHz frequency band. If the signal is sampled at the Nyquist rate (2 * 850 MHz), the sampling period is about 0.6 ns. Useful simulations with such a small sampling time would take a very long time to execute. Therefore, it is more practical to carry out simulations at the base band frequency.

Fig. 3.1 shows the BOSS model of a π/4-DQPSK transmitter. The transmitter consists of the following modules:

1. Random data generator
2. π/4-DQPSK modulator
3. Pulse shaping filter
4. Nonlinear power amplifier

3.3.1 Random Data Generator

A random binary data generator is used to simulate the binary data

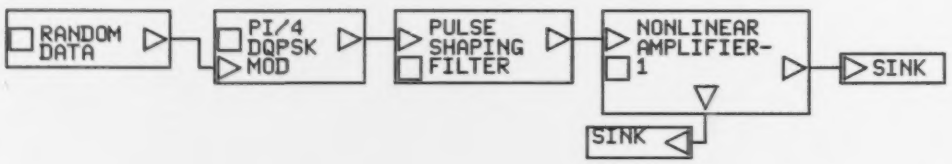

Fig. 3.1 Simulation model of a π/4-DQPSK transmitter

stream. The IS-54 standard specifies a bit rate of 48.6 kb/s, which corresponds to a bit period of 20.576131..... μs. This fractional bit period would cause a cumulative truncation error. To avoid this truncation error, a bit rate of 50 kb/s was used in this project. Each bit is sampled 16 times, which makes the successive samples 1.25 μs apart. The sampling rate must be sufficiently high to prevent undue aliasing of the signals. The BOSS manual [38] recommends a sampling rate of 8 - 16 times the bit rate to ensure that the aliasing is negligible. The BOSS manual also recommends that the sampling period be a power of 2, so that the internal binary representation of the sampling period will not cause any round off error. The sampling period of 1.25 μs satisfies both conditions.

3.3.2 π/4-DQPSK Modulator

The IS-54 standard specifies π/4 shifted, differentially encoded Quadrature Phase Shift Keying (π/4-DQPSK) modulation. A π/4-DQPSK signal constellation has 8 states. These states can be considered to be formed by the superposition of two Quadrature Phase Shift Keying (QPSK) constellations, offset by 45^0 relative to each other, as shown in Fig. 3.2. The two constellations are used alternately to transmit each symbol, and thus the successive symbols have a relative phase difference of $\pm 45^0$ or $\pm 135^0$. The maximum phase change for π/4-DQPSK is $\pm 135^0$, as compared to a maximum phase change of $\pm 180^0$ for QPSK. Therefore, a π/4-DQPSK modulated signal has less envelope fluctuation than a QPSK modulated signal. A smaller envelope fluctuation of the signal results in less spectral spreading of the signal due to nonlinear amplification.

A π/4-DQPSK modulator maps the binary data to the signal constellation. The binary input data stream is first split into two parallel binary streams X_k

and Y_k by a serial-to-parallel converter. The data streams, X_k and Y_k, are then encoded into the in-phase (I_k) and the quadrature phase (Q_k) components of the baseband complex signal according to:

$$I_k = I_{k-1}\cos\Delta\phi_k - Q_{k-1}\sin\Delta\phi_k$$
$$Q_k = Q_{k-1}\sin\Delta\phi_k + Q_{k-1}\cos\Delta\phi_k \quad \text{....(3.1)}$$

where I_{k-1} and Q_{k-1} are the amplitudes in the previous symbol period. The phase change $\Delta\phi_k$ is determined according to Table 3.1.

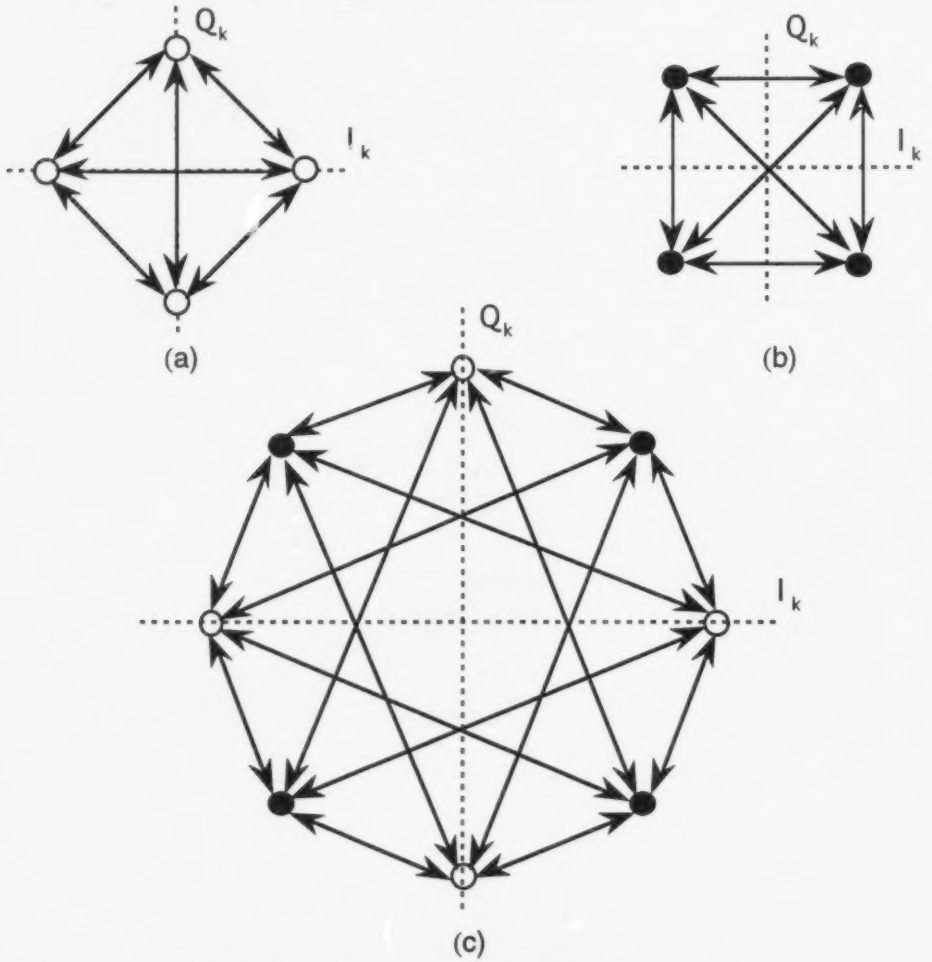

Fig. 3.2 (a), (b) QPSK signal constellation and transitions, (c) π/4-DQPSK signal constellation and transitions

Table 3.1 Phase encoding for π/4-DQPSK modulator

X_k	Y_k	$\Delta\phi_k$
1	1	$-\frac{3}{4}\pi$
0	1	$\frac{3}{4}\pi$
0	0	$\frac{1}{4}\pi$
1	0	$-\frac{1}{4}\pi$

A π/4-DQPSK modulated signal can be detected using a coherent detector, a differential detector or a discriminator followed by an integrate-and-dump filter. Differential detection and discriminator detection both allow simpler receiver realization as compared to coherent detection, which requires carrier recovery. In a fast fading environment, coherent detection results in a higher bit error rate (BER) than differential or discriminator detection.

3.3.3 Pulse Shaping Filter

In communication systems filtering may be done in order to select the desired signals, minimize the effects of noise and interference, modify the spectra of signals, and/or shape the time domain properties such as zero crossings and pulse shapes of digital waveforms. Time domain properties are important in digital communication systems. These properties can be controlled using pulse shaping filters. Bandwidth and zero crossings are two important conditions that the pulses in a digital system must satisfy. For a symbol rate, R_b, the bandwidth of the waveform should be of the order of R_b. Also a

waveform might be required to have zero crossings in the time domain every T_b seconds, where $T_b = 1/R_b$. Such zero crossings will provide zero intersymbol interference (ISI), that is, in the absence of noise, only one symbol will have a non zero value at each sampling time. Nyquist showed that a time domain pulse $p(t)$ will have a zero crossing every T_b seconds (except $t = 0$) if its Fourier transform $P(f)$ satisfies the following constraint [39]:

$$\sum_{k=-\infty}^{\infty} P(f + kR_b) = T_b \qquad for \qquad |f| < R_b/2 \qquad \text{....(3.2)}$$

If $P(f)$ satisfies this constraint, then $p(t)$ has the following properties:

$$p(0) = 1$$
$$p(kT_b) = 0 \qquad k = \pm 1, \pm 2, \ldots\ldots\ldots$$

The IS-54 standard specifies a linear phase and square-root raised cosine frequency response for the transmit filter. That is, the filter response will be given by:

$$|H(f)| = \begin{cases} 1 & for \quad 0 \le f \le \dfrac{1-\alpha}{2T} \\ \sqrt{\dfrac{1}{2}\left(1 - \sin\left(\dfrac{\pi[2fT-1]}{2\alpha}\right)\right)} & for \quad \dfrac{1-\alpha}{2T} \le f \le \dfrac{1+\alpha}{2T} \\ 0 & for \quad f > \dfrac{1+\alpha}{2T} \end{cases}$$

....(3.3)

where T is symbol period. The roll off factor, α, which determines the bandwidth, is specified as 0.35 in the IS-54 standard.

The impulse response of the transmit filter is given by [40]:

$$h(t)=\begin{cases} 1-\alpha+4\dfrac{\alpha}{\pi} & at\ t=0 \\ \dfrac{sin\left(\pi[1-\alpha]\dfrac{t}{T}\right)+4\alpha\dfrac{t}{T}cos\left(\pi[1+\alpha]\dfrac{t}{T}\right)}{\pi\dfrac{t}{T}\left(1-\left[4\alpha\dfrac{t}{T}\right]^2\right)} & for\ t\neq 0,\pm\dfrac{T}{4\alpha} \\ \dfrac{\alpha}{\sqrt{2}}\left(\left[1+\dfrac{2}{\pi}\right]sin\left[\dfrac{\pi}{4\alpha}\right]+\left[1-\dfrac{2}{\pi}\right]cos\left[\dfrac{\pi}{4\alpha}\right]\right) & for\ t=\pm\dfrac{T}{4\alpha} \end{cases}$$

....(3.4)

The impulse response of the transmit filter is shown in Fig. 3.3.

A filter with exactly the same response is used at the receiver. The transmit and the receive filters in cascade form a raised cosine Nyquist filter with an impulse response that goes through zero at each symbol period interval (except $t = 0$). This would ideally, in the absence of any noise or distortion in the channel, result in zero intersymbol interference at the ideal sampling point.

3.3.4 Nonlinear Power Amplifier

The experimentally obtained characteristics of two different amplifiers were used in this research project. The first amplifier is an Avantek 6 Watt class AB amplifier specially designed for the North American cellular frequency band. The AM-AM and AM-PM characteristics of this amplifier were obtained by measuring the input and output power and phase of the amplifier (see Figs. 2.2 and 2.3). This information was provided by NovaTel Communications Ltd. [41]. The second amplifier is an 8 Watt class B amplifier based on a Philips BLV93

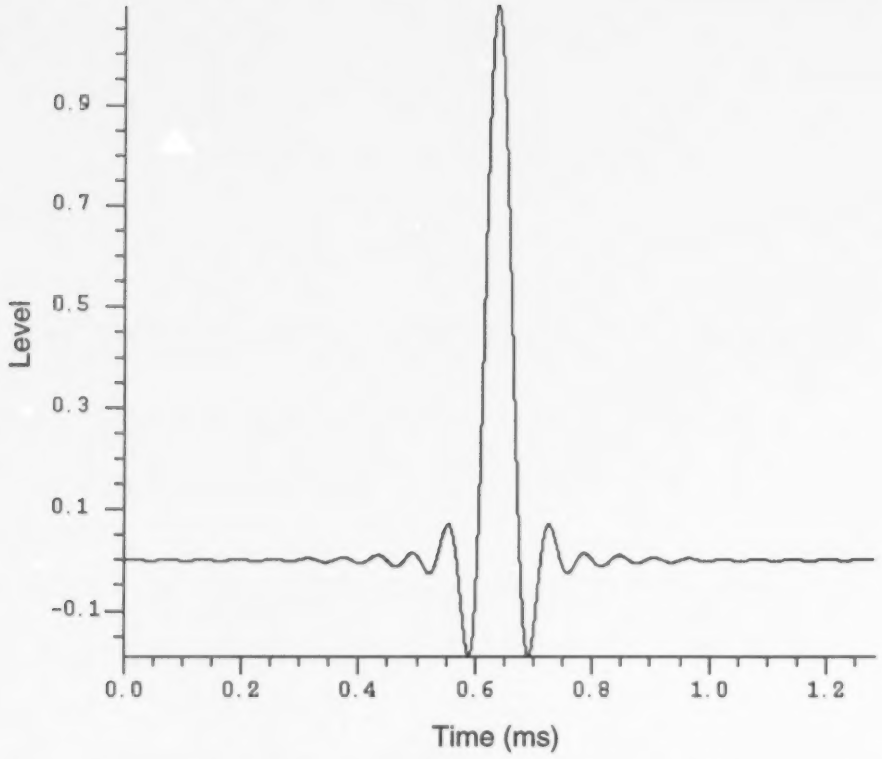

Fig. 3.3 Impulse response of square root raised cosine filter

transistor. The AM-AM and AM-PM characteristics of this amplifier are shown in Figs. 2. 2 and 2.3 [42] .

Fig. 3.4 shows the BOSS model of an amplifier [43]. The normalized magnitude of the input signal is used as an index to two look-up tables that contain the AM-AM and AM-PM conversion factors, respectively. The data for the AM-AM table is normalized so that the maximum gain corresponds to unity (0 dB). The AM-AM and AM-PM conversion tables for both amplifiers are listed in Appendix C.

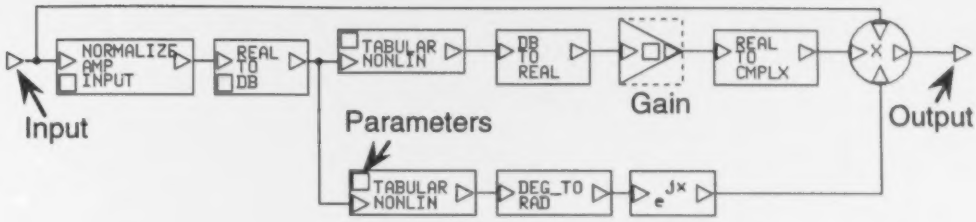

Fig. 3.4 BOSS module of nonlinear power amplifier

3.4 Spline Interpolation Linearizer

Fig. 3.5 shows the BOSS model of a $\pi/4$-DQPSK transmitter with the spline interpolation linearizer. The amplifier output is fed back to estimate the AM-AM and AM-PM characteristics of the amplifier. The spline-points block stores the phase and magnitude of the output signal for different input points. These input points are taken in intervals that are uniformly distributed over the entire input magnitude range. The signal pads in bold (Δ) format in Fig. 3.5 indicate 'vector' signals. There are two spline interpolation blocks for calculating the magnitude and phase distortion values at interpolated points using cubic spline interpolation. The interpolated values are stored in a look-up table. The input to the look-up table is the magnitude of the input signal. The outputs of the look-up table are the magnitude and phase predistortion values. These are vector multiplied with the input signal to obtain the predistorted complex input signal in the predistortion block. A listing of the FORTRAN subroutines for spline interpolation and of the look-up table blocks is given in Appendix D.

Two-tone tests are performed to determine the intermodulation products. For two-tone tests, the random data generator, $\pi/4$-DQPSK modulator and pulse shaping filter blocks are replaced with a two-tone input block to perform

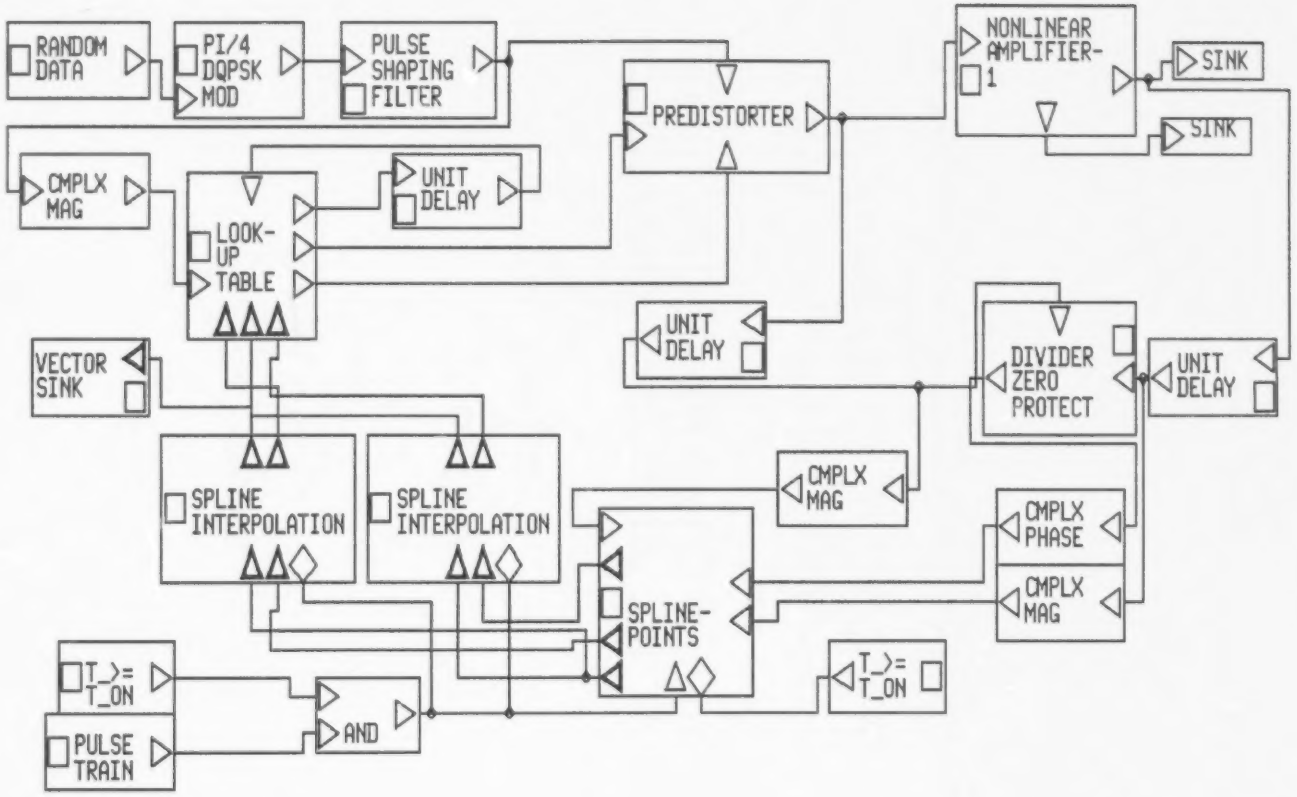

Fig. 3.5 Simulation model of π/4 DQPSK transmitter with spline interpolation linearizer

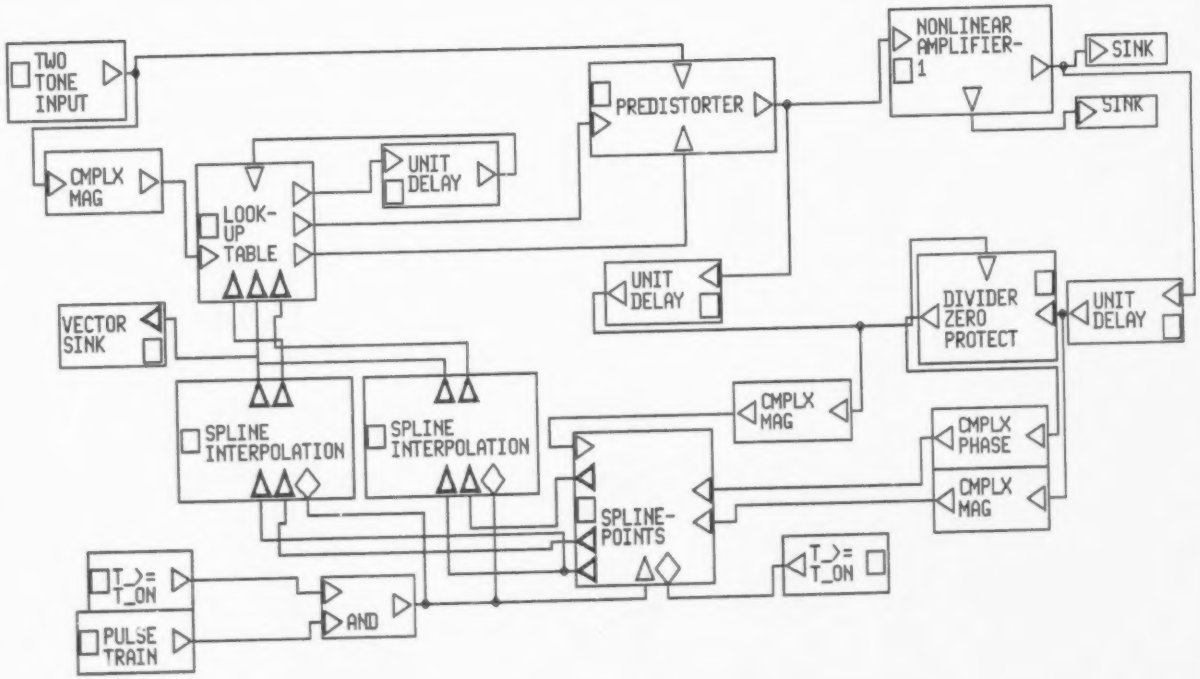

Fig. 3.6 Simulation model of transmitter with spline interpolation linearizer and two-tone input signal

two-tone tests. The two-tone input block generates two complex tones, each with a cosine wave as the i component and a sine wave as the q component. The BOSS model of the transmitter with two-tone input and the spline interpolation linearizer, is shown in Fig. 3.6.

3.5 Complex Gain Predistorter

Fig. 3.7 shows the BOSS representation of the complex gain predistorter [43]. The address block generates the index for the look-up table. The input signal is multiplied by the predistortion coefficients to generate the predistorted signal. The output of the amplifier is compared with the input signal to generate an error signal. The error signal is multiplied by the complex conjugate of the original signal, so that the error vector is independent of the phase of the signal. The update block calculates new predistortion coefficients that are stored in the look-up table. The predistortion coefficients are calculated using the Secant method [29]. A listing of the Fortran subroutine for computing the predistortion coefficients is given in Appendix D.

3.6 Cartesian Coordinate Negative Feedback

This system is a negative feedback system. Fig. 3.8 shows the BOSS representation of the cartesian coordinate feedback system [43]. The loop filter is a single-pole Butterworth filter. This filter is approximated by a low pass infinite impulse response (IIR) filter in BOSS. The 3 dB cut off frequency is at 75 kHz. A single-pole filter is used to control the stability of the feedback loop. The loop filter provides a narrowband response to increase the stability of the system. The performance of the system is critically dependent on the phase adjustment, since phase errors in the feedback path can lead to oscillation. In a practical system, the phase adjustment is made by delaying the local oscillator

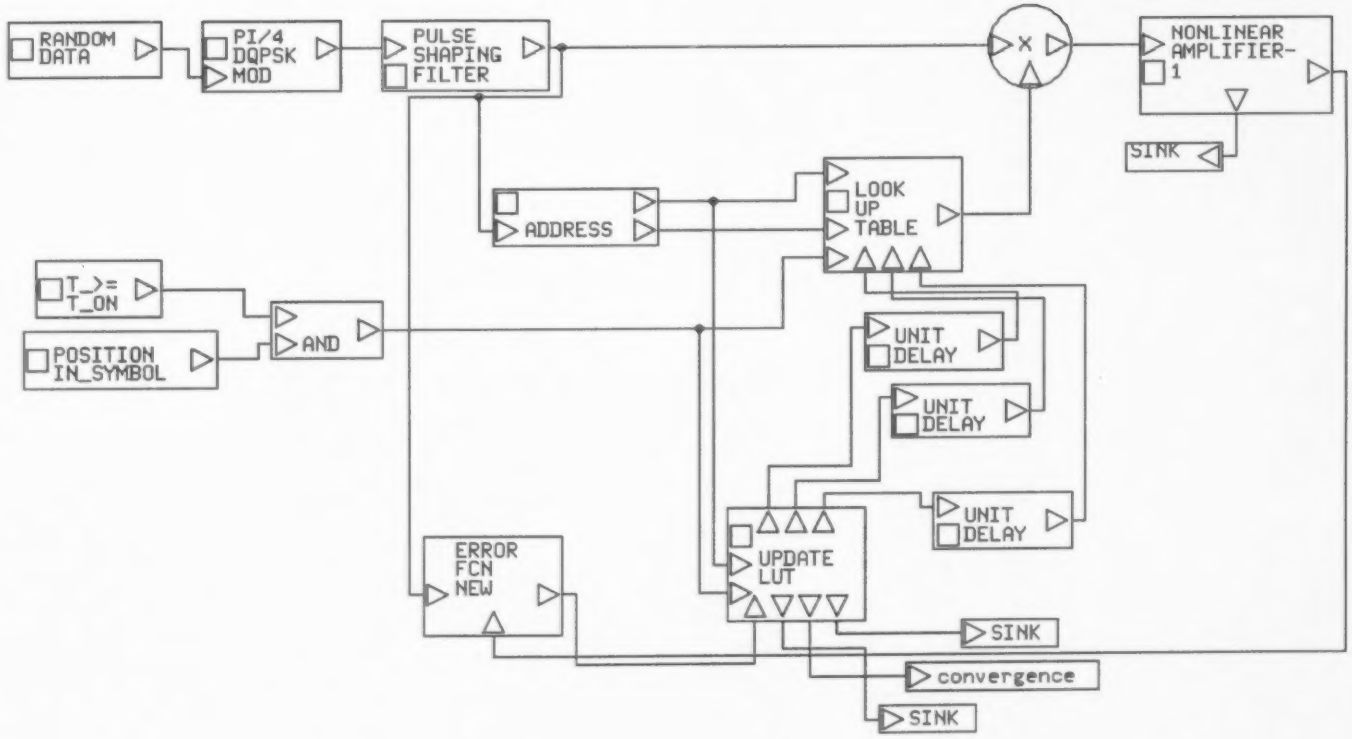

Fig. 3.7 Simulation model of complex gain predistortion system

signal. In BOSS simulations, this is accomplished by adjusting the phase of the complex signal.

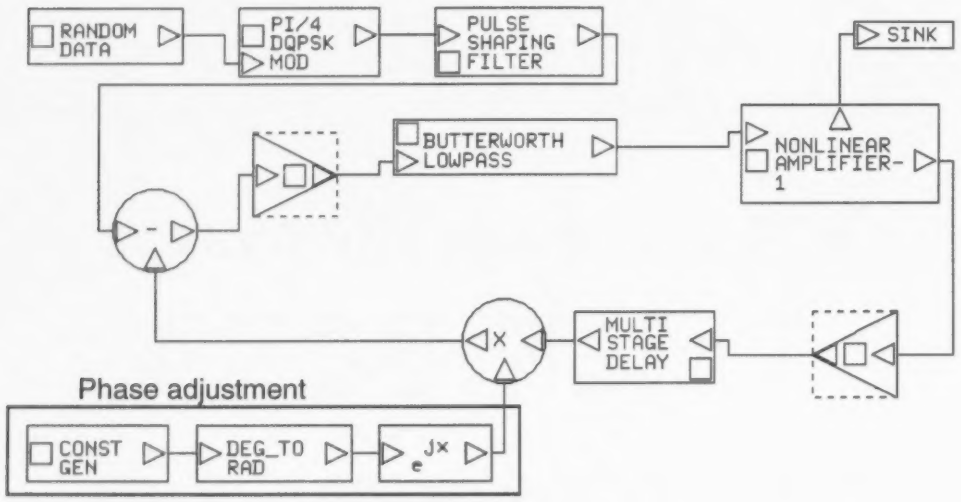

Fig. 3.8 Simulation model of cartesian coordinate negative feedback system

3.7 Modulator

An analog quadrature modulator is required to upconvert the baseband signals. Analog quadrature modulator impairments can be represented by gain imbalance, phase imbalance and dc-offset, as discussed in Section 2.6. The BOSS implementation of a quadrature modulator is shown in Fig. 3.9.

The modulator impairments can introduce phase-dependent distortion in a transmitter, which can adversely affect the performance of a system. A technique to compensate for the modulator impairments has been described in Section 2.8. The compensator module uses the i and q values of the input to the modulator and the magnitude of the output of the modulator at five different

signal points to generate five equations. The signal points should be well spread over the signal constellation, to ensure the convergence of the Newton-Raphson method. The estimated values of the impairments are used to predistort the input signal according to Eqs. 2.32 and 2.33. A listing of the FORTRAN subroutine for the estimation of the modulator impairments is given in Appendix D.

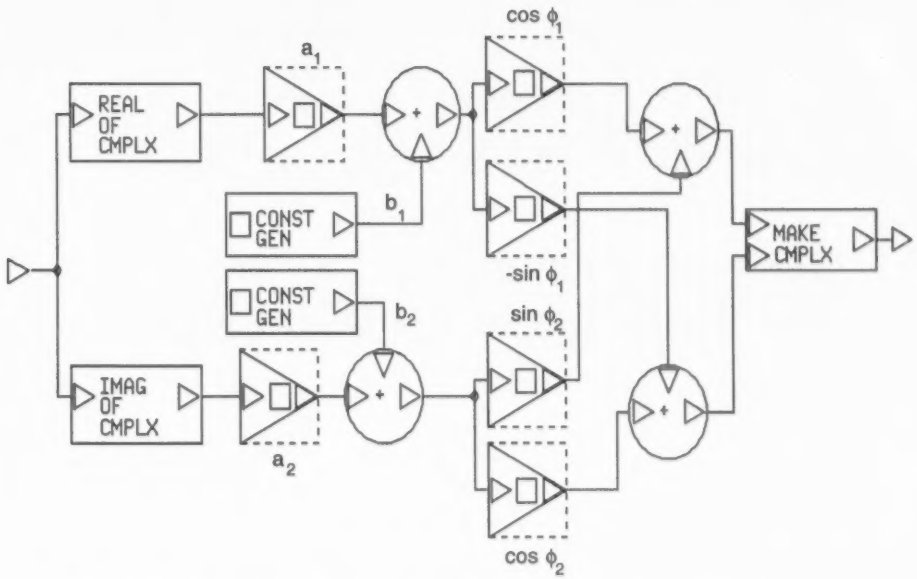

Fig. 3.9 Simulation model of quadrature modulator

3.8 Demodulator

An analog demodulator is required to down-convert the RF signal. A quadrature demodulator is also required in the feedback loop of a RF amplifier linearizer. Like the quadrature modulator impairments, the quadrature demodulator impairments can be represented by gain imbalance, phase imbalance and dc-offset. The BOSS representation of a quadrature demodulator is shown in Fig. 3.10.

Since the demodulator is in the feedback path of the amplifier linearizer, it is especially important to compensate for its impairments, as discussed in Section 2.3.4. A technique to compensate for the quadrature demodulator impairments has been described in Section 2.8. The structure of the demodulator impairment compensator is similar to that of the modulator impairment compensator. A listing of the FORTRAN subroutine for estimation of the demodulator impairments is given in Appendix D. The estimated values of the demodulator impairments are used to post-distort the baseband signal according to Eqs. 2.41 and 2.42.

Fig. 3.11 shows the BOSS representation of a transmitter system with the spline interpolation linearizer, and modulator and demodulator impairment compensators.

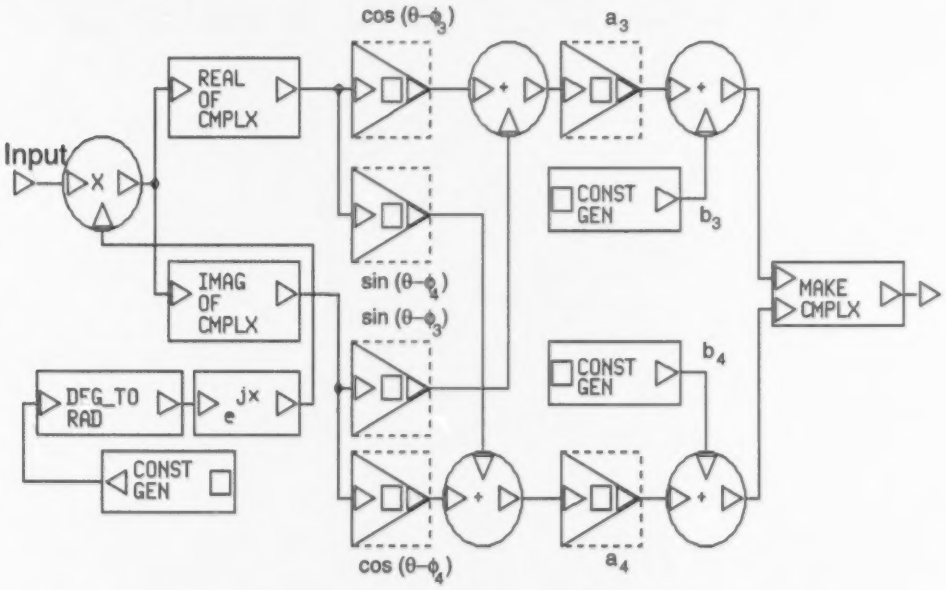

Fig. 3.10 Simulation model of quadrature demodulator

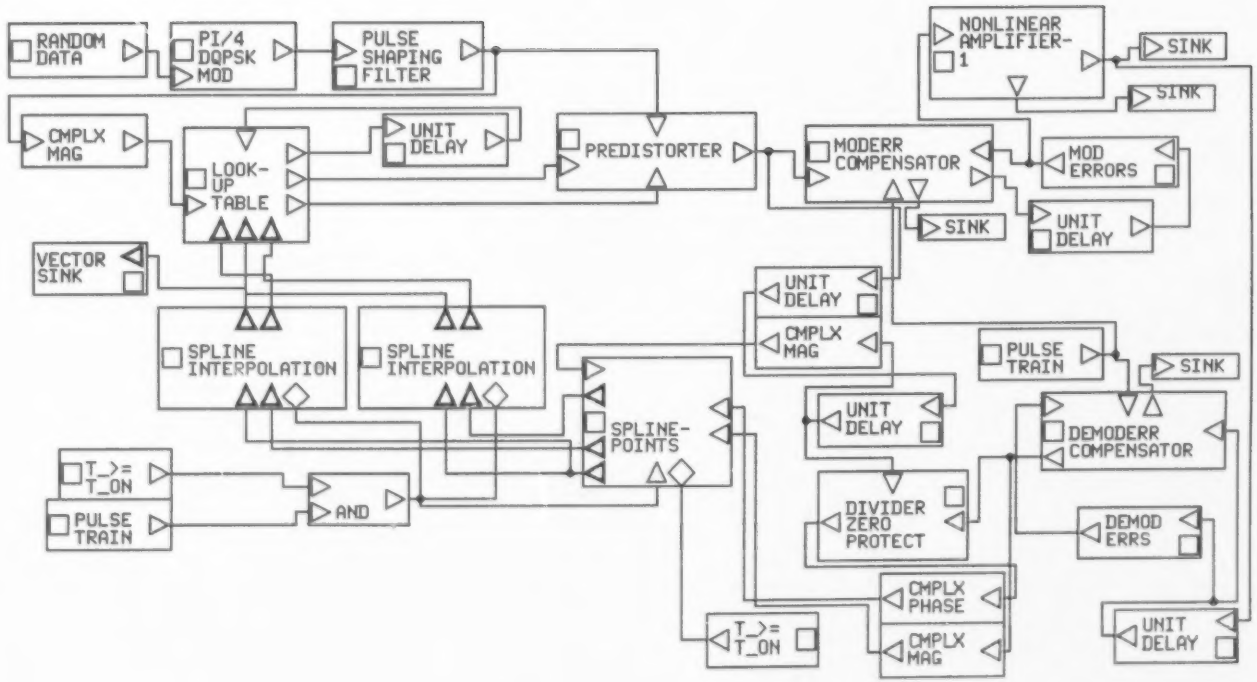

Fig. 3.11 Simulation model of transmitter with spline interpolation linearizer, and modulator and demodulator impairment compensators

4. Results

This chapter presents simulation results for the performance of spline interpolation, complex gain predistortion and cartesian coordinate negative feedback linearizers. The effects of the quadrature modulator and demodulator impairments are investigated. The performance of the quadrature modulator and demodulator impairment compensators is also evaluated.

4.1 Simulation Plan

The first set of simulations was carried out in order to investigate the effects of representative amplifier nonlinearities on the transmitted signal. The results of these simulations are presented in Section 4.3. Simulation results of the performance of the cubic spline interpolation linearizer are given in Section 4.4. In Section 4.5, the method of direct points is described. The performance of the direct method is compared with that of the cubic spline interpolation method. The performance of complex gain predistortion and cartesian coordinate negative feedback linearizers are discussed in Sections 4.6 and 4.7, respectively. Section 4.8 provides a comparison of the above-mentioned linearization techniques. The effects of quadrature modulator and demodulator impairments are described in Sections 4.9 and 4.10. Simulation results of the performance of the modulator and demodulator impairment compensators are presented in Sections 4.11 and 4.12, respectively. Finally, Section 4.13 gives the results of the performance of spline interpolation linearization technique along with the modulator and demodulator impairment compensators.

4.2 Evaluation of Amplifier Linearity

The linearity of an amplifier can be characterized using intermodulation products and spectral spreading of bandlimited input signals. For North American digital cellular systems, the adjacent channels are centered 30 kHz apart. The IS-54 standard [2] specifies the maximum acceptable level of power emission in the adjacent channels, as discussed in Chapter 2. The out-of-band power emission results in inter-channel interference. Therefore, out-of-band power emission must be kept at the minimum level possible.

4.2.1 Estimation of Power Spectrum

The out-of-band power can be evaluated using the power spectral density (PSD) of the amplifier output. The PSD can be estimated using a method called the periodogram [44]. For a periodogram estimation, a Discrete Fourier Transform (DFT) of N equispaced sample points of the function $c(t)$ is computed using the Fast Fourier Transform (FFT) algorithm. The Fourier coefficients are:

$$C_k = \sum_{n=0}^{N-1} c_n e^{j\frac{2\pi kn}{N}} \qquad k = 0,1,2.....N-1 \quad ....(4.1)$$

where the c_n's are the sampled values of $c(t)$.

The periodogram estimate of the power at N/2 + 1 frequencies is given by

$$P(0) = P(f_0) = \frac{1}{N^2}|C_0|^2$$

$$P(f_k) = \frac{1}{N^2}\left[|C_k|^2 + |C_{N-k}|^2\right] \quad for \quad k = 1,2.....\left(\frac{N}{2}-1\right)$$

$$P(f_c) = P\left(N/2\right) = \frac{1}{N^2}\left|C_{N/2}\right|^2 \qquad ....(4.2)$$

where f_k is defined only for zero and positive frequencies:

$$f_k \equiv \frac{k}{N\Delta} = 2 f_c \frac{k}{N}, \qquad k = 0,1,\ldots\ldots\frac{N}{2}$$

where f_c is the Nyquist frequency and Δ is the sampling interval.

The periodogram has a high variance for each discrete frequency f_k. The variance of each $P(f_k)$ is $P^2(f_k)$ for any time interval, T, and for all f_k. The variance does not decrease with an increasing number of data points (N). The additional information goes into producing estimates at a greater number of discrete frequency points. If a longer run of data is obtained using the same sampling rate, the Nyquist frequency is unchanged. However, there is a finer frequency resolution within the frequency interval. On the other hand, if a larger number of points is obtained using a higher sampling rate for the same time interval, the frequency resolution remains the same. However, the Nyquist range will extend up to a higher frequency.

The variance of the periodogram estimate can be reduced by averaging several runs of data. This can be done in two ways. In the first technique, the sampled data are divided into L segments. For each segment, a periodogram is computed. Then L periodograms are averaged together. This technique reduces the variance of the periodogram estimate by a factor of L [44]. For the second technique, L data segments that overlap by one half of their length are taken. Since these segments are not statistically independent, the variance is reduced by a factor of 9L/11 [45].

Another problem with the periodogram estimate is power leakage from one discrete frequency to another. A set of N sample data points is equivalent to an infinite set of sample data points windowed in time. The window function is unity during the sampling time and is zero otherwise. By the convolution

theorem, the Fourier transform of the data with a window function is equal to convolution of the Fourier transform of the data with the Fourier transform of the window function. Since a rectangular window turns off and on instantaneously, its Fourier transform has significant components at high frequencies. This causes power leakage from one discrete frequency to another frequency.

The leakage can be reduced by multiplying the data with a window that changes more gradually from zero to a maximum and then back to zero. There are many different types of window functions [46]. They all involve a trade off between the width of the main lobe and the attenuation of sidelobes. The choice of a window type is governed by the application. Since out-of-band power is small as compared to in-band power, a window with low side lobes is desirable for estimation of out-of-band power emission. The Blackman window [46] is used in this project. The Blackman window function is given by

$$w(t) = 0.42 + 0.5\cos\left(\frac{2\pi t}{T}\right) + 0.08\cos\left(\frac{4\pi t}{T}\right) \quad \text{for} \quad |t| \le \frac{T}{2}$$

....(4.3)

The Fourier transform of the Blackman window is

$$w(f) = \frac{\sin(\pi fT)}{\pi fT}\left[0.42 + \frac{0.5(fT)^2}{1-(fT)^2} - \frac{0.08(fT)^2}{4-(fT)^2}\right]$$

....(4.4)

4.2.2 Intermodulation Products

The intermodulation products obtained using a two-tone test, provide a simple measure of amplifier linearity. The test signal used for evaluating the

intermodulation products has two tones, one at 20 kHz and one at 25 kHz. The spectrum of the two-tone test signal is shown in Fig. 4.1. The third order intermodulation products (IM_3) occur at 30 kHz (upper) and 15 kHz (lower). Similarly, the fifth order intermodulation products (IM_5) occur at 35 kHz (upper) and 10 kHz (lower).

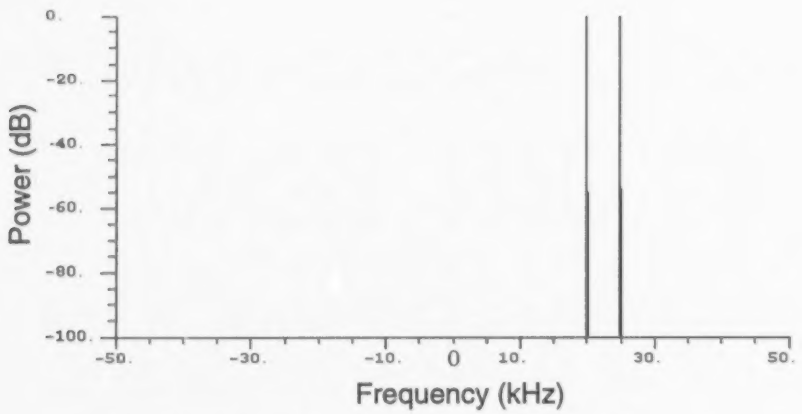

Fig. 4.1 Spectrum of two-tone input signal

4.3 RF Power Amplifier Distortion

An amplifier can be characterized by its AM-AM and AM-PM characteristics, as discussed in Chapter 2. The characteristics of the class AB and class B amplifiers are shown in Figs. 2.2 and 2.3, respectively. The class AB amplifier was an Avantek 6 Watt amplifier specially designed for the North American cellular frequency band. The class B amplifier was an 8 Watt amplifier based on a Philips BLV93 transistor. Fig. 4.2 shows the normalized PSD of a $\pi/4$-DQPSK modulated random data input signal. A square-root raised cosine with a roll-off factor of 0.35, as specified in the IS-54 standard [2], is used. The output PSD of the class AB amplifier is shown in Fig. 4.3. The

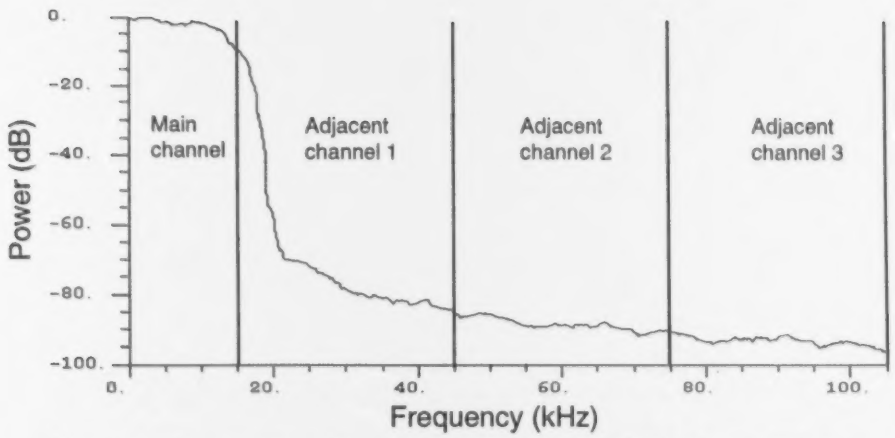

Fig. 4.2 Power spectral density of π/4-DQPSK modulated signal with square-root raised cosine filtering

maximum input power level is specified such that the maximum level of the filtered signal corresponds to the 1 dB compression point of the amplifier gain characteristic. This has been used consistently for all the simulations. The output PSD of the class AB amplifier lies more than 30 dB above the output PSD of an ideal amplifier. Fig. 4.4 shows the output spectrum of the class AB amplifier for the two-tone input signal. The IM_3 and IM_5 are seen to be -28.4 dB

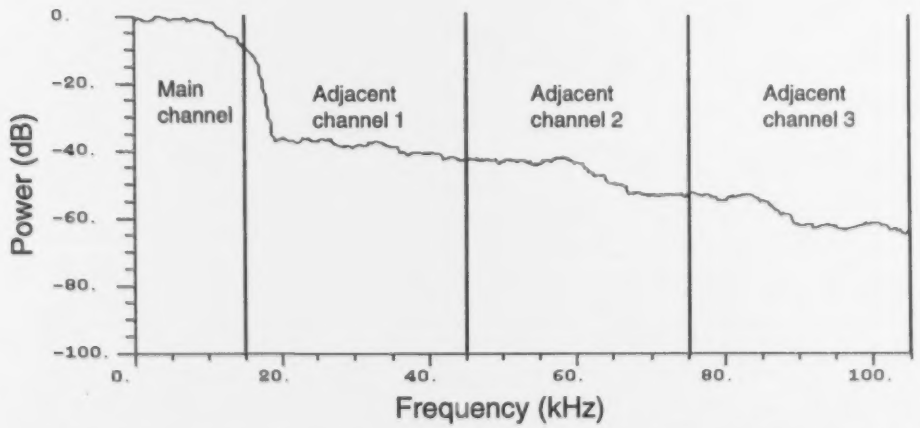

Fig. 4.3 Output power spectral density of class AB amplifier

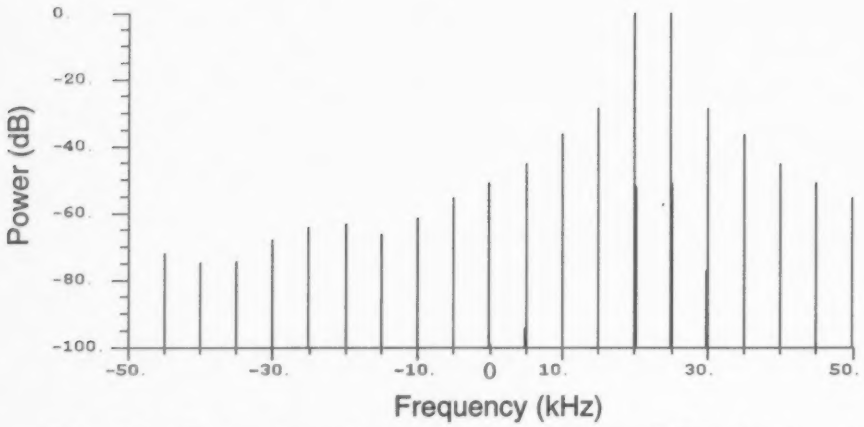

Fig. 4.4 Output spectrum of class AB amplifier for two-tone input signal (20 kHz and 25 kHz)

and -36.6 dB, respectively. The IM_3 is required to be below -44 dB at rated power level [47].

Fig. 4.5 shows the normalized output PSD for the class B amplifier. The output spectrum for the two-tone input signal is shown in Fig. 4.6. The IM_3 and IM_5 are -27.5 dB and -34.5 dB, respectively. The IM_3 is seen to be about

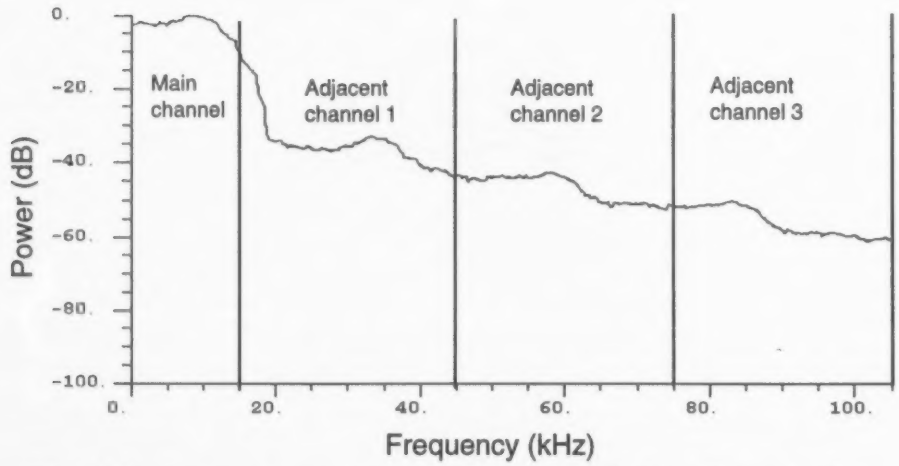

Fig. 4.5 Output power spectral density of class B amplifier

17.5 dB above the acceptable level given in [47]. Fig. 4.7 compares the out-of-band power emission of the class AB and class B amplifiers. The out-of-band power is not significantly different for the class AB amplifier and the class B amplifier. However, the intermodulation products are slightly higher for the class B amplifier than for the class AB amplifier. This can be attributed to a higher cross-over distortion for the class B amplifier.

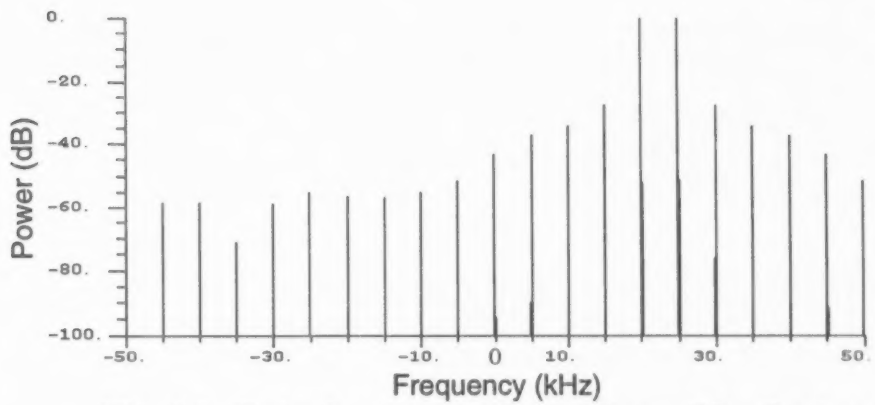

Fig. 4.6 Output spectrum of class B amplifier for two-tone input signal (20kHz and 25 kHz)

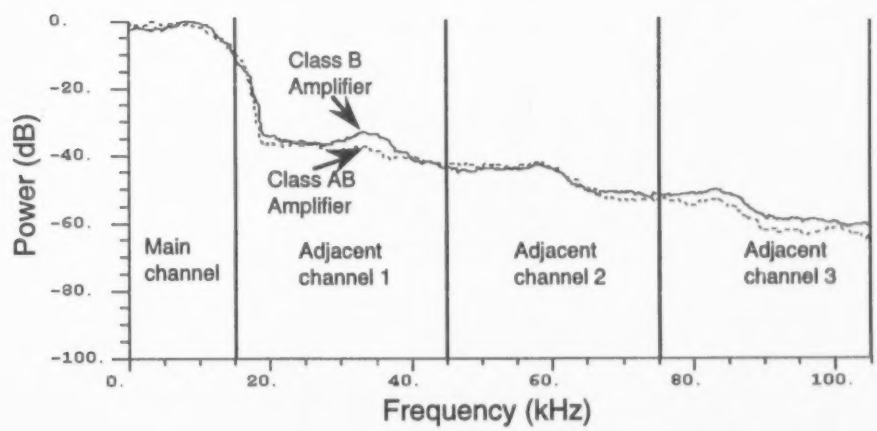

Fig. 4.7 Comparison of output power spectral density of class AB and class B amplifiers

4.4 Cubic Spline Interpolation Linearizer

This section describes the performance of the cubic spline interpolation linearization technique. This technique has been explained in Section 2.5. The simulation models used for the cubic spline interpolation linearizer have been described in Section 3.4. The first two sets of simulations investigate the effects of the number of points used for the spline interpolation and of the look-up table size on the performance of the linearizer. The next set of simulations is for different values of back-off of the amplifier. The class AB amplifier was used for these simulations. The performance of the cubic spline interpolation linearizer for the class B amplifier has also been investigated, and is presented in Section 4.4.4.

4.4.1 Number of Spline Points

The out-of-band power when the number of points used for spline interpolation is varied, is shown in Fig. 4.8. There is a significant reduction in out-of-band power as the number of spline points is increased from 10 to 30 points. There is a diminishing reduction of out-of-band power with an increase in the number of points beyond 30 points. With 30 spline points, the AM-AM and AM-PM characteristics of the amplifier are seen to be sufficiently accurately estimated.

Fig. 4.9 illustrates the suppression of IM_3 and IM_5 with an increase in the number of spline points. There is seen to be about 11 dB improvement in IM_3 as the number of spline points is increased from 10 to 30 points. However, there is only about 1.5 dB improvement in IM_3 as the number of spline points is increased from 30 to 50 points. The IM_5 varies from -78.3 dB to -86.7 dB as the number of spline points changes from 10 to 50 points. The IM_5 also shows

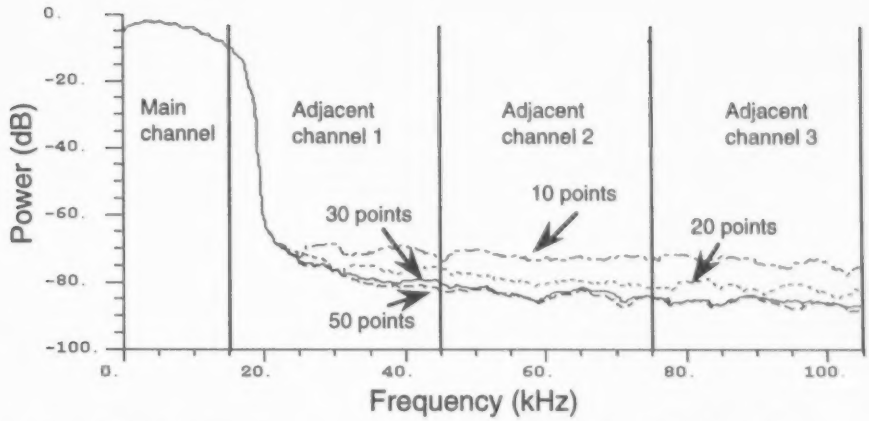

Fig. 4.8 Output power spectral density for different number of spline points

diminishing improvement in the performance of the linearizer beyond 30 spline points.

The spline points are taken in intervals that are uniformly distributed over the entire input magnitude range. The intervals can also be taken

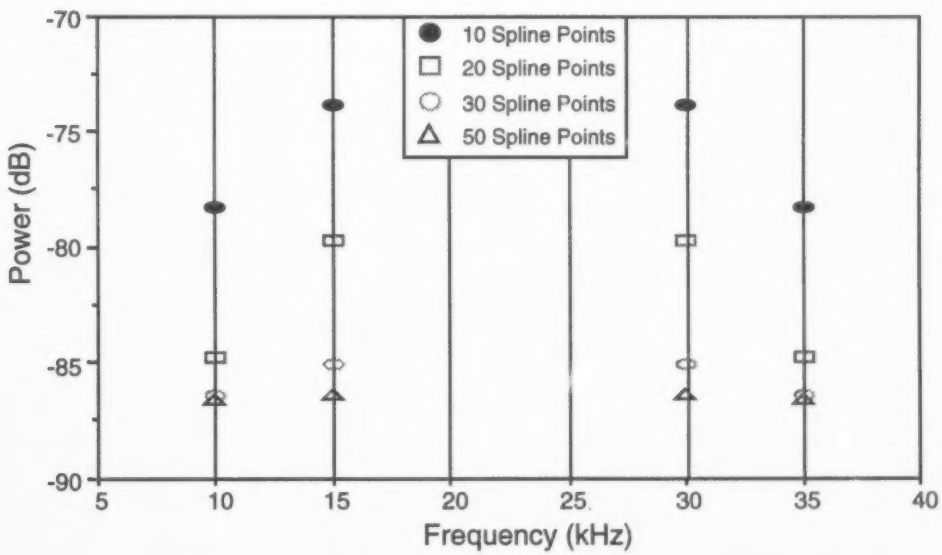

Fig. 4.9 Intermodulation products for different number of spline points

nonuniformly, with more intervals near the saturation and cut off regions, and fewer intervals in the near-linear region of the operating characteristic. However, the disadvantage of a nonuniform distribution of intervals is an increased computational overhead for sorting and a longer required time for updating the look-up table.

4.4.2 Look-Up Table Size

The size of the predistortion look-up table is a further important parameter that affects the performance of the linearizer. The look-up table stores predistortion coefficients for the magnitude and phase errors. It is observed in Fig. 4.10 that there is a considerable improvement in the performance of the linearizer as the look-up table size is increased from 200 to 800 entries. There is no significant improvement in the performance of the linearizer for a look-up table size beyond 3200 points.

The IM_3 and IM_5 for different look-up table sizes are shown in Fig. 4.11.

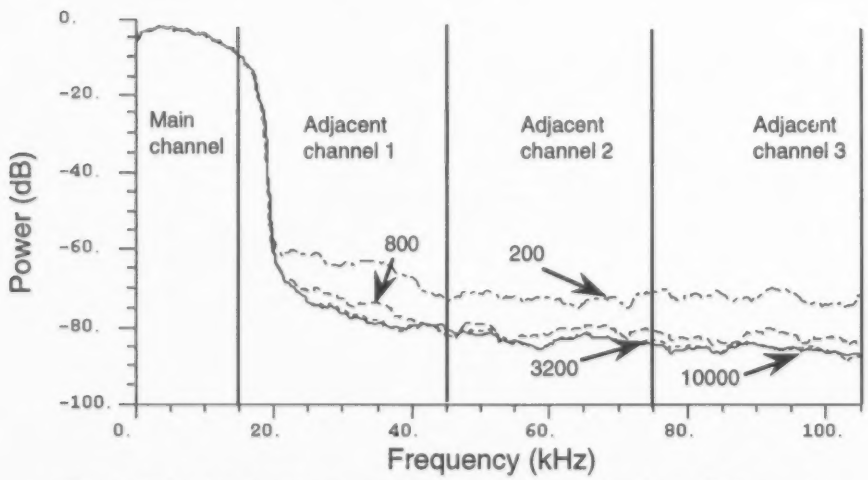

Fig. 4.10 Output power spectral density for different look-up table sizes

There is about a 23.7 dB reduction in IM_3 as the look-up table size increases from 200 to 3200. There is only a 6.5 dB reduction in IM_3 for an increase from 3200 to 10,000 points. Similar improvements are observed for IM_5.

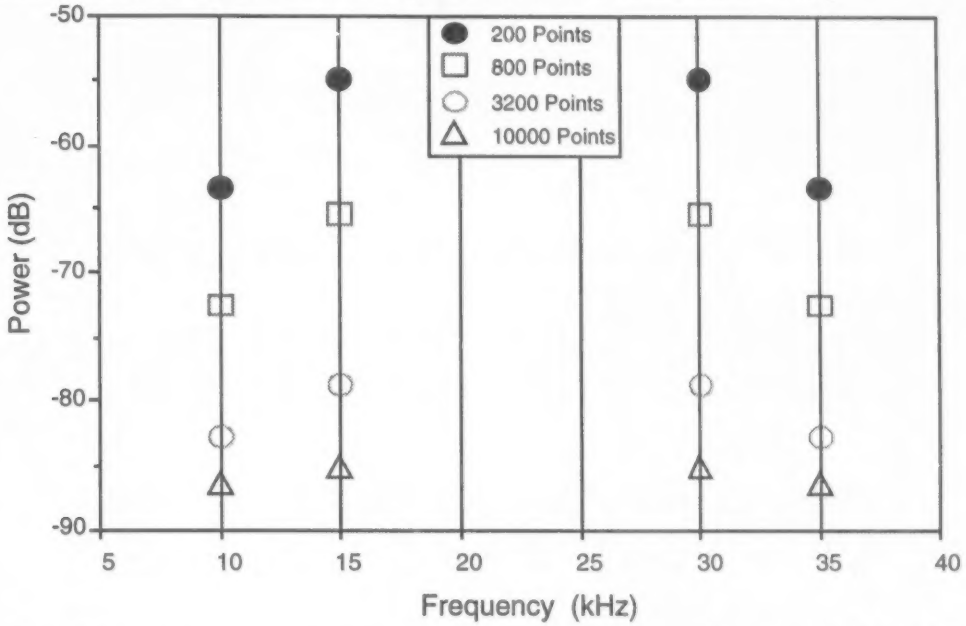

Fig. 4.11 Intermodulation products for different look-up table sizes

4.4.3 Back Off

In cellular radio applications, an amplifier is required to operate at various power levels in order to control the interference in nearby cells. The performance of the linearizer for different values of back-off level was therefore simulated as well. The maximum power is the power level at which the maximum level of the filtered input signal corresponds to the 1 dB gain compression point of the amplifier characteristic. Fig. 4.12 shows the PSD of the amplifier output for peak input levels at 90%, 95% and 100% of the 1 dB gain compression point. This figure illustrates that the amplifier can be operated up to the 1 dB gain compression point without any significant loss of

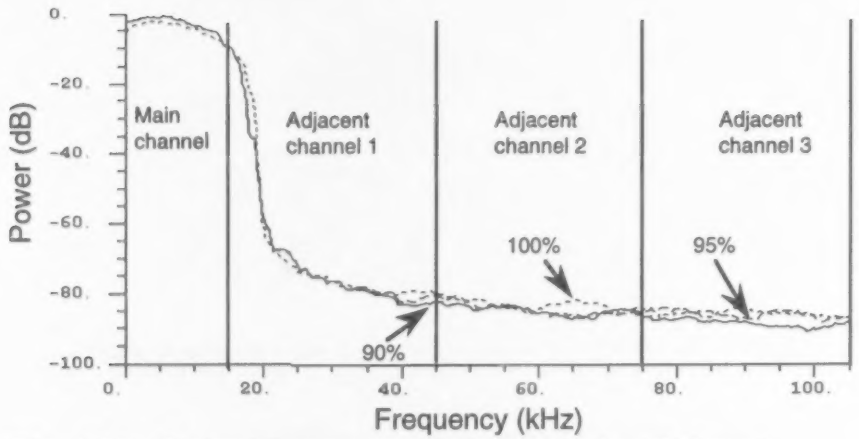

Fig. 4.12 Output power spectral density for different input power levels

amplifier linearity. There is a slight reduction in the out-of-band power with increasing back off levels.

4.4.4 Class B Amplifier Cubic Spline Linearization

Simulations were also carried to evaluate the performance of the cubic spline interpolation linearizer for the class B amplifier. There are 30 spline points, and the look-up table size is 10,000. The IM_3 and IM_5 are -80.6 dB and -81.1 dB, respectively. The PSD is shown in Fig. 4.13. The PSD of the class AB amplifier is also shown for comparison. The out-of-band power of the linearized class B amplifier is seen to be slightly better than that of the class AB amplifier. The IM_3 and IM_5 are 4.5 dB and 5.7 dB higher, respectively, for the linearized class B amplifier than those for the class AB amplifier.

4.5 Direct Points Technique

In this technique, a part of the amplifier output is synchronously demodulated. The demodulated amplifier output is compared with the input

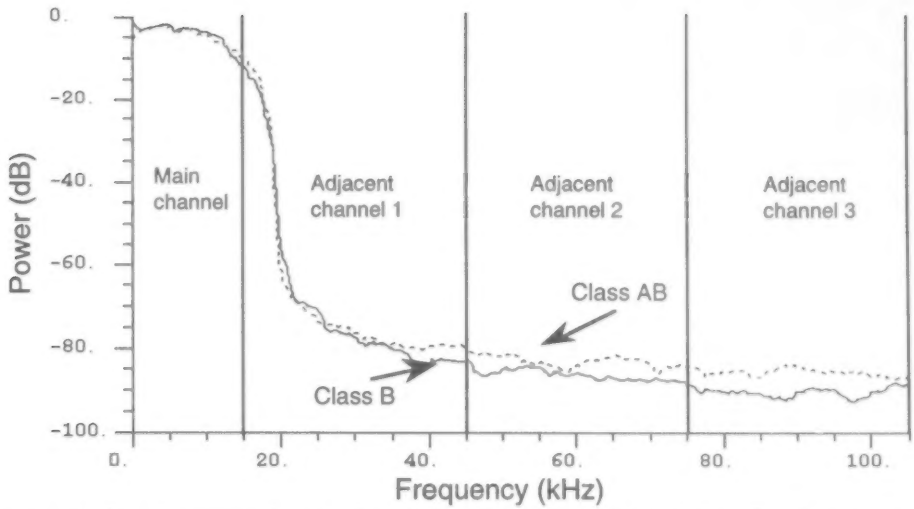

Fig. 4.13 Comparison of output power spectral density of class AB and class B amplifiers with spline interpolation linearizer

signal to estimate the magnitude and phase distortion introduced by the amplifier. These distortion values for different input magnitude levels are stored directly in a look-up table without spline interpolation. The magnitude of the input signal acts as a pointer to the look-up table. The predistortion coefficients are calculated as described in Section 2.5. Fig. 4.14 shows the output PSD of the class AB amplifier with the direct point linearizer. The look-up table size is 200.

A comparison of the direct point and spline interpolation techniques is illustrated in Fig. 4.15. The look-up table size is 200 for both cases. There are 30 spline points for the spline interpolation. It is interesting to note that the performance of both techniques is nearly identical. This demonstrates that spline interpolation is a good method of estimating points on the AM-AM and AM-PM characteristics. The penalty paid is in terms of the additional computational overhead.

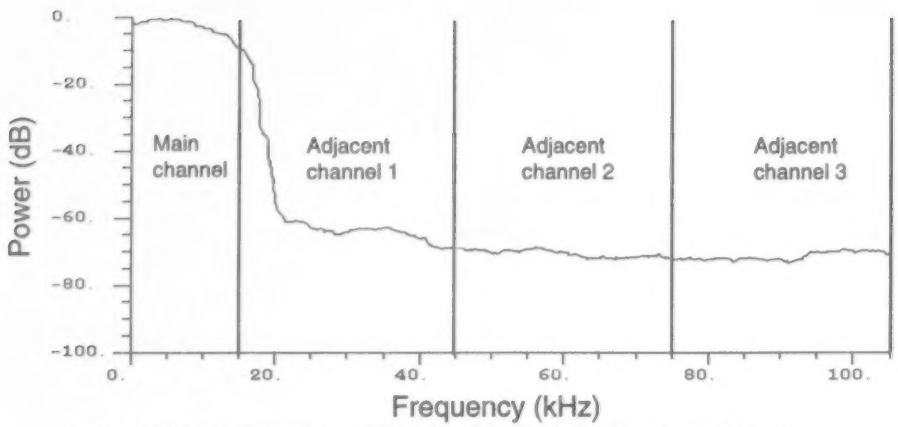

Fig. 4.14 Output power spectral density for direct look-up table points

The amplifier characteristics are more nonlinear near the cut-off and saturation regions. Therefore, it is essential to have a large number of points in these regions to accurately estimate the amplifier distortion. It can be difficult to obtain more points in these regions directly since the points are not uniformly distributed over the entire input magnitude range. The signal points away from

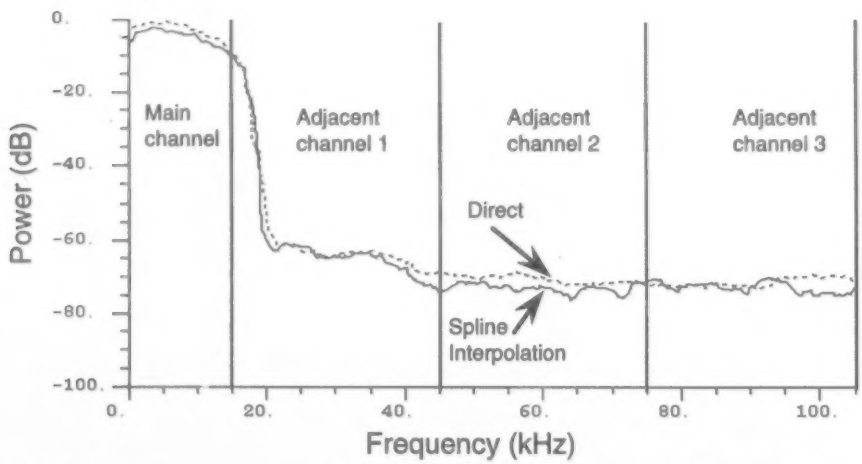

Fig. 4.15 Comparison of output power spectral densities for spline interpolation and direct look-up table points

the constellation points occur less often than points close to the signal constellation points. Since the distribution of points is dependent upon the modulation technique and pulse shaping filter, the direct point method will be modulation-format dependent.

4.6 Complex Gain Predistortion

The complex gain predistortion linearization technique has also been described in Chapter 2. Like the spline interpolation linearization technique, it is also a predistortion linearization technique. The amplifier gain is characterized by its AM-AM and AM-PM characteristics. The predistortion coefficients are stored in a look-up table which is indexed by the input power level. The look-up table entries are calculated using the Secant method, as discussed in Section 2.4.1. Fig. 4.16 shows the output PSD for the class AB amplifier with the complex gain predistortion linearizer. The output spectrum for the two-tone input signal is shown in Fig. 4.17. The IM_3 and IM_5 are -62.3 dB and -70.2 dB, respectively. These results are for a look-up table with 64 complex entries.

Since the complex gain predistortion method uses a successive approximation method for updating the look-up table, ideally the points used for updating should be at the centre of the interval. However, in a practical system the points will be scattered over the quantization interval. This causes adaptation jitter. The adaptation algorithm chases a moving target. This can result in an increase in the output error, and limit the performance of the complex gain predistortion linearizer.

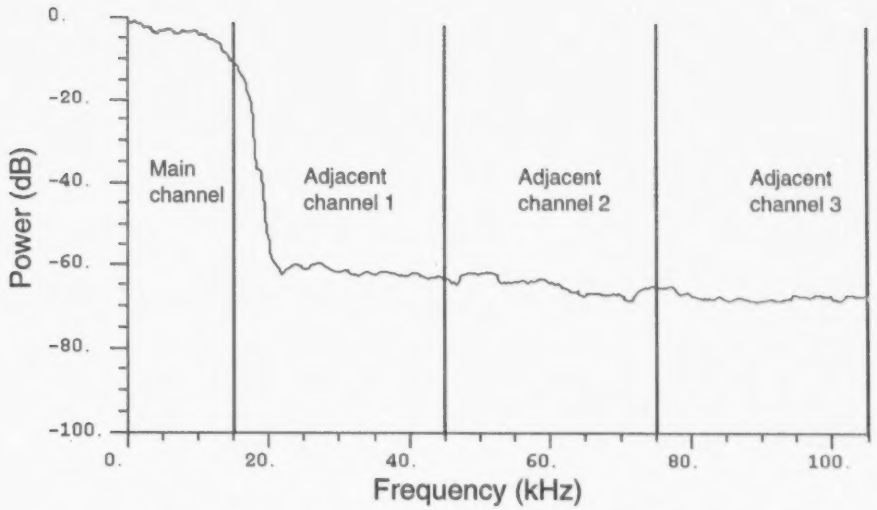

Fig. 4.16 Output power spectral density of class AB amplifier with complex gain predistorter

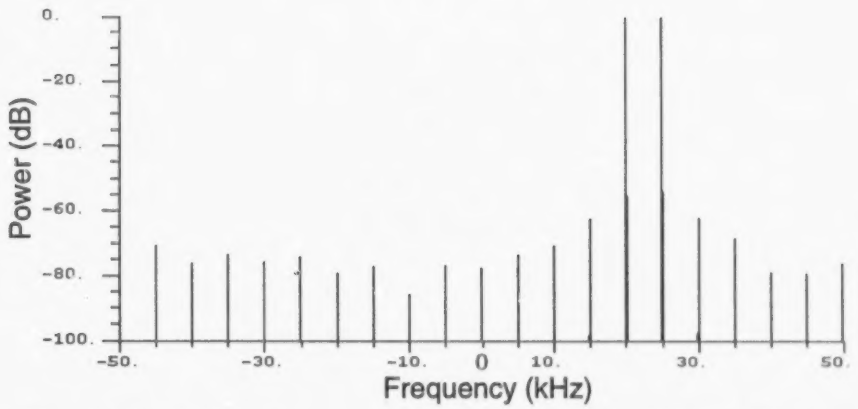

Fig. 4.17 Output spectrum of class AB amplifier with complex gain predistorter for two-tone input signal

4.7 Cartesian Coordinate Negative Feedback

The cartesian coordinate negative feedback system uses negative feedback to linearize the amplifier. This technique has also been described in Chapter 2. Loop gain is an important parameter of the cartesian coordinate negative feedback system. If the loop gain is too high, the system can oscillate. On the other hand, if the loop gain is too small, the system will not correct for amplifier nonlinearity. The amplifier distortion is reduced by a factor equal to the loop gain, as illustrated by Eq. 2.16. Fig. 4.18 shows the output PSD for the class AB amplifier. A loop gain of 15 was used for these simulations. The IM_3 and IM_5 have been found to be -54.9 dB and -60 dB, respectively.

The cartesian coordinate negative feedback system is simple to implement, but requires a phase adjustment that depends on the RF carrier frequency. If proper phase adjustment is not done, the feedback can cause

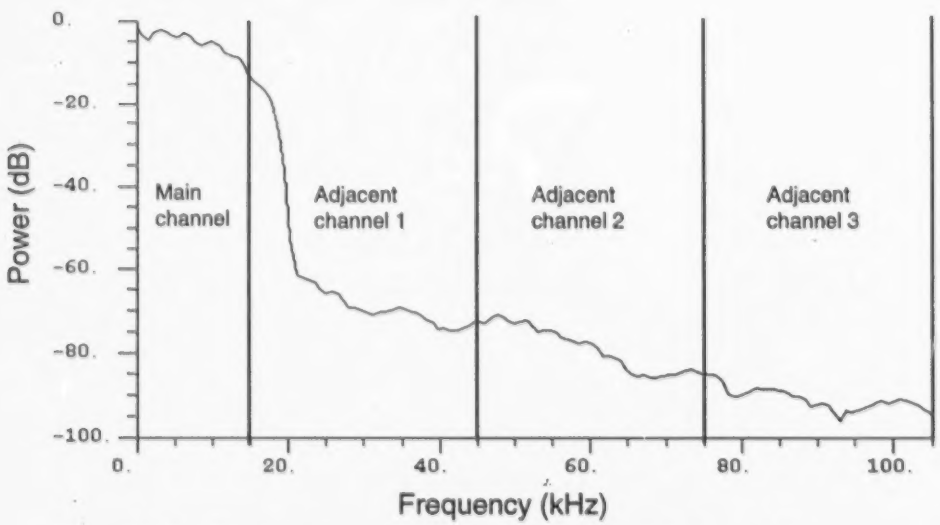

Fig. 4.18 Output power spectral density of class AB amplifier with cartesian coordinate negative feedback

oscillation.

4.8 Comparison of Performance of Spline Interpolation, Complex Gain and Cartesian Systems

Fig 4.19 shows the output PSD of the class AB amplifier for three linearization techniques, namely: spline interpolation, complex gain predistortion and cartesian coordinate negative feedback. The spline interpolation system had 30 spline points and a look-up table with 10,000 points. The complex gain system had a look-up table with 64 entries. The cartesian coordinate negative feedback system had a loop gain of 15. The spline interpolation method has better performance than the cartesian coordinate method in the first adjacent channel and in the first half of the second adjacent channels, and cartesian system has better performance than

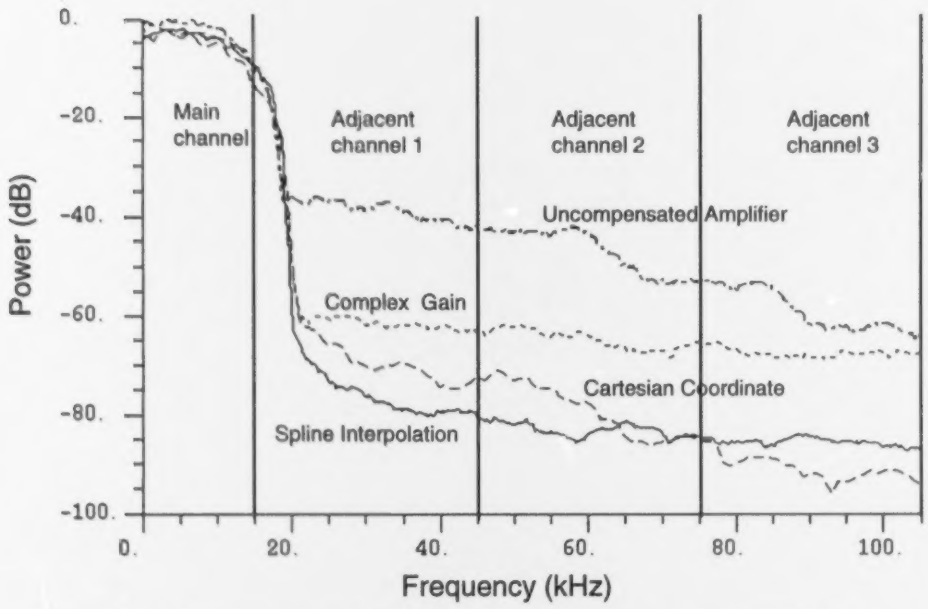

Fig. 4.19 Comparison of output power spectral densities of class AB amplifier

the spline in the third adjacent channel.

A comparison of the IM_3 and IM_5 for all three techniques is shown in Fig. 4.20. The spline interpolation technique reduces the IM_3 and IM_5 to -85.1 dB and -86.4 dB, respectively. The reduction of IM_3 is seen to be about 23 dB better than that provided by the complex gain predistortion system which in turn has about 7 dB more reduction of IM_3 than that provided by the cartesian coordinate negative feedback system.

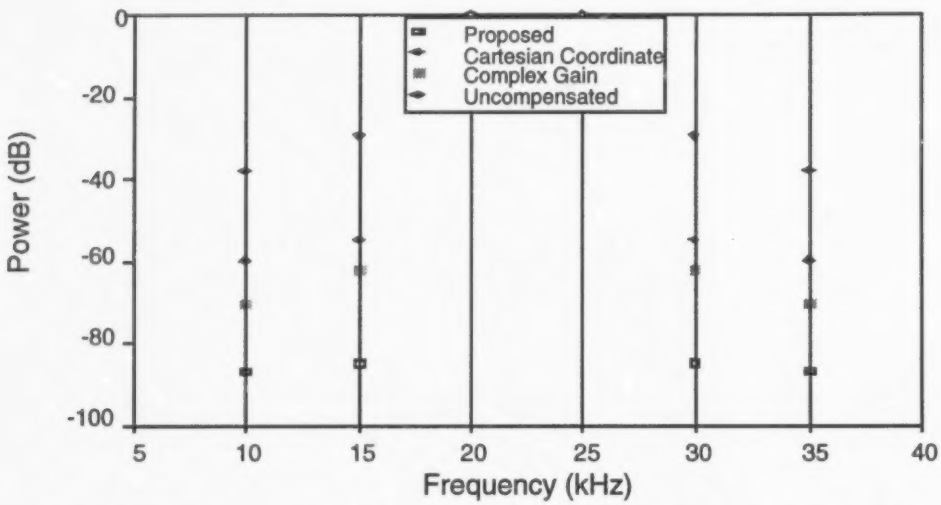

Fig. 4.20 Comparison of intermodulation products of class AB amplifier with spline interpolation, complex gain and cartesian coordinate negative feedback linearizers

4.9 Modulator Distortion

The interface between the baseband signal and the RF transmission channel is an analog quadrature modulator that generates the amplitude and phase modulated RF signal. An analog quadrature modulator has three major impairments, namely: gain imbalance, phase imbalance and dc-offset. These impairments are discussed in Chapter 2. The modulator impairments can

distort the transmitted signal and degrade the performance of an adaptive predistortion amplifier linearizer. In this section, the effects of these impairments are investigated.

4.9.1 Effects of Gain Imbalance

Ideally gains in the i and q channels should be equal. However, a practical quadrature modulator has different gains in the i and q channels. The gain imbalance results in a spurious tone at a frequency f_m below the carrier frequency for an input tone of frequency f_m. The effects of the gain imbalance are evaluated using a complex tone of 20 kHz. The i component of the modulator input signal is a cosine wave and the q component is a sine wave. The undesired sideband level at $f = (f_c - f_m)$ is measured as a ratio (in dB) below the desired sideband level at $f = (f_c + f_m)$. Fig. 4.21 shows the level of the undesired sideband $(f_c - f_m)$ in a quadrature modulator as a function of the gain imbalance, with phase imbalance as a parameter. A mathematical expression for this function is given in [33]. This figure presents the theoretical limit for suppression of the undesired sideband level for different values of

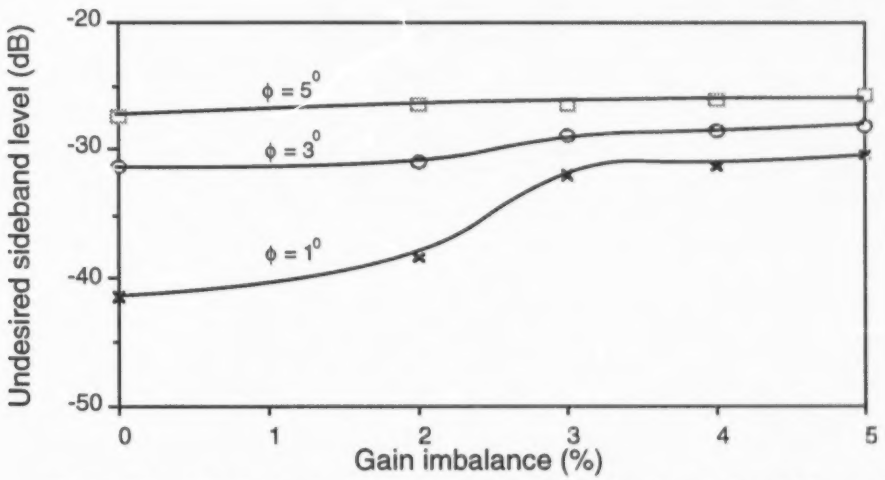

Fig. 4.21 Gain imbalance versus undesired sideband level

gain and phase imbalances. Simulation results illustrate that 40 dB suppression can be obtained with 1^0 phase imbalance and gain imbalance below 1% of the absolute gain. This is a rather stringent condition for a practical quadrature modulator.

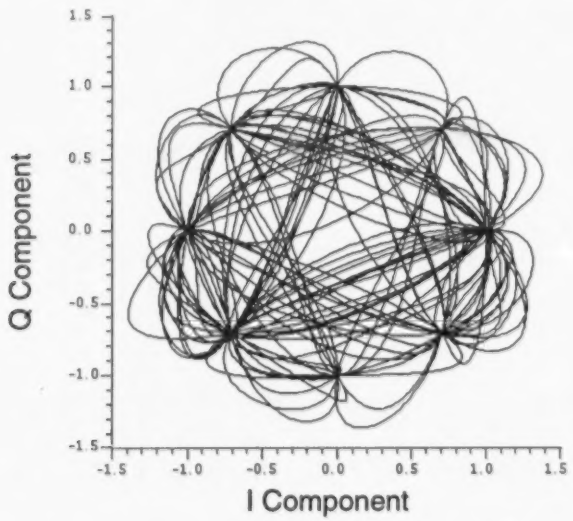

Fig. 4.22 Signal constellation of a π/4-DQPSK modulated signal with raised cosine filtering (Time is a parameter along the phasor trajectory)

Fig. 4.22 shows the signal constellation diagram of the π/4-DQPSK modulated signal with raised cosine filtering. The signal constellation points lie on a circle, and are equidistant from the origin. The effect of the gain imbalance in the modulator is illustrated in Fig. 4.23. The constellation points now lie on ellipse instead of on a circle. A gain imbalance of 50% was used for this simulation to illustrate the effect of the gain imbalance.

4.9.2 Effects of Phase Imbalance

The phase difference between the local oscillator signals that multiply i and q components should be exactly 90^0. But this is not the case for a

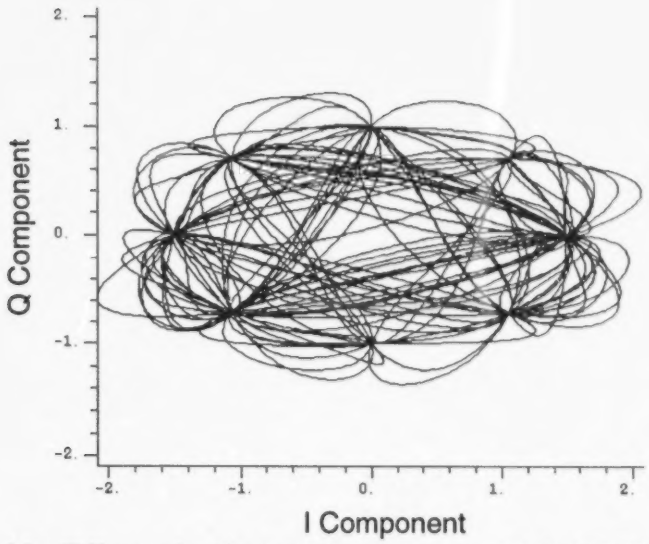

Fig. 4.23 Effect of gain imbalance on a π/4-DQPSK modulated signal

practical quadrature modulator that has a phase imbalance. A difference in the length of the two RF paths (see Fig. 2.20) can also result in phase imbalance. For a single tone input with frequency f_m, the phase imbalance will generate a spurious signal at a frequency $f_c - f_m$. Fig. 4.24 shows the undesired sideband level as a function of phase imbalance, with gain imbalance as a parameter. This figure presents the same information as Fig. 4.22.

The effect of phase imbalance on a π/4-DQPSK modulated raised cosine filtered signal is illustrated in Fig. 4.25. The phase imbalance distorts the circular constellation into a rotated elliptical constellation. A phase imbalance of 10^0 was used for this simulation.

4.9.3 Effects of DC-Offset

Carrier feedthrough in the modulator gives an unwanted RF component at the carrier frequency. Fig. 4.26 shows the level of the unwanted signal at the carrier frequency as a function of dc-offset.

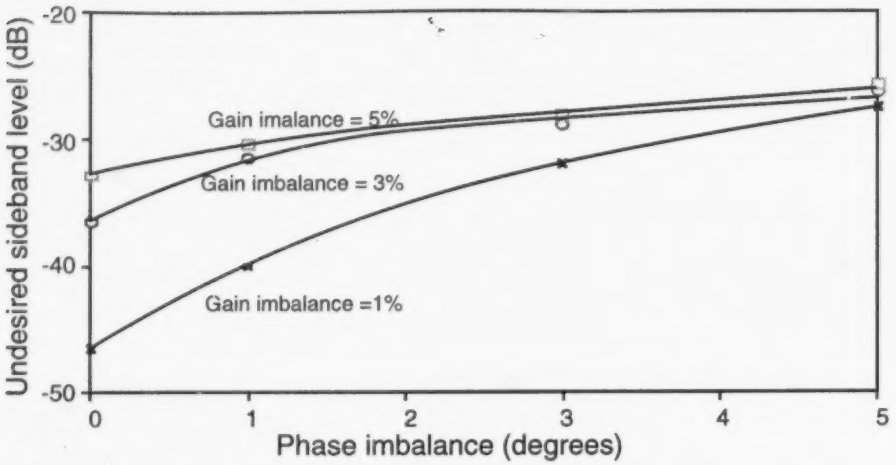

Fig. 4.24 Phase imbalance versus undesired sideband level

The effect of dc-offset on a π/4-DQPSK modulated signal with raised cosine filtering is illustrated in Fig. 4.27. All signal constellation points are shifted by an equal amount.

4.10 Demodulator Distortion

An analog quadrature demodulator is the interface between the

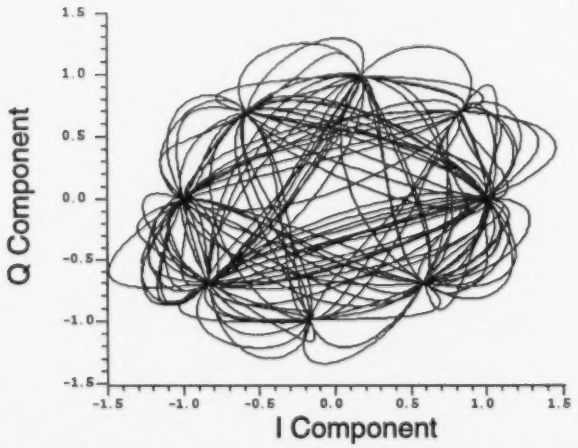

Fig. 4.25 Effect of phase imbalance on a π/4-DQPSK modulated signal

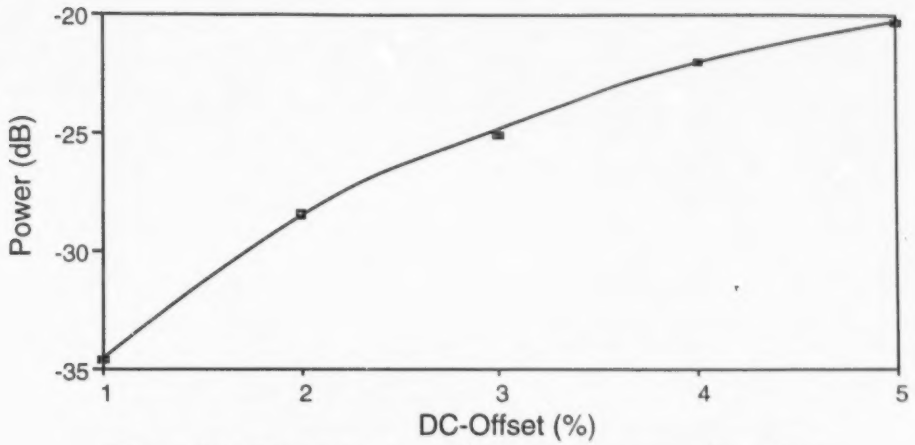

Fig. 4.26 Undesired carrier signal versus dc-offset

received RF signal and the baseband signals. An analog quadrature demodulator suffers from the same three major impairments as a quadrature modulator, namely: gain imbalance, phase imbalance and dc-offset. In this section, the effects of these impairments are investigated.

4.10.1 Effects of Gain Imbalance

In an ideal quadrature demodulator the gains in i and q channels

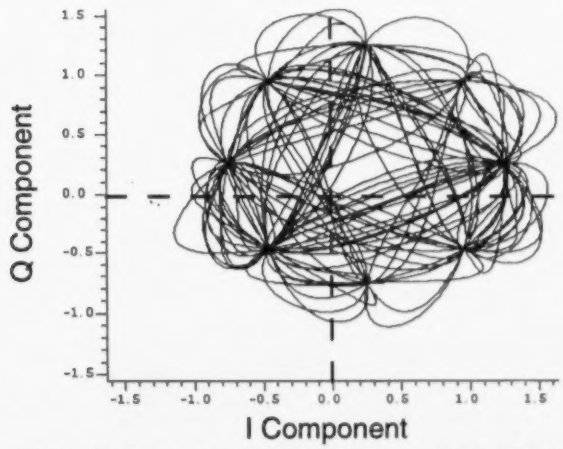

Fig. 4.27 Effect of dc-offset on a π/4-DQPSK modulated signal

should be exactly equal. However, a practical quadrature demodulator has different gains in the i and q channels. The gain imbalance in the demodulator causes an image signal at a frequency $f_{if} - f_m$, where f_{if} is the intermediate frequency. Fig. 4.28 shows the level of the image signal below the desired signal level as a function of gain imbalance, with phase imbalance as a parameter. This figure presents the theoretical limit for the image signal level for different values of gain and phase imbalance. For this set of simulations, a complex tone of 20 kHz was used as the input signal. The i component of the input signal was a cosine wave and the q component was a sine wave. The image signal level increases with increase in the gain imbalance in the demodulator.

4.10.2 Effects of Phase Imbalance

The phase imbalance also causes an image signal of the input signal. Fig. 4.29 shows the level of the image signal below the desired signal level as a function of phase imbalance, with gain imbalance as a parameter. It can be

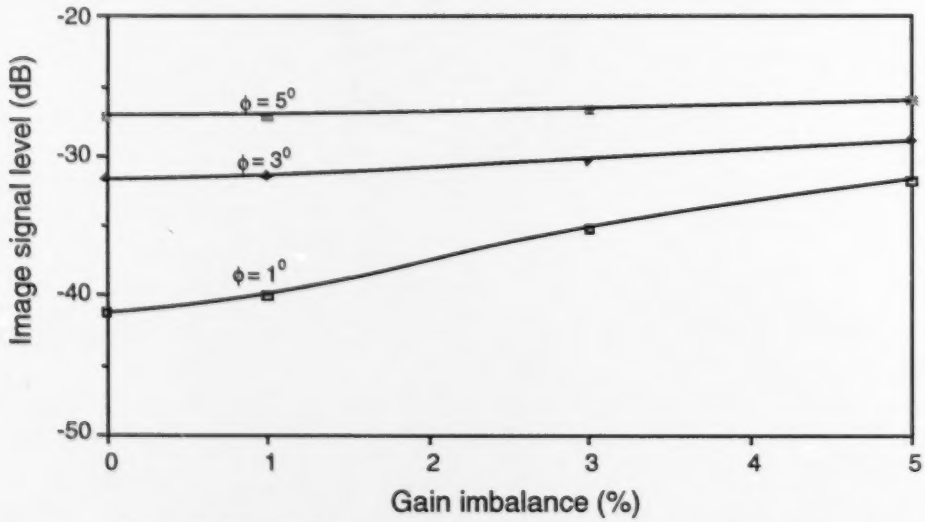

Fig. 4. 28 Gain imbalance versus image signal level

seen that the image signal level can, at best, be about 30 dB below the desired signal level for a phase imbalance of 3^0 and gain imbalance of 3%. Figure 4.29 presents the same information as Fig. 4.28. The image signal level increases with increase in the phase imbalance in the demodulator.

4.10.3 Effects of DC-Offset

The local oscillator signal leaks into the input RF ports of the i and q channel mixers causing self mixing of the local oscillator signal. This can result in dc-offset in the i and q baseband channels. Dc-offset is independent of the gain and phase imbalances in the demodulator. Fig. 4.30 shows the dc signal level below the desired signal level for different values of the self mixing of the local oscillator signal.

4.11 Performance of Modulator Impairment Compensator

The quadrature modulator impairments can distort the signal constellation of the transmitted signal, thereby degrading the performance of a system. It can cause phase dependent distortion in a transmitter. Therefore, it

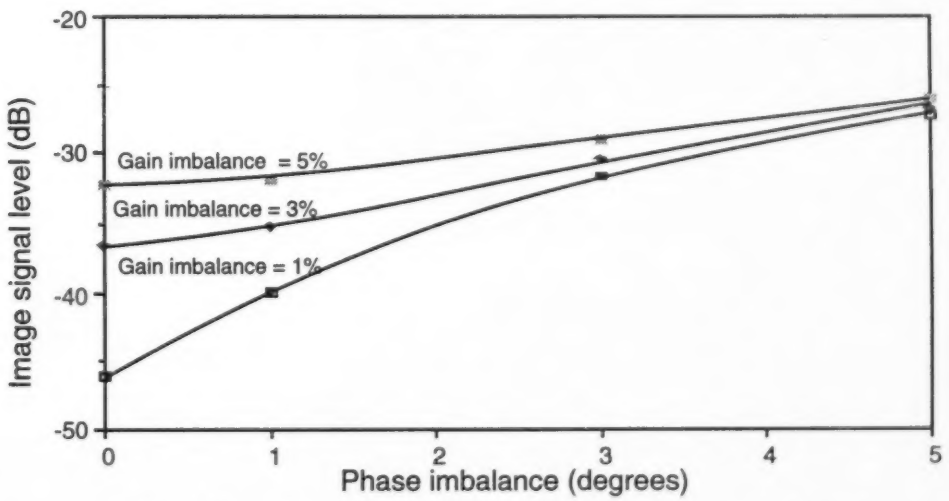

Fig. 4.29 Phase imbalance versus image signal level

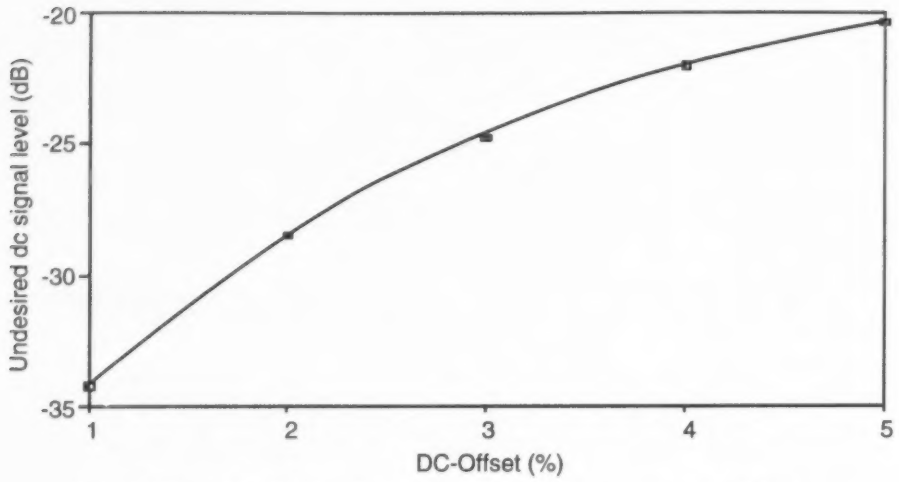

Fig. 4.30 Undesired dc signal level versus dc-offset

is important to keep the modulator impairments to the minimum level possible. A technique to compensate for the modulator impairments was discussed in Chapter 2. In this section, the performance of this technique is evaluated.

Fig. 4.31 shows the undesired sideband level for different values of gain and phase imbalance. The undesired sideband level is at least 75 dB below the desired sideband level when the compensator is used. A convergence bound of 10^{-3} was used for these simulations. There is about a 20 dB variation in the suppressed undesired sideband level. This variation is attributable to the convergence characteristics of the iterative process in the Newton-Raphson method. The convergence is not monotonic, and depends on the starting value. As a result, the undesired sideband level for a higher gain imbalance and/or phase imbalance can actually be less than that for a smaller imbalance.

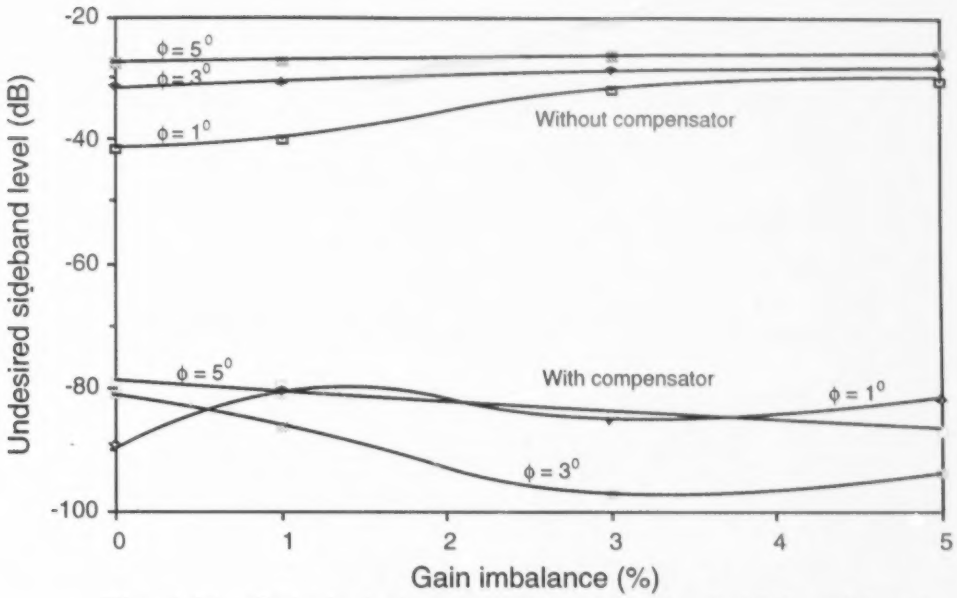

Fig. 4.31 Gain imbalance versus undesired sideband level

Fig. 4.32 shows the undesired sideband level of a modulator as a function of the convergence bound. It is seen that decreasing the convergence bound increases the suppression of the undesired sideband. Decreasing the convergence bound, however, requires more iterations of the convergence

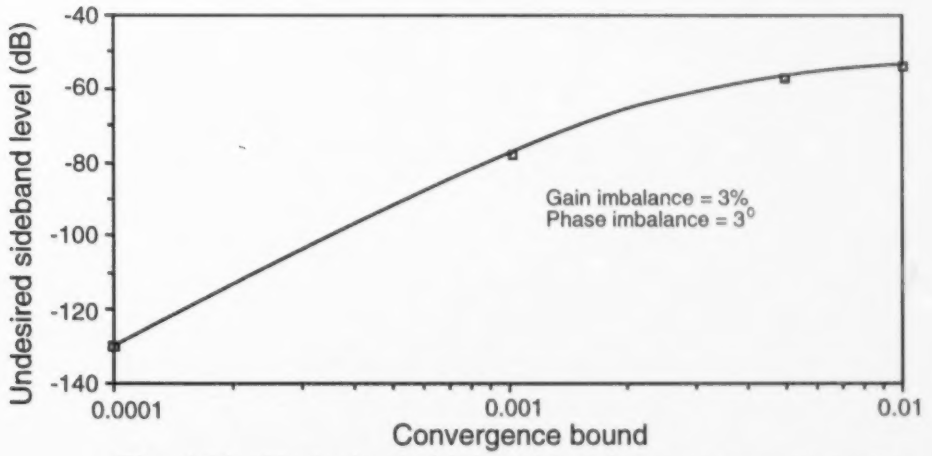

Fig. 4.32 Undesired sideband level versus convergence bound of compensated modulator

algorithm. With a convergence bound of 10^{-3}, the number of iterations is normally less than 20, which represents a reasonable trade-off.

4.12 Performance of Demodulator Impairment Compensator

A technique to compensate for the quadrature demodulator impairments was discussed in Chapter 2. In this section, the performance of the compensator is evaluated. A complex tone of 20 kHz is used as a test signal to determine the image signal level due to the gain and phase imbalances. Fig. 4.33 shows the image level below the desired signal level for different values of gain and phase imbalances. The image signal level is at least 75 dB below the desired signal level when the compensator is used. A convergence bound of 10^{-2} was used for these simulations. There is about a 20 dB variation in the suppressed image signal level. As for the case of the modulator, this variation is attributable to the convergence characteristics of

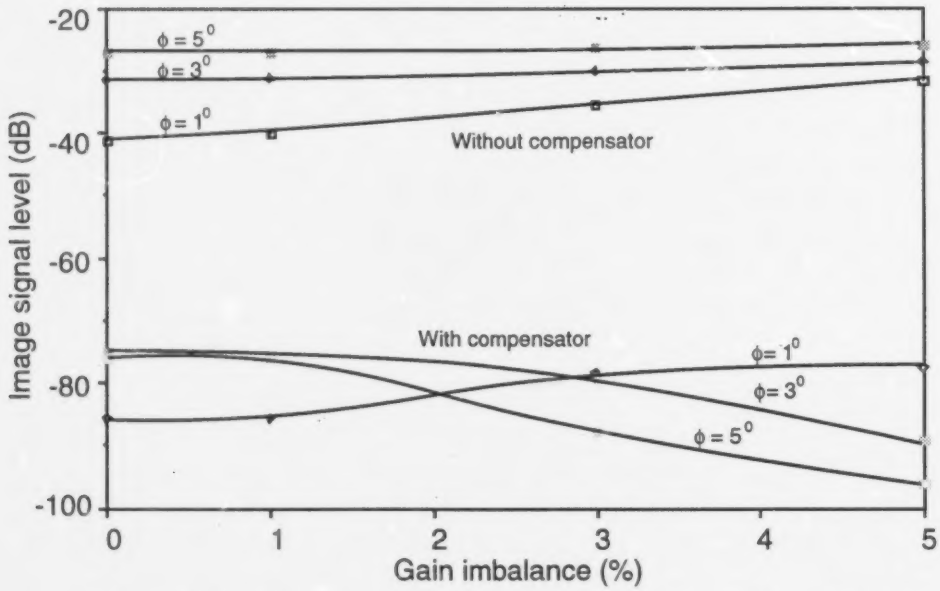

Fig. 4.33 Gain imbalance versus image signal level (dB)

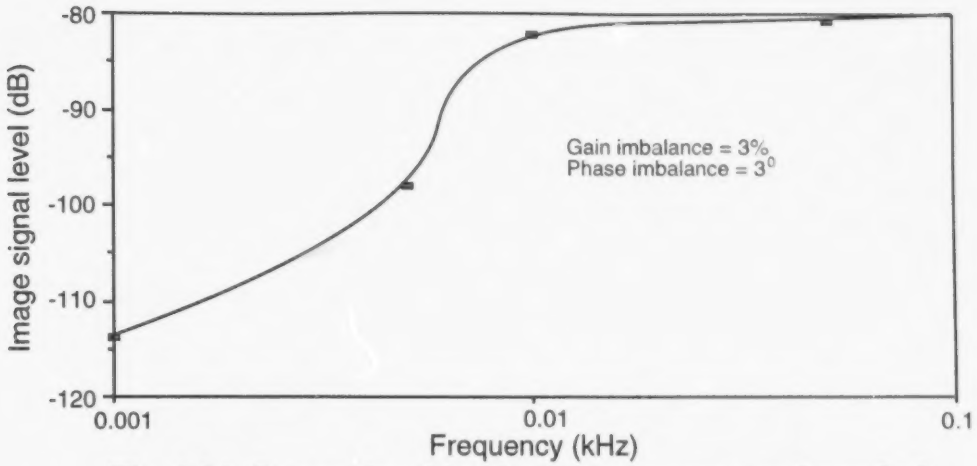

Fig. 4.34 Image signal level versus convergence bound of demodulator impairment compensator

the iterative process in the Newton-Raphson method.

Fig. 4.34 shows the image signal level of a demodulator as a function of convergence bound. It is seen that decreasing the convergence bound increases the suppression of the image signal. Decreasing the convergence bound, however, requires more iterations of the convergence algorithm. With a convergence bound of 10^{-2}, the number of iterations is normally less than 15.

4.13 Performance of Spline Interpolation Linearizer with Modulator and Demodulator Impairment Compensators

The spline interpolation linearizer assumes the amplifier distortion to be dependent only on the magnitude of the input signal. However, the quadrature modulator impairments in the forward path and the quadrature demodulator impairments in the feedback path can introduce phase dependent distortions. Therefore, it is important to compensate for these impairments.

Fig. 4.35 shows the performance of the spline interpolation linearizer along with the modulator and demodulator impairment compensator for the class AB amplifier. The modulator had 3% gain imbalance, 3^0 phase imbalance and 3% dc-offset. The demodulator also had 3% gain imbalance, 3^0 phase imbalance and 3% dc-offset. There were 30 spline points. The look-up table had 10,000 points. It can be seen from Fig. 4.35 that the decreasing convergence bound for the modulator and demodulator impairment compensators, decreases the out-of-band power emission, or, in other words, improves the linearizer performance. However, decreasing the convergence bound also requires more iterations of convergence algorithm and a consequently greater computational overhead.

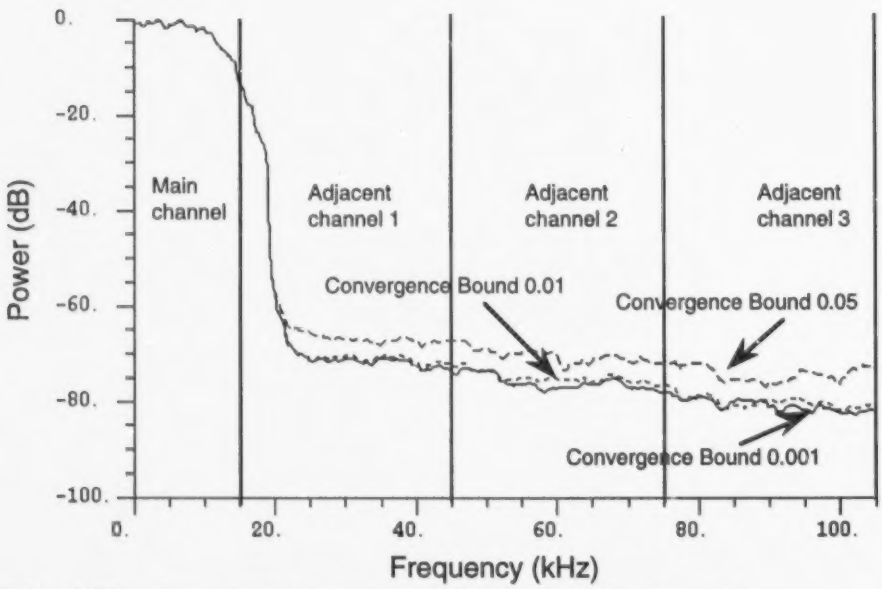

Fig. 4.35 Output power spectral density of class AB amplifier with spline interpolation linearizer and modulator and demodulator impairment compensators

5. Summary and Conclusions

The output of an ideal amplifier is a simple scaled replica of the original input signal. However, practical amplifiers introduce nonlinear distortion. Amplifier distortion can be characterized using amplitude-to-amplitude (AM-AM) and amplitude-to-phase (AM-PM) distortion. AM-AM distortion arises because the power gain of the amplifier is not constant. The gain of an amplifier decreases as the saturation is approached. AM-PM distortion is caused by a nonconstant phase delay in the amplifier. The phase shift introduced by an amplifier is a function of the input signal level, due to the transistor nonlinear capacitances. The effective capacitance at any frequency depends on the signal level.

In this project, a new adaptive predistortion technique for RF power amplifier linearization has been developed. The AM-AM and AM-PM characteristics of the amplifier are estimated, using cubic spline interpolation, from a look-up table of distortion values that are obtained using synchronous demodulation from the amplifier output itself. These estimated characteristics are then used to predistort the input signal so that, when the predistorted signal passes through the nonlinear amplifier, the net result is a linearly amplified signal.

The proposed linearizer is suitable for baseband implementation. Since it has basically an open configuration, it is unconditionally stable. The feedback loop is closed only for updating the predistortion coefficients. This linearization method is not restricted by the modulation format, because the signal is predistorted after the pulse shaping filter.

A complex envelope simulation model has been used to compare the performance of the different linearization techniques. Bandpass signals are

represented by equivalent lowpass signals. The simulation models include the data source, $\pi/4$-DQPSK modulator, and pulse shaping filter. The filter has a square-root raised cosine frequency response and a linear phase response. The parameters used for the amplifier models were obtained from actual measurements of the AM-AM and AM-PM characteristics of class AB and class B experimental amplifiers designed for digital cellular radio applications. The Block Oriented System Simulator (BOSS), a software package from Comdisco Systems, Inc., was used in this research project.

The performance of the proposed technique has been compared with that of the cartesian coordinate negative feedback and complex gain predistortion methods. The intermodulation products and out-of-band power emission are used as criteria for assessing the amplifier linearity. Two complex tones at 20 kHz and 25 kHz, respectively, are used to measure the intermodulation products. The third-order intermodulation products (IM_3) occur at 30 kHz (upper) and 15 kHz (lower), while the fifth-order products occur at 35 kHz (upper) and 10 kHz (lower). The out-of-band power is evaluated using the power spectral density of the output signal. The output data is windowed by a Blackman window to reduce spectral leakage. Overlapping sets of data are averaged together to reduce the variance in each frequency sample.

The cubic spline interpolation linearizer has about 23 dB and 16 dB better suppression of third and fifth order intermodulation products, respectively, than that provided by the complex gain predistortion system , and about 31 dB and 26 dB better suppression, respectively, than that provided by the cartesian coordinate negative feedback system. The complex gain predistortion linearizer reduced the output power spectral density to about -60 dB, whereas the output power spectral density was reduced to about -80 dB with the cubic spline

interpolation linearizer. The cubic spline interpolation linearizer was seen to have better performance than the cartesian coordinate negative feedback system in the first adjacent channel and in the first half of the second adjacent channel. The cartesian coordinate negative feedback system had the best performance in the third adjacent channel.

The interface between the baseband signals and the RF transmission channel is an analog quadrature modulator, which generates the amplitude and phase modulated RF signal. The baseband i and q components are recovered from the RF signal using an analog quadrature demodulator. Both analog modulator and demodulator have three major impairments, namely: gain imbalance, phase imbalance and dc-offset. These impairments result in spurious signals, which degrade the performance of the linearization system.

A technique to compensate for analog quadrature modulator and demodulator impairments has also been proposed in this research project. A part of the modulator output signal is fed to an envelope detector. The detector output and the i and q signal component values are used to generate five equations for five different signal points (at five different time instants). These equations are solved using the Newton-Raphson method to estimate the gain imbalance, phase imbalance and dc-offset. The estimated values are then used to compensate for the modulator impairments. Similarly, for the quadrature demodulator, a part of the RF signal is fed to an envelope detector. The quadrature demodulated i and q components along with the envelope detector output are then used to estimate the impairments, as before. These estimated values are used to compensate for the quadrature demodulator impairments. The spurious signal level can be suppressed below 70 dB when the compensator is used. There was a 20 dB variation in the suppressed undesired

sideband level. This is attributed to the fact that the convergence of the Newton-Raphson method is not monotonic. As a result, the undesired sideband level for a higher gain imbalance and/or phase imbalance can be actually less than that for a smaller imbalance.

In this research project, computer simulations have been carried out in order to investigate the performance of the cubic spline interpolation linearizer, and the quadrature modulator and demodulator impairment compensators. A hardware prototype needs to be developed to demonstrate the feasibility of these techniques in a real system.

The quadrature modulator and demodulator impairment compensators require an envelope detector to measure the magnitude of the signal. The performance of the compensator will be sensitive to this magnitude measurement. The effect of inaccuracy in the magnitude on the performance of the compensator needs to be investigated.

A more efficient algorithm to estimate the quadrature modulator and demodulator impairments should also be explored. There is an on-going project at TR labs in which quadrature modulator and demodulator impairment compensation techniques will be investigated further.

Digital techniques for the linearization of broadband RF power amplifiers should also be investigated. Linear broadband amplifiers are required for the amplification of multicarrier signals.

References

[1] C.E.W. Sundberg, N. Seshadri, "Digital cellular systems for North America", in *Proc. IEEE Globecom '90*, San Diego, California, Dec.1990, pp. 533-537.

[2] EIA/TIA Interim Standard, *Cellular System Dual-Mode Mobile Station - Base Station Compatibility Standard, IS-54,* Electronic Industries Association, May 1990.

[3] J. Uddenfeldt, K. Raith, B. Hedberg, "Digital technologies in cellular radio", in *Proc. 38th IEEE Veh. Technol. Conf.*, Philadelphia, Pennsylvania, June 1988, pp. 516-519.

[4] C.C. Hsieh, "Linear amplification techniques in 2 GHz microwave radio", in *Proc. NTC Conf.*, Los Angeles, California, Dec. 1977, pp.16:3-1 - 16:3-3.

[5] S.A. Hetzel, A. Bateman, J.P. McGeehan, "A LINC transmitter", in *Proc. 41st IEEE Veh. Technol. Conf.*, St. Louis, Missouri, May 1991, pp. 133-137.

[6] F.H. Raab, "Efficiency of outphasing RF power-amplifier systems", *IEEE Trans. Commun.,* vol. COM-33, no.10, pp. 1094-1099, Oct.1985.

[7] D.C. Cox, "Linear amplification with nonlinear components", *IEEE Trans. Commun.*, vol. COM-22, pp.1942-1945, Dec. 1974.

[8] F. Casadevall, J.J. Olmos, "On the behavior of the LINC transmitter", in *Proc. 40th IEEE Veh. Technol. Conf.*, Orlando, Florida, May 1990, pp. 29-34.

[9] R.D. Stewart, F.F. Tusubira, "Feedforward linearization of 950 MHz amplifiers", *Inst. Elec. Eng. Proc.*, vol. 135, pt H, no. 5, pp.347-350, Oct. 1988.

[10] A. Bateman, "The combined analogue locked loop universal modulator (CALLUM)", in *Proc. 42nd IEEE Veh. Technol. Conf.*, Denver, Colorado, May 1992, pp. 759-763.

[11] A. Bateman, R.J. Wilkinson, J.D. Marvill, "The application of digital signal processing to transmitter linearisation", in *Proc. 8th European Conf. on Electrotechnis*, Stockholm, Sweden, June 1988, pp. 64-67.

[12] S. Ono, N. Kondoh, Y. Shimazaki, "Digital cellular system with linear modulation", in *Proc. 39th IEEE Veh. Technol. Conf.*, San Francisco, California, May 1989, pp. 44-49.

[13] A. Bateman, D. Haines, "Direct conversion transceiver design for compact low-cost portable mobile radio terminals", in *Proc. 39th IEEE Veh. Technol. Conf.*, San Francisco, California, May 1989, pp. 57-62.

[14] M. Johansson, T. Mattsson, " Transmitter linearization using cartesian coordinate negative feedback for linear TDMA modulation", in *Proc. 41st IEEE Veh. Technol. Conf.*, St. Louis, Missouri, May 1991, pp. 439-444.

[15] A. Bateman, D. Haines, R. Wilkinson, "Direct conversion linear transceiver design", in *Proc. 5th Inst. Elec. Eng. Int. Conf. on Mobile Radio and Personal Commun.*, Coventry, UK, Dec. 1989, pp. 53-56.

[16] A. Bateman, D.M. Haines, R.J. Wilkinson, " Linear transceiver architectures", in *Proc. 38th IEEE Veh. Technol. Conf.*, Philadelphia, Pennsylvania, June 1988, pp. 478-484.

[17] Y. Nagata, " Linear amplification technique for digital mobile communications", in *Proc. 39th IEEE Veh. Technol. Conf.*, San Francisco, California, May 1989, pp. 159-164.

[18] J. Namiki, "An automatic controlled predistorter for multilevel quadrature amplitude modulation", *IEEE Trans. Commun.*, vol. COM-31, pp. 707-712, May-1983.

[19] A.A.M. Saleh, J. Salz, " Adaptive linearization of power amplifier in digital radio systems", *Bell Syst. J.*, vol. 62, pp. 1019-1033, Apr. 1983.

[20] S. Pupolin, L.J. Greenstein, "Performance analysis of digital radio links with nonlinear amplifiers", *IEEE J. Select. Areas Commun.*, vol. SAC-5, pp. 534-546.

[21] S.P. Stapleton, F.C. Costescu, "An adaptive predistorter for a power amplifier based on adjacent channel emissions", *IEEE Trans.Veh. Technol.*, vol. 41, no. 1, pp. 49-56, Feb. 1992.

[22] S. Kumar, "Power amplifier linearization using MMICs", *Microwave J.*, pp. 97-104, Apr. 1992.

[23] T. Nojima, T. Konno, "Cuber predistortion linearizer for relay equipment in 800 MHz band land mobile telephone system", *IEEE Trans. Veh. Technol.*, vol. VT-34, no. 4, pp. 169-177, Nov. 1985.

[24] S.P. Stapleton, F.C. Costescu, "An adaptive predistortion system", in *Proc. 42nd IEEE Veh. Technol. Conf.*, Denver, Colorado, May 1992, pp. 690-693.

[25] A.S. Wright, "Digital linearization techniques for nonlinear amplifiers", *Report No. LPA-003-ASW*, Jan. 1991.

[26] S.P. Stapleton, J.K. Cavers, "A new technique for adaptation of linearizing predistorters", in *Proc. 41st IEEE Veh. Technol. Conf.*, St. Louis, Missouri, May 1991, pp. 753-758.

[27] R.D. Stewart, F.F Tusubira, "Predistortion linearisation of amplifiers for UHF mobile radio", in *Proc. 8th European Conf. on Electrotechnis*, Stockholm, Sweden, June 1988, pp.1017-1022.

[28] J.K. Cavers, "Amplifier linearization using a digital predistorter with fast adaptation and low memory requirements", *IEEE Trans. Veh. Technol.*, vol. VT-39, no. 4, pp. 374-382, Nov. 1990.

[29] Y. Jaluria, *Computer Methods for Engineering*, Englewood Cliff, New Jersey:Prentice-Hall, 1988.

[30] A.S. Wright, W.G. Durtler, "Experimental performance of an adaptive digital linearized power amplifier", *IEEE MTT-S Int. Symp. Dig.*, Albuquerque, New Mexico, June 1922, vol. 2, pp. 1105-1108.

[31] A.S. Wright, W.G. Durtler, "Experimental performance of an adaptive digital linearized power amplifier", *IEEE Trans. Veh. Technol.*, vol. 41, no. 4, pp. 395-400, Nov. 1992.

[32] D.E. Norton, S.A. Massa, P. O'Donovan, "I and Q modulators for cellular communications systems", *Microwave J.*, pp. 63-80, Oct. 1991.

[33] J. Roome, "Analysis of quadrature detectors using complex envelope notation", *Inst. Elec. Eng. Proc.*, vol. 136, pt. F, no. 2, pp. 95-100, Apr. 1989.

[34] J.K. Cavers, M. Liao, "Adaptive compensation for imbalance and offset losses in direct conversion transceivers", in *Proc. 41st IEEE Veh. Technol. Conf.*, St. Louis, Missouri, May 1991, pp. 578-583.

[35] K. Anvari, M. Kaube, B. Hriskevich, "Performance of a direct conversion receiver with $\pi/4$-DQPSK modulated signal", in *Proc. 41st IEEE Veh. Technol. Conf.*, St. Louis, Missouri, May 1991, pp. 822-827.

[36] M. Faulkner, T. Mattsson, W. Yates, "Automatic adjustment of quadrature modulators", *Electron. Lett.*, vol. 127, no. 3, pp. 214-216, Jan. 1991.

[37] D. Hilborn, S.P. Stapleton, J.K. Cavers, "An adaptive direct conversion transmitter", in *Proc. 42nd IEEE Veh. Technol. Conf.*, Denver, Colorado, May 1992, pp. 764-767.

[38] COMDISCO Systems Inc., Block Oriented Systems Simulator (BOSS), *User Guide*, 1989.

[39] M.C. Jeruchim, P. Balaban, K.S. Shanmugan, *Simulation of Communication Systems*, New York: Plenum Press, pp. 344-348, 1992.

[40] S. Chennakeshu, G.J. Saulnier, " Differential detection of $\pi/4$-shifted-DQPSK for digital cellular radio", in *Proc. 41st IEEE Veh. Technol. Conf.*, St. Louis, Missouri, May 1991, pp. 186-191.

[41] Correspondence with NovAtel,1991,1992.

[42] B. Cain, "Temperature effects on an RF power amplifier", *M.Sc. Thesis*, University of Alberta, pp. 99-110, 1991.

[43] Y.J. den Otter, "Adaptive linearization of power amplifiers for digital cellular radio", *M.Sc. Thesis,* University of Alberta, 1992.

[44] A.V. Oppenheim, R.W. Schafer, *Digital Signal Processing*, New Delhi: Prentice-Hall, pp. 532-577, Dec. 1988.

[45] P.D. Welch, "The use of Fast Fourier Transform for the estimation of power spectra: a method based on time averaging over short, modified periodograms", *Modern Spectrum Analysis*, New York, IEEE Press, 1978.

[46] W.D. Stanley, G.R. Dougherty, R. Dougherty, *Digital Signal Processing*, Reston: Reston Publishing Company, Inc., pp. 301-309, 1984.

[47] N.L.Wang, W.J. Ho, J.A. Higgins, "High linearity power operation of AlGaAs/GaAs HBT at 10 GHz", *Electron. Lett.*, vol. 28, no. 1, pp. 55-56, Jan. 1992.

Appendix A

Cubic Spline Interpolation

Spline interpolation is an interpolation method based on curve fitting of small subset of data points. Interpolating polynomials are called spline functions. It is known from linear beam theory that the fourth derivative of the displacement of a beam is zero in the interval that has no external force acting on the beam. Since the fourth derivative is zero, the function can be a cubic polynomial. A general form of a cubic function is:

$$f_i(x) = a_0 + a_1 x + a_2 x^2 + a_3 x^3 \qquad \text{for} \quad x_i \le x \le x_{i+1}$$

There are four unknowns in the above equation. There should be four conditions that the polynomial must satisfy in order to determine the unknown constants. Since the polynomial must pass through the end points of the interval, the following conditions must be satisfied:

$$f(x_i) = a_0 + a_1 x_i + a_2 {x_i}^2 + a_3 {x_i}^3$$

$$f(x_{i+1}) = a_0 + a_1 x_{i+1} + a_2 {x_{i+1}}^2 + a_3 {x_{i+1}}^3$$

The remaining two conditions are provided by the fact that the first and second derivatives should be continuous. The second order derivatives of cubic functions are a straight line over each interval, and can be expressed as

$$f_i''(x) = f''(x_i)\frac{x_{i+1} - x}{x_{i+1} - x_i} + f''(x_{i+1})\frac{x - x_i}{x_{i+1} - x_i}$$

$$\text{for} \quad x_i \le x \le x_{i+1}$$

Integrating this equation and simplifying the equation using the first condition, $f_i(x)$, can be written as

$$f_i(x) = f''(x_i)\frac{(x_{i+1}-x)^3}{6\Delta x_i} + f''(x_{i+1})\frac{(x-x_i)^3}{6\Delta x_i} +$$

$$\left[\frac{f(x_i)}{\Delta x_i} - \frac{\Delta x_i}{6} f''(x_i)\right](x_{i+1}-x) +$$

$$\left[\frac{f(x_{i+1})}{\Delta x_i} - \frac{\Delta x_i}{6} f''(x_{i+1})\right](x-x_i)$$

where $\Delta x = x_{i+1} - x_i$

The second derivatives in the above equation are calculated using the fact that the first derivatives are continuous. $f_i(x)$ is differentiated and evaluated at x_i; similarly, $f_{i-1}(x)$ is differentiated and evaluated at x_i. The two results are equated to generate a set of linear simulation equations of the form

$$\Delta x_{i-1} f''(x_{i-1}) + 2(x_{i+1} - x_{i-1}) f''(x_i) + x_i f''(x_{i+1})$$

$$= 6\left[\frac{f(x_{i+1}) - f(x_i)}{\Delta x_i} - \frac{f(x_i) - f(x_{i-1})}{\Delta x_{i-1}}\right]$$

For n data points, there are (n-1) cubic spline functions. However, there are n unknown second derivatives. Two additional conditions at the end points are taken as

$$f''(x_0) = 0 \quad \text{and} \quad f''(x_n) = 0$$

This type of spline interpolation is known as a natural cubic spline interpolation. The system of simultaneous equations is tridiagonal and can be easily solved using gaussian elimination.

Appendix B

Newton-Raphson Method

The Newton-Raphson method is an iterative procedure to solve nonlinear equations. The method is based on the Taylor series expansion of functions. The first-order Taylor series expansion of a function, $f(x_1, x_2, \ldots\ldots x_n)$, at $(x_1', x_2' \ldots\ldots x_n')$ can be written as:

$$f_i(x_1', x_2' \ldots\ldots x_n') \approx f_i(x_1, x_2 \ldots\ldots x_n) + \left(\frac{\partial f_i}{\partial x_1}\right)(x_i' - x_1)$$

$$+ \ldots\ldots\ldots + \left(\frac{\partial f_i}{\partial x_n}\right)(x_n' - x_n)$$

where partial derivatives are evaluated at $(x_1, x_2 \ldots\ldots x_n)$. If $(x_1', x_2' \ldots\ldots x_n')$ is an exact solution of f_i's, then

$$f_i(x_i', x_2', \ldots\ldots x_n') = 0 \quad \text{for} \quad i = 1, 2 \ldots\ldots n$$

The unknown Δx_i, where $\Delta x_i = x_i' - x_i$, can be computed using

$$\begin{bmatrix} \frac{\partial f_1}{\partial x_1} & \frac{\partial f_1}{\partial x_2} & \ldots\ldots & \frac{\partial f_1}{\partial x_n} \\ \frac{\partial f_2}{\partial x_1} & & & \frac{\partial f_2}{\partial x_n} \\ & & & \\ \frac{\partial f_n}{\partial x_1} & & & \frac{\partial f_n}{\partial x_n} \end{bmatrix} \begin{bmatrix} \Delta x_1 \\ \Delta x_2 \\ \\ \\ \Delta x_n \end{bmatrix} = \begin{bmatrix} -f_1 \\ -f_2 \\ \\ \\ -f_n \end{bmatrix}$$

The next approximation is obtained as:

$$x_i^{(l+1)} = x_i^{(l)} + \Delta x_i^{(l)}$$

The initial guess of the values of unknowns is taken arbitrarily. However, the algorithm may not converge if the initial guess is too far off from the exact solution.

Appendix C

AM-AM and AM-PM Characteristics of Class AB and Class B Amplifiers

The following table gives normalized AM-AM and AM-PM conversion factors for an Avantek 6 Watt class AB amplifier.

Table C.1 Normalized AM-AM and AM-PM conversion factors for the class AB amplifier

Input (dB)	Output (dB)	Phase (degrees)
-10.45757	-11.1362	-1.4177
-10.17277	-10.8118	-1.2986
-9.89700	-10.49822	-0.9026
-9.62972	-10.18631	0.1879
-9.37042	-9.87333	0.2171
-9.11864	-9.56188	0.3197
-8.87395	-9.26077	0.4832
-8.63597	-8.98124	0.531
-8.40433	-8.72045	0.6520
-8.17871	-8.46666	0.7282
-7.95880	-8.21628	0.8450
-7.74432	-7.97391	1.0429
-7.53501	-7.74200	1.2496
-7.33063	-7.51773	1.4585
-7.13095	-7.29805	1.6598
-6.93575	-7.08246	1.8540
-6.74484	-6.87164	2.0455
-6.55804	-6.66650	2.2355
-6.37517	-6.46834	2.4180
-6.19608	-6.27834	2.5864
-6.02060	-6.09450	2.7355
-5.84860	-5.91185	2.8619
-5.67993	-5.72592	2.9635

Table C.1 Normalized AM-AM and AM-PM conversion factors for the class AB amplifier

Input (dB)	Output (dB)	Phase (degrees)
-5.51448	-5.53890	3.0529
-5.35212	-5.35741	3.1531
-5.19275	-5.18765	3.2852
-5.03624	-5.02982	3.4447
-4.88250	-4.87969	3.6083
-4.73144	-4.73302	3.7523
-4.58296	-4.58793	3.8705
-4.43698	-4.44568	3.9793
-4.29340	-4.30776	4.0967
-4.15217	-4.17518	4.2351
-4.01319	-4.04680	4.3830
-3.87640	-3.92093	4.5228
-3.74173	-3.79589	4.6368
-3.60912	-3.67141	4.7166
-3.47850	-3.54917	4.7670
-3.34982	-3.43105	4.7935
-3.22302	-3.31882	4.8021
-3.09804	-3.21246	4.7997
-2.97483	-3.11031	4.7945
-2.85335	-3.01061	4.7945
-2.73354	-2.91163	4.8077
-2.61537	-2.81279	4.8339
-2.49877	-2.71473	4.8641
-2.38373	-2.61816	4.8892
-2.27019	-2.52377	4.8999
-2.15811	-2.43215	4.8912

Table C.1 Normalized AM-AM and AM-PM conversion factors for the class AB amplifier

Input (dB)	Output (dB)	Phase (degrees)
-2.04746	-2.34346	4.8687
-1.93820	-2.25785	4.8391
-1.83030	-2.17545	4.8092
-1.72372	-2.09638	4.7853
-1.61844	-2.02032	4.7641
-1.51441	-1.94666	4.7358
-1.41162	-1.87476	4.6903
-1.31003	-1.80398	4.6176
-1.20961	-1.73376	4.5093
-1.11035	-1.66425	4.3694
-1.01220	-1.59587	4.2071
-0.915150	-1.52908	4.0318
-0.819172	-1.46434	3.8527
-0.724243	-1.40208	3.6787
-0.630341	-1.34244	3.5110
-0.537443	-1.28535	3.3471
-0.445528	-1.23076	3.1841
-0.354575	-1.17861	3.0194
-0.264565	-1.12884	2.8501
-0.175478	-1.08137	2.6731
-8.72959E-02	-1.03606	2.4848
0.	-0.992751	2.2816

The following table gives normalized AM-AM and AM-PM conversion factors for an 8 Watt class B amplifier based on a Philips BLV93 transistor.

Table C.2 Normalized AM-AM and AM-PM conversion factors for the class B amplifier

Input (dB)	Output (dB)	Phase (degrees)
-10.45757	-10.23587	1.1364
-10.17277	-9.89631	1.4085
-9.89700	-9.57408	1.6790
-9.62972	-9.26515	1.9216
-9.37042	-8.96375	2.0990
-9.11864	-8.66448	2.1763
-8.87395	-8.36234	2.1212
-8.63597	-8.05572	1.9220
-8.40433	-7.76260	1.6864
-8.17871	-7.50415	1.5497
-7.95880	-7.27244	1.5400
-7.74432	-7.04606	1.6338
-7.53501	-6.80979	1.8116
-7.33063	-6.57164	2.0681
-7.13095	-6.34480	2.4015
-6.93575	-6.13149	2.7942
-6.74484	-5.92413	3.2149
-6.55804	-5.71631	3.6355
-6.37517	-5.50827	4.0402
-6.19608	-5.30236	4.4176
-6.02060	-5.10080	4.7572
-5.84860	-4.90569	5.0489
-5.67993	-4.71838	5.2877
-5.51448	-4.53863	5.4803
-5.35212	-4.36599	5.6342

Table C.2 Normalized AM-AM and AM-PM conversion factors for the class B amplifier

Input (dB)	Output (dB)	Phase (degrees)
-5.19275	-4.20004	5.7567
-5.03624	-4.04035	5.8550
-4.88250	-3.88655	5.9355
-4.73144	-3.73827	6.0046
-4.58296	-3.59514	6.0681
-4.43698	-3.45685	6.1317
-4.29340	-3.32306	6.2006
-4.15217	-3.19348	6.2797
-4.01319	-3.06785	6.3699
-3.87640	-2.94598	6.4691
-3.74173	-2.82766	6.5755
-3.60912	-2.71270	6.6873
-3.47850	-2.60094	6.8027
-3.34982	-2.49218	6.9203
-3.22302	-2.38627	7.0384
-3.09804	-2.28306	7.1555
-2.97483	-2.18239	7.2703
-2.85335	-2.08411	7.3814
-2.73354	-1.98809	7.4875
-2.61537	-1.89421	7.5882
-2.49877	-1.80239	7.6838
-2.38373	-1.71255	7.7750
-2.27019	-1.62460	7.8622
-2.15811	-1.53848	7.9459
-2.04746	-1.45411	8.0267
-1.93820	-1.37142	8.1050

Table C.2 Normalized AM-AM and AM-PM conversion factors for the class B amplifier

Input (dB)	Output (dB)	Phase (degrees)
-1.83030	-1.29036	8.1811
-1.72372	-1.21084	8.2557
-1.61844	-1.13281	8.3290
-1.51441	-1.05622	8.4014
-1.41162	-0.981005	8.4732
-1.31003	-0.907139	8.5445
-1.20961	-0.834591	8.6153
-1.11035	-0.763333	8.6855
-1.01220	-0.693339	8.7550
-0.915150	-0.624582	8.8239
-0.819172	-0.557036	8.8922
-0.724243	-0.490680	8.9597
-0.630341	-0.425488	9.0265
-0.537443	-0.361438	9.0925
-0.445528	-0.298506	9.1578
-0.354575	-0.236673	9.2222
-0.264565	-0.175916	9.2859
-0.175478	-0.116215	9.3487
-8.72959E-02	-5.75530E-02	9.4106
0.	9.31885E-05	9.4717

Appendix D

Listing of Fortran Codes for BOSS Primitives

This appendix gives listings of Fortran codes for cubic spline interpolation, look-up table, computation of the quadrature modulator and demodulator impairment values using the Newton-Raphson method, and secant method. These subroutines are used to construct primitive BOSS modules which can be used along with the standard BOSS library modules.

```
**********************************************************************************
*****************This subroutine is for spline interpolation block*****************
**********************************************************************************

      subroutine splinetable(v,t,vt,tt,m,its)

      dimension a(1000),b(1000),c(1000),d(1000)
      real v(m),t(m),t2(1000),vt(its),tt(its)

**    Calculate the second derivatives at the given points

      c(1)=v(2)-v(1)
      do 1 i=2,m-1
            a(i)=v(i)-v(i-1)
            b(i)=2.0*(v(i+1)-v(i-1))
            c(i)=v(i+1)-v(i)
            d(i)=6.0*((t(i+1)-t(i))/c(i)-(t(i)-t(i-1))/a(i))
  1   continue

      do 2 i=3,m-1
            b(i)=b(i)-a(i)*c(i-1)/b(i-1)
            d(i)=d(i)-a(i)*d(i-1)/b(i-1)
  2   continue

      t2(1)=0.0
      t2(m)=0.0
      t2(m-1)=d(m-1)/b(m-1)
      do 3 i=2,m-2
            in=m-i
            t2(in)=(d(in)-c(in)*t2(in+1))/b(in)
  3   continue

      del =1.05*vv(m)/(its-1.0)

*     Spline calculations
```

```
      do 10 k=1,its
            vp=(k-1.0)*del
            do 5 i=1,m-1
                  if(vp.le.v(i+1)) then
8                       s1=v(i+1)-v(i)
                        s2=vp-v(i)
                        s3=v(i+1)-vp
                        tp=t2(i)*s3*(s3**2/s1-s1)/6.0+t2(i+1)*s2*(s2**
     +                        2/s1-s1)/6.0+t(i)*s3/s1+t(i+1)*s2/s1
                        goto 6
                  elseif (vp.gt.v(m)) then
                        i=m-1
                        goto 8
                  endif
5     continue
6     vt(k)=vp
            tt(k)=tp
10    continue
      return
      end
```

```
**********************************************************************************
***********This subroutine is for the look-up table block**********************
**********************************************************************************
      subroutine table(m,erm,erp,im,om,op,in,jj,kk)

      real im(m),om(m),op(m),in

      j=jj
2     if (in.ge.om(j)) then
            j=j+1
            if (j.ge.ml then
                  j=m
                  goto 6
            endif
            goto2
      endif

3     if (in.lt.om(j-1)) then
            j=j-1
            if (j.le.1) then
                  j=1
                  goto 6
            endif
            goto 3
      endif

6     erm=im(j)
      kk=j

4     if (erm.ge.im(j)) then
            if (j.ge.m) then
                  j=m
                  goto 7
            endif
            j=j+1
            goto 4
      endif

5     if (in.lt.im(j-1)) then
            if (j.le.1) then
                  j=1
                  goto 7
            endif
            j=j-1
            goto 5
      endif
```

```
7   erp=op(j)
    return
    end
```

```
*****************************************************************************************
**********This subroutine is for estimating the modulator impairments*********
*****************************************************************************************
      subroutine fivevarmod (ib1,ib2,ia1,ia2,ip1,eps,a1,a2,b1,b2,p1
     &i1,i2,i3,i4,i5,m1,m2,m3,m4,m5,q1,q2,q3,q4,q5,en)

      logical *1 en
      real i1,i2,i3,i4,i5,q1,q2,q3,q4,q5,m1,m2,m3,m4,m5
      real a1,a2,b1,b2,old,p1,ia1,ia2,ib1,ib2,ip1
      real i(5),q(5),m(5),z(5,6),d(5)
      integer n,nn
*     Initialization of variables
      i(1)=i1
      i(2)=i2
      i(3)=i3
      i(4)=i4
      i(5)=i5
      q(1)=q1
      q(2)=q2
      q(3)=q3
      q(4)=q4
      q(5)=q5
      m(1)=m1
      m(2)=m2
      m(3)=m3
      m(4)=m4
      m(5)=m5
      a1=ia1
      a2=ia2
      b1=ib1
      b2=ib2
      p1=ip1
      pi=3.1415926

      do 20 n=1,5
            en=.true.
      s=sin(p1)
      z(n,3)=-2*(b1+a1*i(n)-(b2+a2*q(n))*s)
      z(n,4)=-2*(b2+a2*q(n)-(b1+a1*i(n))*s)
      z(n,1)=i(n)*z(n,3)
      z(n,2)=q(n)*z(n,4)
      z(n,5)=2*(b1+a1*i(n))*(b2+a2*q(n))*cos(p1)
      z(n,6)=m(n)**2-((a1*i(n)+b1)*cos(p1))**2-((a1*i(n)+
     +     b1)*(-sin(p1))+(a2*q(n)+b2))**2
      z(n,6)=-z(n,6)
20    continue
```

```
      do 28 n=1,5
            d(n)=0
            do 29 nn=1,6
                  if (abs(z(n,nn)).lt.eps/10) then
                        z(n,nn)=0
                  endif

                  z(n,nn)=z(n,nn)*10000
29          continue
28    continue
      do 39 j=1,4
            do 38 k=j,5
                  if (abs(z(k,j)).gt.abs(z(j,j))) then
                        do 37 kk=1,6
                              old=z(k,kk)
                              z((k,kk)=z(j,kk)
                              z(j,kk)=old
37                      continue
                  endif
38          continue
            do 36 k=j+1,5
                  do 41 kk=6,j,-1
                        if (abs(z(j,j)).lt.1) then
                              en=.false.
                              goto 70
                        else
                        z(k,kk)=z(k,kk)-z(j,kk)*z(k,j)/z(j,j)
                        endif
41                      continue
36          continue
39    continue
      do 43 j=5,1,-1
            old=0
            do 42 k=1,5
                  old=old+z(j,k)*d(k)
42          continue
            if (abs(z(j,j)).lt.1) then
                  en=.false.
                  goto70
            else
                  d(j)=(z(j,6)-old)/z(j,j)
            endif
43    continue
      if (abs(d(n)).lt.eps/10) then
            d(n)=0
      endif
      do 60 n=1,5
```

```
            if (abs(d(n)).gt.eps) then
                  en=.false.
            endif
            if (abs(d(n)).gt.10) then
                  d(n)=0
            endif
60    continue

      a1=a1+d(1)
      a2=a2+d(2)
      b1=b1+d(3)
      b2=b2+d(4)
      p1=p1+d(5)
      if (a1.lt.0) then
            a1=-a1
            b1=-b1
            p1=-p1
      endif
      if (a2.lt.0) then
            a2=-a2
            b2=-b2
            p1=-p1
      endif
      if (en.eq.true.) then
            if (cos(p1).lt.0) then
                  p1=-p1
            endif
62          if (p1.gt.1) then
            p1=p1-pi
            goto 62
            elseif (p1.lt-1) then
            p1=p1+pi
            goto 62
            endif
      endif
70    return
      end
```

```
*******************************************************************************************

**********This subroutine is for estimating the demodulator impairments********
*******************************************************************************************

      subroutine fivevardemod (ib3,ib4,ia3,ia4,ip3,eps,a3,a4,b3,b4
     &,p3,i1,i2,i3,i4,i5,m1,m2,m3,m4,m5,q1,q2,q3,q4,q5,en)

      logical *1 en
      real i1,i2,i3,i4,i5,q1,q2,q3,q4,q5,m1,m2,m3,m4,m5
      real a3,a4,b3,b4,p3,old,ia3,ia4,ib3,ib4,ip3
      real i(5),q(5),m(5),z(5,6),d(5)
      integer n,nn
*     Initialization of variables
      i(1)=i1
      i(2)=i2
      i(3)=i3
      i(4)=i4
      i(5)=i5
      q(1)=q1
      q(2)=q2
      q(3)=q3
      q(4)=q4
      q(5)=q5
      m(1)=m1
      m(2)=m2
      m(3)=m3
      m(4)=m4
      m(5)=m5
      a3=ia3
      a4=ia4
      b3=ib3
      b4=ib4
      p3=ip3
      pi=3.1415926
5     d0 20 n=1,5
            en=.true.
            s1=(i(n)-b3)/a3
            s2=9q(n)-b4)/a4
            z(n,3)=8*(a4*(b3-i(n))+(b4-q(n))*sin(p3)*a3)/a4*
     +           (cos(p3)*a3)**2
            z(n,4)=8*(a3*(b4-q(n))+(b3-i(n))*sin(p3)*a4)/a3*
     +         (cos(p3)*a4)**2
            z(n,1)=z(n,3)*s1
            z(n,2)=z(n,4)*s2
            z(n,5)=4*((3-cos(2*p3))*s1*s2+2*sin(p3)*
     +          (s1**2+s2**2))/(cos(p3))**2
            z(n,6)=(2*m(n))**2-(4*s2**2+4*((s1+s2*sin(p3))/
```

```
     +          (cos(p3)))**2)
20   continue
     do 28 n=1,5
          d(n)=0
          do 29 nn=1,6
               if (abs(z(n,nn)).lt.eps/10) then
                    z(n,nn)=0
               endif
               z(n,nn)=z(n,nn)*10000
29        continue
28   continue
     do 39 j=1,4
          do 38 k=j,5
               if (abs(z(k,j)).gt.abs(z(j,j))) then
                    do 37 kk=1,6
                         old=z(k,kk)
                         z((k,kk)=z(j,kk)
                         z(j,kk)=old
37                  continue
               endif
38        continue
     do 36 k=j+1,5
          do 41 kk=6,j,-1
               z(k,kk)=z(k,kk)-z(j,kk)*z(k,j)/z(j,j)
41             continue
36        continue
39   continue
     do 43 j=5,1,-1
          old=0
          do 42 k=1,5
               old=old+z(j,k)*d(k)
42        continue
          if (abs(z(j,j)).lt.1) then
               en=.false.
               goto70
          else
               d(j)=(z(j,6)-old)/z(j,j)
          endif
43   continue
     if (abs(d(n)).lt.eps/10) then
          d(n)=0
     endif
     do 60 n=1,5
          if (abs(d(n)).gt.eps) then
               en=.false.
          endif
          if (abs(d(n)).gt.10) then
```

```
                d(n)=0
            endif
60      continue
        a3=a3+d(1)
        a4=a4+d(2)
        b3=b3+d(3)
        b4=b4+d(4)
        p3=p3+d(5)
        if (a3.lt.0) then
            a3=-a3
            b3=-b3
            p3=-p3
        endif
        if (a4.lt.0) then
            a4=-a4
            b4=-b4
            p3=-p3
        endif
        if (en.eq.true.) then
            if (cos(p3).lt.0) then
                p3=-p3
            endif
62          if (p3.gt.1) then
            p3=p3-pi
            goto 62
            elseif (p3.lt-1) then
            p3=p3+pi
            goto 62
            endif
        endif
70      return
        end
```

```
*****************************************************************************************
**********This subroutine performs the calculation for a secant iteration*******
*****************************************************************************************

      subroutine secant1(fk0,fk1,eg0,eg1,enable,n,n1,
     &        wr_enable,finished,fk2,try1,try2,max_iter, err_min,err_max)

      logical*1  enable,wr_enable,finished
      integer n,n1,max_iter
      complex fk0,fk1,eg0,eg1,fk2,try1,try2
      real err_min,err_max
      wr_enable=.false.
      finished=.false.

      if (.not.enable) then
            goto200

      if(n.eq.0) then
            fk2=try1
            n1=1
            wr_enable=.true.
            goto200
      endif

      if (n.eq.1) then
            fk2=try2
            n1=2
            wr_enable=.true.
            goto 200
      endif

      if (cabs(eg1).gt.err_max) then
            goto 50
      endif

      if (n.gt.max_iter) then
            goto200
      endif

      if (n.eq.max_iter) then
            n1=n+1
            finished=.true.
            goto200
      endif
50    coninue

      if((eg1-eg0).eq.0) then
```

```
            fk2=fk1+0.25*eg1
        else
            fk2=(fk0*eg1-fk1*eg0)/(eg1-eg0)
        endif
        n1=n+1
        wr_enable=.true.

    200 continue

        return
        end
```